IL
NUOVO CIMENTO
ORGANO DELLA SOCIETÀ ITALIANA DI FISICA
SOTTO GLI AUSPICI DEL CONSIGLIO NAZIONALE DELLE RICERCHE

VOL. XI, N. 6 *Serie decima* 16 Marzo 1959

To Introduce the Impact Parameter into the Analysis of Multiple Meson Processes.

H. EZAWA

Department of Physics, University of Tokyo - Tokyo

(ricevuto il 6 Ottobre 1958)

Summary. — To introduce the concept of impact parameter into the analysis of high energy events seems possible and also useful. Showing the inadequacy of Fermi's theory with impact parameter, we propose another way to infer the impact parameter for each event in the emulsion from the experimentally observable quantities. The impact parameters introduced in this way have admissible order of magnitude and are shown to have a somewhat definite functional relation with the multiplicity of mesons whose plot versus primary energy has been known to suffer large fluctuation. Consistency with the uncertainty principle is also discussed.

1. – Introduction.

Since HEISENBERG pointed out the possibility of the explosive production of meson in high energy nuclear impacts, [1], many people have attempted to reveal, both theoretically and experimentally, characteristic features of this phenomenon, the investigation of which is expected to bring us into a glittering expanse of virgin country.

Various opinions have been stated by different authors. HEISENBERG [1] has emphasized the possible existence of second kind interactions and the

[1] W. HEISENBERG: *Zeits. f. Phys.*, **101**, 35 (1936); **113**, 61 (1939); **126**, 569 (1949); **133**, 65 (1952).

classical behavior of highly excited states; FERMI [2,3], the statistical nature of many meson systems; LANDAU [4], the inadequacy of particle picture in the early stage of Fermi's process; LEWIS, OPPENHEIMER and WOUTHUYSEN [5], the instantaneity of the production process; and so on.

These theories have indeed constituted convenient references for experimentalists, whose attempts have thus consisted in deciding which one of those features prevails in nature. Unfortunately, the rarity of events and therefore the poorness of statistics hindered the decision. As is very natural in the traditional application of quantum mechanics, only one parameter, the energy of primary nucleons in the center-of-mass system (C.M.S.) $2\gamma_c Mc^2$, has hitherto been used to specify the initial condition in all the theories but those of FERMI [3]. The analysis of experiments has also been carried through it. For example, the multiplicity of meson production n_s (*) has been analysed through the relation $n_s = f(\gamma_c)$, which is predicted differently theory by theory and therefore considered to serve as a crucial point. However, this way of analysis has been not so successful because of the poorness of statistics and of the large fluctuation of the multiplicity itself. Taking this situation for granted, it seems desirable to find another way to push our investigation forward. We have to adapt our method of investigation to the new field of physics under consideration, the extremely high energy region.

Recently, angular distributions of secondary particles have been found to vary considerably event by event, even when we restrict ourselves to those with similar primary energy. In the usual scattering experiments, we at first classify events with respect to their primary energy and then add up the number of events to give the angular distribution which is to be compared with theory. In this paper, however, we give the term « angular distribution » a meaning different from that usual in ordinary scattering experiments; our angular distribution is the distribution of many secondary particles, *one for each event*. To compare the distributions with the theory hitherto proposed, we must average over the events with the same or at least a similar primary energy.

In the multiple meson processes, there are many quantities which are observable in the emulsion, say, multiplicity of mesons, angular distribution, inelasticity etc.; they are fluctuating event by event. Instead of averaging, we may

---

[2] E. FERMI: *Prog. Theor. Phys.*, **5**, 4 (1950). See also reference [13].

[3] E. FERMI: *Phys. Rev.*, **81**, 115 (1951).

[4] L. D. LANDAU: *Usp. Akad. Nauk SSSR.* **17**, 51 (1953); S. Z. BELEN'KIJ and L. D. LANDAU: *Usp. Fiz. Nauk*, **56**, 309 (1955).

[5] H. W. LEWIS, J. R. OPPENHEIMER and S. A. WOUTHUYSEN: *Phys. Rev.*, **73**, 127 (1948).

(*) In this paper the number of charged swift particles is used as a representative of the multiplicity.

also inquire about the correlation between any two of these fluctuating quantities. When there are many quantities correlated with each other, we may combine them with some parameters (parametric representation). In addition these parameters themselves will have some physical meaning.

Thus, I should like to point out, in this paper, that the experimental facts suggest the possibility to introduce one more parameter other than the primary energy, the impact parameter b of nuclear collision, and then to analyze the multiplicity, for example, through $n_s = g(\gamma_c, b)$. This point of view will enable us to draw more information from experiments.

There may indeed be many questions as to the introduction of such a parameter, to the discussion of which we will return later. One remark to be stressed here is that the usefulness of the impact parameter, a rather geometrical concept, is a characteristic feature of high energy phenomena.

To conclude this section, we summarize the experimental material to be used in this paper. Besides the number of charged swift secondaries n_s, the inelasticity K and the Lorentz factor of colliding nucleons in the C.M.S. γ_c, we use the index of peakedness of the angular distribution m. This index m is, according to T. F. HOANG ([6]) and the Bristol group ([7]), defined through the angular distribution (C.M.S.) of secondary particles as

$$\frac{\mathrm{d}\, n_s(\theta)}{\mathrm{d}\cos\theta} \simeq \alpha \cos^m \theta \,. \tag{1.1}$$

Although some authors ([8]) call our attention to the fact that the angular distribution is not monotonic even in one of the separate cones, forward and backward, but has a maximum in each cone, we shall not, at present, enter into such a discussion. The Bristol group ([7]) showed that m can be conveniently calculated by the formula:

$$\langle \mathrm{cosec}\, \theta \rangle_{\mathrm{av}} \simeq 1.25\sqrt{m} \qquad \text{(for large } m\text{)}, \tag{1.2}$$

the average being taken over the charged swift secondaries. Hereafter we shall regard Eq. (1.2) as the equation defining m (*), keeping in mind its meaning expressed in Eq. (1.1).

([6]) T. F. HOANG: *Journ. Phys. et Rad.*, **14**, 395 (1953).

([7]) B. EDWARDS, J. LOSTY, D. H. PERKINS and J. REYNOLDS: *Phil. Mag.*, **3**, 237 (1958). The data of this paper are supplemented by a private communication from Dr. J. IWADARE, to whom the present author is very grateful. The m for the event $p20$ is taken to be 2000.

([8]) K. NIU: *Lecture at the Annual Meeting of the Physical Society of Japan*, (Oct. 1957). *Uchusen-Kenkyu* (Mimeographed circular in Japanese), **3**, 85 (1958). The paper will appear in *Nuovo Cimento*; G. COCCONI: *Phys. Rev.*, **111**, 1699 (1958).

(*) Use is made of this definition also for small m.

2. – The Fermi theory with impact parameter.

FERMI developed a theory to describe the angular distribution of each event. It is the only theory hitherto proposed which takes the impact parameter into account. We shall briefly summarize his results and compare them with experiments, showing some discrepancies. In the following, the equation cited as, for example, (F.20) refers to the Eq. (20) in FERMI's paper [3].

Fermi's theory gives for the angular distribution of secondary particles when observed in C.M.S., the formula (*)

$$\text{(F.21)} \qquad \frac{\mathrm{d}n_s}{\mathrm{d}\eta} = g(\beta) f_4(\varrho\eta) ,$$

where $g(\beta)$ is a certain function of β, β corresponding to the hot spot temperature $\beta \equiv c/kT$, and

$$\text{(F.22)} \qquad f_4(\alpha) \equiv [2/\alpha^2(1-\alpha^2)] - (1/\alpha^2) \ln [(1+\alpha)/(1-\alpha)] .$$

$\eta \equiv \cos\theta$, and ϱ is related to the impact parameter b by (F.20), $b/R = 3f_1(\varrho)/2f_2(\varrho)$ ($R \equiv \hbar/\mu c$, $\mu = \pi$-meson mass), as to the right hand side of which the reader may consult the Table I of his paper.

The numbers of charged secondaries are given by (F.15) and (F.17) after some modifications of numerical coefficients to take the charge independence into account ($a \to 3a$, $b \to 3b$, and taking two thirds of n for n_s):

$$\text{(2.1)} \qquad n_s = 3.4 [2K(\gamma_c - 1)]^{\frac{1}{2}} \cdot f(\varrho)/[f_2(\varrho)]^{\frac{3}{4}} ,$$

where

$$f(\varrho) \equiv [(1+\varrho^2)/\varrho^3] \ln (1+\varrho)/(1-\varrho) - 2/\varrho^2 ,$$

and

$$f_2(\varrho) \equiv [1/\varrho] \ln (1+\varrho)/(1-\varrho) + 2/(1-\varrho^2) .$$

The angular distribution (F.21) agrees qualitatively with experiments. As a first step towards the quantitative comparison we shall take up the value m defined in Eq. (1.2), the agreement of which with experiment is a necessary

---

(*) Some changes of notation: γ, r in Fermi's paper are changed into β and b respectively.

condition for the theory to be correct. According to Eq. (1.2) and (F.20),

$$1.25\sqrt{m} = \frac{\int_0^{\pi/2} f_4(\varrho \cos\theta)\, d\theta}{\int_0^{\pi/2} f_4(\varrho \cos\theta) \sin\theta\, d\theta}. \tag{2.2}$$

That m is independent of γ_c is a characteristic of Fermi's theory.

Thus comparing Eq. (2.1) and (2.2), we see that, in Fermi's theory $n_s/[2K(\gamma_c - 1)]^{\frac{1}{2}}$ is connected uniquely with m through ϱ, and therefore through

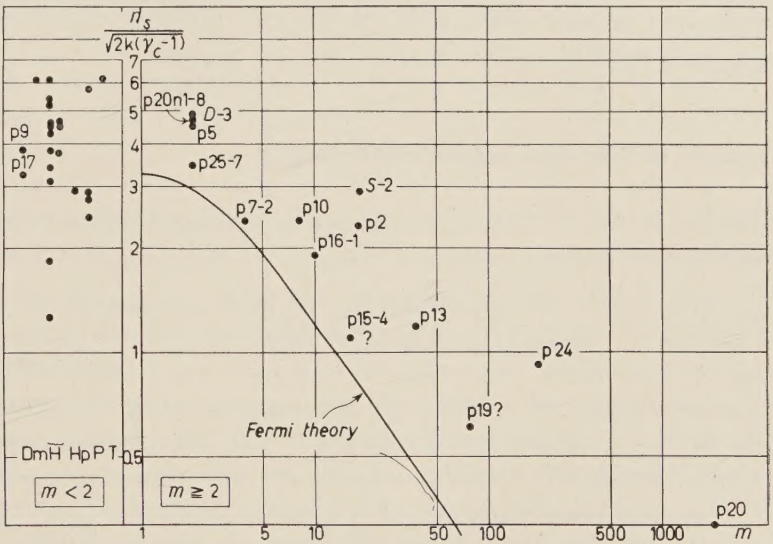

Fig. 1. – The relation between multiplicity of charged particles n_s and m, the latter being defined by Eq. (1.2). The curve shows the relation due to Fermi's theory. The points with question mark correspond to the events with apparent lack of forward-backward symmetry in C.M.S. The numbers beside the points show the number of gray tracks. For the events without gray tracks and for the events with $m < 2$ (gray tracks < 4), nothing is written. The events with $m < 2$ are separately listed. The references are designated: $p25$ etc.: Bristol group [7], D: DEBENEDETTI *et al.* [9], Dm: DEMEUR *et al.* [10], H: HOANG [6], H_p: HOPPER *et al.* [11], P. PICKUP *et al.* [12], S: SCHEIN [13], T: TEUCHER *et al.* [14]. The inelasticities for the events of PICKUP *et al.* are taken to be 1, those of the Bristol group to be their K'.

---

[9] A. DEBENEDETTI, C. M. GARELLI, L. TALLONE and M. VIGONE: *Nuovo Cimento*, **4**, 1142 (1956).

[10] M. DEMEUR, C. DILWORTH and M. SCHÖNBERG: *Nuovo Cimento*, **9**, 92 (1952).

[11] V. D. HOPPER, S. BISWAS and J. F. DARBY: *Phys. Rev.*, **84**, 457 (1951).

[12] E. PICKUP and L. VOYVODIC: *Phys. Rev.*, **84**, 1190 (1951).

[13] R. G. GLASER, D. M. HASKIN, M. SCHEIN and J. J. LORD: *Phys. Rev.*, **99**, 1555 (1955).

[14] K. GOTTSTEIN and M. TEUCHER: *Zeits. f. Naturf.*, **8***a*, 120 (1953).

the impact parameter b. While a certain relation between them is apparent in the experimental plot (cf. Fig. 1) (*), the discrepancy with Fermi's theory is so deep that the conventional procedure to adjust the hot spot volume $4\pi R^3/3$ (to translate the theoretical curve upwards or downwards) does not work.

That the experiments show values for $n_s/[2K(\gamma_c - 1)]^{\frac{1}{2}}$ higher than those expected in the theory, seems to show the inadequacy of Eq. (F.21) and consequently of Eq. (2.2). It seems probable that, in contrast to Fermi's theory, m depends also on γ_c in such a way that the higher value of m does not necessarily correspond to the more distant collision.

Thus, it is shown that Fermi's theory is not adequate for us to infer the impact parameter of each event from the angular distribution. In the next section, we shall provide another method for this purpose.

3. – A method to infer the impact parameter.

The discussion in this Section is very crude, and the method presented is rather heuristic in nature.

(i) To begin with, we shall consider the physical meaning of m introduced in Section **1**. Since m is originally defined to be the power of $\cos\theta$ in the angular distribution of mesons, it may have some relationship to the angular momentum of each meson; the following reasoning will confirm this to some extent and lead us to the conclusion that « the angular momentum of each meson is probably perpendicular to the direction of incidence of a nucleon having initiated the process (this direction is hereafter referred to as z-axis), and the most frequent value (the mode, in the terminology of statistics) of the angular momentum among secondary mesons of the jet in question will be $m\hbar/2$ ».

As described in the introduction, our angular distributions are different from those in the usual scattering experiments which are the average taken over impact parameters. When we restrict ourselves to the event with definite impact parameter, we can, in principle, calculate the wave function of secondary particles using the wave packet for the primary nucleons.

a) Consider a case where the angular part of the wave function for the secondary meson-system is given by

$$\Psi(\theta_1\varphi_1;\,\theta_2\varphi_2;\,\ldots;\,\theta_n\varphi_n) = \sum_{\mathrm{P}} \mathrm{P}\cdot \mathrm{P}_{\lambda_1}^{\mu_1}(\cos\theta_{j_1}) \exp[-i\mu_1\varphi_{j_1}]\cdot \tag{3.1}$$

$$\cdot \mathrm{P}_{\lambda_2}^{\mu_2}(\cos\theta_{j_2}) \exp[-i\mu_2\varphi_{j_2}]\cdot\ldots\cdot \mathrm{P}_{\lambda_n}^{\mu_n}(\cos\theta_{j_n}) \exp[-i\mu_n\varphi_{j_n}]\,,$$

(*) As for the Bristol data (7), their K' is taken for our K.

where $\sum_{\mathrm{P}} \mathrm{P}$ is the symmetrizing operator, $P_{\mu}^{\lambda}(\cos\theta)$, the associated Legendre function. λ's and μ's are assumed to be different from each other. Then the angular distribution of mesons is:

$$\frac{\mathrm{d}n}{\mathrm{d}\Omega} \propto \int \mathrm{d}\Omega_2 \ldots \mathrm{d}\Omega_n |\Psi|^2 , \qquad \propto \sum_i |P_{\lambda_i}^{\mu_i}(\cos\theta)|^2 , \tag{3.2}$$

since the interference term vanishes on account of our assumption.

Alternatively, consider the other extreme case

$$\lambda_1 = \lambda_2 = \ldots = \lambda_n (\equiv \lambda) , \qquad \mu_1 = \mu_2 = \ldots = \mu_n \quad (\equiv \mu) \quad \text{in (3.1), then}$$

$$\frac{\mathrm{d}n}{\mathrm{d}\Omega} \propto |P_{\lambda}^{\mu}(\cos\theta)|^2 . \tag{3.3}$$

In fact, the wave function of secondary mesons may be more complicated than those assumed above; the angular momentum state for each meson may not be pure, and so on. We cannot at present enter into such a discussion. In connection with this, the observation of possible azimuthal anisotropy may be of interest ([15]).

b) Experiments show us that the angular distribution is peaked forwards and backwards, and therefore that we may assume $\mu_i = 0$ (cf. Eq. (3.2), (3.3)). The angular momenta of mesons are thus perpendicular to the z-axis.

c) Owing to the fact that, in experiments, the angular distribution is expressed by the term $\cos^m\theta$ alone, $m/2$ may be interpreted as the λ in Eq. (3.3) or the λ around which the density of λ_i in Eq. (3.2) is greatest. This is the reason why we have called $m\hbar/2$ the most probable angular momentum among secondary mesons of the jet in question.

d) One additional remark. Although $P_{\lambda}^{\mu}(\cos\theta)$ contains also terms $\cos^k\theta$, $k<\lambda$, it is the highest power term $\cos^{\lambda}\theta$ that is responsible for the peaks, forward and backward. And the shape of the angular distribution near $\theta = 0$ or π is important in the determination of the index m, because of the weight factor $\operatorname{cosec}\theta$ in the defining equation (1.2). Thus the neglect of $\cos^k\theta$, $k<\lambda$, and the choice $\lambda = m/2$ is justified (*).

([15]) K. Niu: *Soryusiron-Kenkyu* (Mimeographied circular in Japanese), **7**, 836 (1955); Z. Koba and S. Takagi: *Nuovo Cimento*, **10**, 755 (1958).

(*) Mr. K. Kobayakawa, Osaka University, remarked that we have to pick up the term $\cos^k\theta$ with the greatest coefficient in the expansion $|P_{\lambda}(\cos\theta)|^2$, then to take $m = k$. The change in guess into $\lambda = \alpha m$ ($\alpha =$ some numerical constant other than $\frac{1}{2}$) is not so serious to our present discussion.

ii) Now the knowledge of the total angular momentum of secondary mesons J_M allows a guess on the impact parameter b through the conservation law:

$$Mc\gamma_c \cdot b = J_M \,, \qquad (M = \text{nucleon mass}). \tag{3.4}$$

The left-hand side is the angular momentum of two nucleons in the initial stage, that is still perpendicular to the z-axis. In the right-hand side, the omission of the angular momenta carried off by particles other than mesons may be admitted (*), taking into account the crudeness of our argument.

iii) Let us consider how to obtain the total angular momentum J_M. No detailed mechanism of the production process being as yet known, we cannot but rely upon a probability-theoretical argument (*). According to the theory of random walk ([16]), the probability distribution for the resultant $\boldsymbol{R}$ of N ($\gg 1$) vectors $\boldsymbol{x}_i$ whose magnitudes and directions are randomly distributed over a plane (2-dimensional random walk),

$$W(\boldsymbol{R})\mathrm{d}\boldsymbol{R} = \frac{1}{\pi N\sigma^2} \exp\left[-\frac{R^2}{N\sigma^2}\right] \mathrm{d}\boldsymbol{R} \,. \tag{3.5}$$

That this distribution is characterized only by $\sigma^2 \equiv \langle x_i^2 \rangle_{\mathrm{av}}$ is the merit of our assumption $N \gg 1$.

The most probable value of R is obtained from

$$\frac{\mathrm{d}}{\mathrm{d}R}[2\pi R \cdot W(R)] = 0 \,,$$

as

$$R^* = \sqrt{\tfrac{1}{2} N\sigma^2} \,. \tag{3.6}$$

Now identifying

$$\sigma = \frac{m\hbar}{2} \,, \qquad N = \frac{3n_s}{2} \,, \tag{3.7}$$

we obtain for the most probable resultant angular momentum,

$$J_M = \sqrt{\frac{1}{2}\frac{3n_s}{2}\left(\frac{m\hbar}{2}\right)^2} = \frac{\sqrt{3}}{4} m\sqrt{n_s}\,\hbar \,. \tag{3.8}$$

(*) Cf. K. KOBAYAKAWA's comment, which will be published in the near future.

([16]) K. HUSIMI: *Kakuritsu-ron oyobi Tôkei-ron* (Kawade-Syobô, 1940), p. 215. It is not difficult to take into account the Markoffian correlation, into the discussion of which we have not entered. See loc. cit. p. 260; S. CHANDRASEKHAR: *Rev. Mod. Phys.*, **15**, 1 (1943).

iv) Thus eq. (3.4) gives, as the most probable value (*)

$$b = \frac{\sqrt{3}}{4} \frac{m\sqrt{n_s}}{\gamma_c} \frac{\hbar}{Mc}, \qquad (M\text{: nucleon mass}). \tag{3.9}$$

The impact parameters obtained in this way are found to range from $(1/50)(\hbar/Mc)$ to $10(\hbar/Mc)$, admissible order of magnitude, showing that Eq. (3.9) is sufficiently trustworthy.

Other facts supporting Eq. (3.9) are the systematic functional relations found between b and some other quantities, for example, multiplicity of mesons (see next section).

As to the statistical distribution of the impact parameter over all events observed in the emulsion, b does not seem to obey Prob $(r < b < r + \mathrm{d}r) \propto \propto 2\pi r\,\mathrm{d}r$. It is not yet clear whether this results from the poorness of statistics or more profound nature of the process in question.

When we assume a law $n_s \propto \gamma_c^{\frac{1}{2}} b^{-\alpha}$ partially invoking the statistical theory of multiple production, then

$$m \propto b^{1+\alpha/2} \gamma_c^{\frac{3}{4}} . \tag{3.10}$$

This shows, in contrast to Fermi's theory, that m is not only a function of b, but also an increasing function of γ_c: this agrees with the guess at the end of Section **2**.

4. – The impact parameter and other observable quantities.

In this Section some graphs are presented to show the possible existence of systematic functional relations between the quantities observable in emulsion experiments and the impact parameter introduced in the last section.

Besides the impact parameter, there is another parameter that characterizes the initial condition, the energy of nucleons γ_c; it is therefore desirable to investigate the relation, for example, in the form $n_s = g(\gamma_c, b)$. In the following, we draw graphs with impact parameter b as abscissa and discriminate the energy γ_c by some marks. The dependence on γ_c will be found weaker than that on b.

Since the argument in the last Section was probability-theoretic in nature, so should be the relation of any quantity with b. The fluctuations seen in the graphical representation $n_s = g(\gamma_c, b)$ are definitely smaller than in the usual

(*) As to the events with $m = 0$ see Sect. **5**.

representation $n_s = f(\gamma_c)$. This fact shows the importance of the impact parameter for the analysis of experiments.

The experiments referred to are the same as in Fig. 1.

i) *Multiplicity and impact parameter.* See Fig. 2. The question marks beside the points tell the lack of forward-backward symmetry in the corresponding events. The numbers just after the hyphen mean the number of

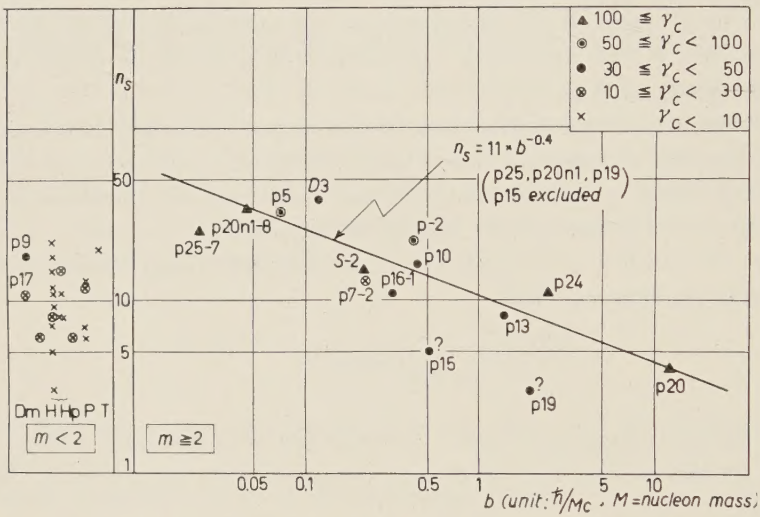

Fig. 2. – The relation between the multiplicity of charged particles n_s and the impact parameter calculated through Eq. (3.9). The experimental materials are the same as those of Fig. 1.

heavy tracks accompanying the events. For example $p25$-7 is accompanied with 7 heavy tracks and is inadequate for our analysis. The events with $m < 2$ are separately listed (*).

The multiplicity (of charged particles) n_s decreases rather systematically with increasing impact parameter b; this is very natural. The deviation of those points with question mark from such a trend may be considered to support, though negatively, our method of analysis. From the graph, roughly,

$$n_s \propto b^{-0.4} .$$

However, this relation should not be taken seriously because of many uncertain

(*) Under the restriction to integer value, m (< 2) must be zero on account of the forward-backward symmetry of the angular distribution.

factors in the argument of Section 3. It is the only aim of this paper to indicate the possible rôle taken by the impact parameter.

ii) *Inelasticity and impact parameter.* – The Bristol group (7) introduced two kinds of inelasticity, K' and K''. K' is defined on the assumption that all the secondary particles are π-mesons with transverse momenta 0.5 GeV/c. K'' is calculated on the same basis but excluding the particles (about 20%) emitted at the smallest forward and backward angles as « x » particles different from π's.

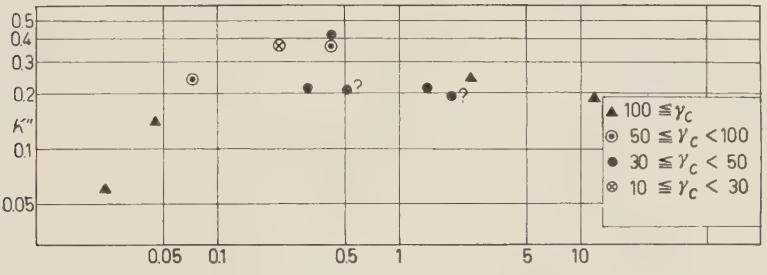

Fig. 3.

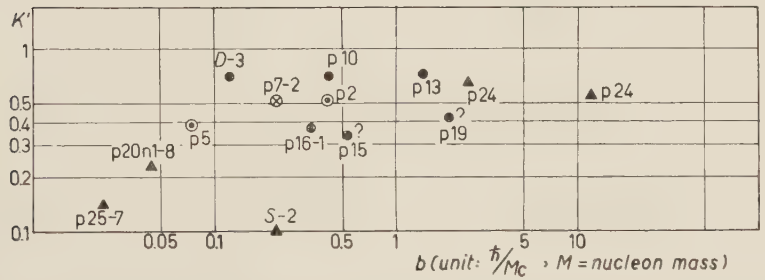

Fig. 4.

Fig. 3 and 4. – The relation between the inelasticity and the impact parameter calculated through Eq. (3.9). The experimental materials are the same as those of Fig. 1. As to the definitions of K' and K'' see the text.

We identify the inelasticities used by authors other than the Bristol group with K'. (See Fig. 3 and 4). We see, in the region of small impact parameter, the fact that the inelasticity decreases with the decrease of the impact parameter; this trend is surprising. However, the fact that this trend is more prominent for K'' makes us surmise the increase in the proportion of « x » particles (*) as the impact parameter decreases. If this is in fact the case, the investigation on high energy collisions will yield some knowledge about nucleon structure.

(*) This terminology was introduced by the Bristol group (7).

5. – The impact parameter and the uncertainty principle.

To introduce the concept of impact parameter, we have to examine its compatibility with the uncertainty principle. We shall, meanwhile, consider the problem in the laboratory system (hereafter abbreviated as L.S.), the z-axis being taken parallel to the direction of incidence of the primary nucleon. Denoting the uncertainty in the position and momentum of the incident nucleon Δx, ...,; Δp_x, ..., respectively, the uncertainty relations are

$$\Delta x \cdot \Delta p_x \gtrsim \frac{\hbar}{2}, \quad \text{etc.} . \tag{5.1}$$

To make the impact parameter b meaningful, the condition $\Delta x < b$ must be satisfied. When the momentum p of the incident nucleon is large enough, Δp may also be large and Δx small, allowing us to use the concept of impact parameter; this is the conventional argument. In addition to the largeness of Δp, however, there must be an appropriate relation among the Fourier amplitudes to realize a small wave packet. (For example, in the non-relativistic theory, to obtain a minimum packet for which $\Delta x \cdot \Delta p_x = \hbar/2$,

$$\psi(x) = \int f(p_x) \exp[ip_x x] \mathrm{d}p_x ,$$

we must take the amplitude $f(p_x)$ to be a function of gaussian type.) As to the realization of the latter relation we know nothing. An observation of position causes the wave packet to contract. But observation with an atom (ionization) is insufficient to localize the nucleon in such a way as to be able to speak of its impact parameter. The idea which arises next is to observe, in the emulsion, many ionized atoms. Does a line suitably drawn to pass them enable us to find the nucleon path more accurately than observing one atom? This does not seem to be the case even when we note that the nucleon in question is extremely relativistic and that the spreading of the wave packet is very slow because of the well known retardation of a moving clock, since the momentum transfer to an atom is very small and randomly oriented for different atoms in emulsion.

Then, how can we understand the regularity found in Section **4**? The present author can't answer this question. In this connection, we remember that the direction of motion can be determined to 10^{-4} radian in the emulsion experiments; this fact implies that $\Delta p_x/p_z$ of a particle traversing emulsion is smaller than 10^{-4}, and that

$$\Delta x \gtrsim \frac{\hbar}{2\Delta p_x} > 10^4 \cdot \frac{\hbar}{2p} = \frac{10^4}{4\gamma_c^2} \cdot \frac{\hbar}{Mc} . \tag{5.2}$$

Thus, for $\gamma_c \sim 100$, the impact parameter (*) *may* be definite to the extent

$$b \sim \frac{\hbar}{4Mc}. \tag{5.3}$$

This fact will afford a basis for the introduction of the impact parameter.

In connection with this, we notice the following facts: there is only one event found with $m \neq 0$ for $\gamma_c < 30$, and few events with $m = 0$ for $\gamma_c > 30$ (**). See Fig. 2. The reader may be perplexed with the fact that the events with $m = 0$ (which would have $b \cong 0$ if Eq. (3.9) were applied) have rather small mutiplicity. The reason is that the events with $m = 0$ are also of low energy. These facts seem to show the inadequacy of the impact-parameter concept for low energy events.

The above arguments show only the possibility of introducing the impact parameter and it should be decided only by further experiments whether or not the nucleon-wave packet is so small as to make the parameter useful.

6. – Conclusions and discussions.

i) The importance of the impact parameter for the description of experimental results in the high energy region is pointed out. In this connection, Fermi's theory with impact parameter is examined. The relation between n_s and m, resulting from this theory, is shown not to be in accord with experiments; and so this theory cannot be used to infer the impact parameters for each event. An alternative method, heuristic in nature, for this purpose is proposed. In spite of the crudeness of reasoning, the impact parameter, calculated in the latter way from experimentally observable quantities, is satisfactory in various respects: (i) admissible order of magnitude

$$\frac{1}{50}\frac{\hbar}{Mc} \lesssim b \lesssim 10\,\frac{\hbar}{Mc}, \qquad (M\text{: nucleon mass}),$$

and, (ii) rather definite functional relations with multiplicity and probably with inelasticity.

(*) For the sake of eliminating the uncertain situation as to the target nucleon, the reader may consider the problem in C.M.S., remembering the Lorentz transformation of angle $\theta_{\text{C.M.S.}} = 2 \cdot \gamma_c \theta_{\text{L.S.}}$.

(**) See footnote on page 754.

The concept of impact parameter is possibly compatible with the uncertainty principle for the high energy region under consideration. However no positive basis that the nucleon wave packet must be small enough could be found.

ii) Now that the importance and utility of the impact parameter for high energy events is established, there arise many possibilities for theory and experiments, the examples of which will be described below.

For experiments, it is interesting not only to confirm the relations mentioned in Section **4**, but also to investigate the composition of secondary particles as a function of the impact parameter. Especially it is interesting to investigate whether there arises a knick-like behavior in the functional relation with b. Isn't there, for example, a sudden increase in the nucleon pair production at some small values of b? This knowledge should contribute much to our understanding of the nucleon-structure.

Theoretically, it becomes possible to treat, as a first step, only events with large impact parameter; a rather easier problem being separated from the complicated whole. This method is the same as that which is advocated by Prof. M. TAKETANI ([17]) and is adopted by Japanese workers on nuclear force problems.

* * *

The author expresses his sincere gratitude to Prof. H. UMEZAWA for his continual guidance. Thanks are also due to the authorities in the Institute for Nuclear Study, University of Tokyo, and the Institute for Fundamental Physics, University of Kyoto for discussions. Especially, the author should like to note here, with grateful recognition, that Prof. Y. FUJIMOTO and J. NISHIMURA have called his attention to the angular distribution problem of high energy jets, and that K. KOBAYAKAWA gave him critical comments. Last but not least, the author expresses his gratitude to the Iwanami Fûjukaj Fellowship for the financial aid.

([11]) M. TAKETANI, S. NAKAMURA and M. SASAKI: *Prog. Theor. Phys.*, **6**, 581 (1951). See also, *Suppl. of Prog. Theor. Phys.*, **3** (1956).

Note added in proof.

(i) Although we have not been able to find any positive basis that a small nucleon wave packet is realized in nature, we may still make some arguments in favour of the concept of impact parameter, from another point of wiew.

When the incident nucleon is duly expressed by plane waves rather than by a wave packet, we may ascribe impact parameter $b = l\hbar/p$ to the partial waves with angular momenta $\sim l\hbar$ (p being the momentum of the nucleon). Doubtful as it may

appear at first sight whether we can ascribe an impact parameter to each event in the emulsion (many partial waves may contribute to the cross section), this doubt will be resolved when we can assume the phase relations to bo very complicated among the matrix elements of those partial waves. Since interferences are destructed, the cross section will be practically identical to that which would be calculated for the « Gemisch » of nucleon states, each of these states belonging to a rather small range of angular momentum. If this is the case, a member of the « Gemisch » corresponds to each event in the emulsion, thus allowing the concept of impact parameter. This is again a characteristic feature of high energy phenomena.

Other points of view will also be possible.

These are essentially the same as the arguments given by Prof. Z. Koba on the Annual Meeting of the Physical Society of Japan (Oct. 1958). Also, the author owes much to the members of the symposium on Interpretation of Quantum Mechanics and Quantum Field Theories (Feb. 1959). To all of them, the author expresses his sincere gratitude.

(ii) We have to note, with great pleasure, that Koba and Takagi's introduction of « classifying variables » is similar in spirit to our introduction of the impact parameter. Their argument is adapted for the framework of field theory. See, Z. Koba and S. Takagi: Fortschritte der Physik, in press.

RIASSUNTO (*)

L'introduzione del concetto di parametro d'impatto nell'analisi degli eventi di alta energia appare possibile ed opportuna. Dimostrando l'insufficienza della teoria di Fermi col parametro d'impatto, proponiamo un'altra via per ricavare il parametro d'impatto per ogni evento in emulsione in base alle grandezze sperimentalmente osservabili. I parametri d'impatto introdotti in tal modo hanno ordine di grandezza ammissibile e, come si dimostra, una abbastanza definita relazione funzionale con la molteplicità dei mesoni il cui diagramma in funzione dell'energia primaria presenta, come è noto, grande fluttuazione. Si discute anche la compatibilità col principio d'indeterminazione.

(*) *Traduzione a cura della Redazione.*

IL NUOVO CIMENTO Vol. XI, N. 6 16 Marzo 1959

Extended Invariance Properties of Quantum Fields.

I. – Lagrangian formalism.

M. E. Mayer (*)

Joint Institute for Nuclear Research - Dubna
Laboratory of Theoretical Physics

(ricevuto il 15 Novembre 1958)

Summary. — This is the first paper from a series in which the consequences of invariance of Quantum Field Theory under an f-parameter Lie group are investigated. Part I deals with the consequences of invariance of a general Lagrangian under such a group. It is shown that the invariance leads to the conservation of f « current density operators », the corresponding charge operators being a representation of the Lie group on the state vector space. Invariance under extended transformations, *i.e.* transformations in which the parameters are functions of the space-time point leads to the necessity of introducing f non-commuting vectors fields. The general structure of the Lagrangian corresponding to these fields is established and their possible physical counterparts are discussed. Part II will contain a similar investigation in the framework of an S-matrix theory, and Part III will be devoted to a detailed classification of possible transformation groups and the corresponding calssification of particle fields and their interactions.

(*) On leave of absence from the Faculty for Mathematics and Physics of the C.I. Parhon University, Bucharest and the Institute for Atomic Physics of the Academy of the Rumanian People's Republic, Bucharest. This work was started at these Institutions in 1956. Present address: Physico-Mathematical Faculty, C.I. Parhon University, Bucharest.

1. – Introduction.

During the last years considerable progress has been made in the study of elementary particle interactions and the selection rules governing them, and there have been several, more or léss successful attempts at theoretical interpretations or classifications of the corresponding interactions, the best-known of which is the GELL-MANN–NISHIJIMA interpretation in terms of the strangeness quantum number, and the various modifications of this scheme.

Although it has been clear that any conservation law in quantum field theory must be the consequence of some invariance property of the fields under investigation, there have been relatively few attempts to study in quite a general form the consequences of the invariance of a theory (we will specify below what exactly is meant by this term) and to investigate the possibility of obtaining all possible fields and their interactions on the basis of the fundamental postulates of quantum field theory and the structure of the admissible transformation groups, which, as will be shown below, are Lie groups which turn out to possess the important (from the mathematical point of view) property of being compact and which are well studied in the mathematical literature.

Such an investigation has been started by the author in 1956 and some of the results obtained have been quoted in an unpublished dissertation [1]. Essentially the same results have been published at about the same time by UTIYAMA [2] and are mostly a generalization of Schwinger's analysis of constant phase transformations and their extension to gauge transformations, which leads to the introduction of the electromagnetic field [3,4]. These results, together with some general properties of the groups which leave invariant the Lagrangian form of quantum field theory, form the contents of Sections 2 and 3 of this paper. It is shown that the « internal degrees of freedom » (as contrasted to the space-time properties) of the fields are such that the « internal space » is a finite dimensional Euclidian space so that the corresponding transformations are orthogonal linear transformations. The invariance of the (quantum) Lagrangian with respect to such transformations leads to the con-

[1] M. E. MAYER: *Some Functional Methods in Quantum Field Theory* (in rumanian). Unpublished Dissertation, Parhon University, Bucharest (1956).

[2] R. UTIYAMA: *Phys. Rev.*, **101**, 1597 (1956).

[3] J. SCHWINGER: *Phys. Rev.*, **91**, 713 (1953); *Proc. Nat. Acad. Sci. U.S.A.*, **44**, 223 (1958).

[4] M. E. MAYER: *Cimpuri Cuantice si Particule Elementare* (in rumanian), (Bucharest, 1959).

servation of f charges, where f is the number of parameters characterizing the given group, and the commutation relations of the corresponding operators coincide with those of the infinitesimal operators of the group, so that the charge operators are a representation of these infinitesimal operators in the state-vector space of the system.

In Section **3** the notion of « extended invariance » is introduced. This means that invariance of the Lagrangian is required not only for transformations in which the parameters are constant in space-time, but also under point-dependent transformations. Physically such a requirement can be motivated by imposing the condition that if a theory is invariant under a group of internal symmetry transformations, this invariance must not depend upon the point of location of the observer, so that two observers in distinct space-time points should be able to carry out independently arbitrary transformations from the group under consideration, without destroying the invariance of the observable quantities. In order to ensure the invariance of the Lagrangian formalism under such extended transformations it becomes necessary to introduce supplementary operator fields (in the same manner as the Maxwell field can be introduced to reestablish the invariance of a charged field Lagrangian, when extending constant phase transformations to gauge transformations). The covariant vector fields introduced in this manner are subjected under our group to generalized gauge transformations of the second kind (3.7). The possible general form of the « free Lagrangian » corresponding to these vector fields is also investigated and it turns out, that it leads to complicated non-linear field equations, which have not been investigated in the general case.

A similar analysis, but in the framework of an S-matrix theory is the subject of Part II of this series and Part III will contain a detailed analysis of the structure of admissible transformation groups with the final scope ot obtaining a classification of « elementary » particles and the structure of the corresponding Lagrangian (this was in part carried out by SCHWINGER ([3])) or S-matrices. This investigation is only a preliminary step to the construction of a quantum field theory in which physically meaningless quantities, such as interacting field operators etc., no longer occur and the basic quantities of the theory are closely connected with group representations and invariant transition amplitudes (in this connection attention must be called to attempts in this direction by SEGAL ([5]), which are however in a much too abstract form as yet).

([5]) I. E. SEGAL: *Proc. Nat. Acad. Sci. U.S.A.*, **41**, 1103 (1955); **42**, 670 (1956) and other mathematical papers to which references can be found there.

2. – Lie Groups, infinitesimal transformations, structural costants and current densities.

We take as our starting point Schwinger's general form of the Lagrangian density ([3,4])

$$L(\chi) = \tfrac{1}{2}[\chi A^{\mu}\partial_{\mu}\chi - \partial_{\mu}\chi A^{\mu}\chi] - H(\chi)\,, \tag{2.1}$$

where A^{μ} are a set of antihermitian matrices and χ sets of hermitian field operators. The matrix indices of A^{μ} refer only to the space-time transformation properties of the operators χ.

In order to be able to describe various physical properties of the particles associated with the fields χ the latter must possess some internal degrees of freedom (*i.e.* they must consist of sets of components suitably labelled) which can be subjected to various transformation groups. The following natural requirements are to be imposed on such « internal transformations »: i) L must be invariant under the transformations of the group G, or at least invariant up to the addition of a divergence; ii) all physically significant relations, such as commutation relations, expectation values of S-matrix elements etc., should also be left invariant. From these requirements it follows immediately that the internal space, *i.e.* the system of components of χ, must have some sort of scalar product defined in it, which shall assure the positive definite character of *e.g.* the anticommutator of fermion operators or the energy density of bosons (cf. also ([6])).

Thus the internal space must be a Riemannian manifold, but if we do not want to get entangled with non-linear field equations it is reasonable to suppose it a finite-dimensional Euclidian space. The corresponding transformations of the internal space are consequently linear orthogonal transformations = rotations.

Consider the f-parameter group of linear transformations of the n-dimensional internal space

$$'\chi_r = \sum_{s=1}^{n} M_{rs}(\lambda_1, ..., \lambda_f)\chi_s\,, \tag{2.2}$$

The infinitesimal operators of this group can be written in the form

$$M_{rs}(\delta\lambda_1, ..., \delta\lambda_f) = \delta_{rs} - i\sum_{a=1}^{f}\delta\lambda_a T^a_{rs} \tag{2.3}$$

([6]) J. Schwinger: *Ann. of Phys.*, **2**, 407 (1957). Cf. also *Proceedings of the 7th Annual Rochester Conference* (1957).

or in obvious matrix notation

$$'\chi = (I - i\delta\lambda_a T^a)\chi \,. \tag{2.4}$$

In order to preserve the Hermitian character of the field operators it is necessary that the matrices T^a be imaginary.

The A^μ commute with the T^a as they refer to different degrees of freedom, so that the invariance requirement on the Lagrangian leads to the Hermitian property of the infinitesimal matrices

$$T^{a\,T} = -T^a \,, \qquad (T^a)^+ = T^a \,. \tag{2.5}$$

Let the structural constants of the group, C_k^{ij} be defined by the f relations

$$[T^i, T^j] = T^i T^j - T^j T^i = \sum_{K=1}^{f} C_k^{ij} T^k, \tag{2.6}$$

with the well known properties

$$\begin{cases} C_k^{ij} = -C_k^{ji} \,, \\ \sum\limits_m (C_k^{im} C_m^{jn} + C_k^{jm} C_m^{ni} + C_k^{nm} C_m^{ij}) = 0 \,. \end{cases} \tag{2.7}$$

A variation of the Lagrangian with respect to λ_a can be put into the form (*)

$$\delta_\lambda L = -i \sum_{a=1}^{f} (\chi A^\mu T^a \chi)\, \partial_\mu \delta\lambda_a(x) \,, \tag{2.8}$$

and defines the current densities

$$j_a^\mu(x) = -i(\chi A^\mu T^a \chi) \,, \qquad a = 1, 2, \ldots, f, \tag{2.9}$$

which satisfy the conservation laws

$$\begin{cases} \int \mathrm{d}^4x\, \partial_\mu j^\mu(x) = 0 \,, \\ Q^a = \int\limits_\sigma \mathrm{d}\sigma^\mu j_\mu^a(x) = \text{const} \,. \end{cases} \tag{2.10}$$

(*) Here $\delta\lambda_a(x)$ are arbitrary functions of the co-ordinates, vanishing on the two limiting spacelike surfaces which intervene in the action principle; cf. for example (4), § 21.

Repeating the usual argument (*e.g.* (4), § 22) it can be seen that

$$[\chi, Q^a] = T^a\chi\,, \tag{2.11}$$

and (2.6) implies

$$[Q^a, Q^b] = \sum_c C_c^{ab} Q^c\,, \tag{2.12}$$

that is, the various charges do not commute in general.

On the other hand, the transformation (2.2) can be expressed as a unitary transformation of the field operators

$$'\chi = M\chi = U^+\chi U\,, \qquad U^+U = UU^+ = I\,, \tag{2.13}$$

with U acting on the state vectors (*e.g.* in the occupation number representation U can be expressed in terms of the creation and annihilation operators). For infinitesimal transformations (2.3) U can be expressed by means of Hermitian operators Q^a in the form

$$U = I + i\sum_a Q^a \delta\lambda_a\,. \tag{2.14}$$

It is easy to verify that the operators Q_a satisfy the commutation relations (2.11) and (2.12) and are thus identical with the operators (2.10). Thus for finite transformations we obtain

$$U = \exp\left[i\sum_a Q^a\lambda_a\right] = \exp\left[i\sum_a \int \mathrm{d}\sigma^\mu j_{l\mu}^a \sigma\lambda_a\right]. \tag{2.15}$$

Now let us consider briefly the structure of the possible transformation groups. As shown in Chapter XI of (7) the Lie algebra of an euclidian space is compact and decomposes into the direct sum of its center (the commutative subgroup) and a set of simple compact non-commutative algebras which are ideals in the original algebra. The vector space of the Lie algebra is unitary with the Hermitian scalar product

$$(a, b) = -\sum C_{\alpha j}^i C_{\beta i}^j a^\alpha b^\beta \equiv g_{\alpha\beta} a^\alpha b^\beta. \tag{2.16}$$

Thus it is sufficient to consider separately commutative and purely non-commutative algebras.

(7) L. Pontrjagin: *Topological Groups* (Princeton, 1939); second russian edition (1953).

The commutative groups, which can be considered as rotations around an axis in the internal space, or alternatively as constant phase transformations have been thoroughly studied in ([3]) and ([4]) and will not be considered here. We only note that the « charges » associated with various phase or gauge transformations commute and can be used for classification of the states of a system (this problem will be treated in detail in Part III of this series of papers). Examples of non-commutative groups have been investigated by different authors ([5-11]), and some special examples will be investigated below (Part III) (*).

3. – Extended group invariance and associated vector fields.

As a generalization of the extension of the group of constant phase transformations that leads to the introduction of the electromagnetic field with its own gauge transformation of the second kind (cf. ([4]), Sect. 22, or SCHWINGER's original work ([3])) we will now consider « extended » transformation groups in which the parameters λ_a are arbitrary functions of the space-time co-ordinates. This extension is based upon the independence of the internal degrees of freedom on the space-time transformation properties and means that we may apply to each space-time point its own internal transformation (**).

Consider the extended transformations

$$(3.1) \qquad {}'\chi(x) = M(\lambda_1(x), \ldots . \lambda_f(x))\,\chi(x) ,$$

or their infinitesimal form

$$(3.2) \qquad {}'\chi(x) = (I - i\sum_a \delta\lambda_a(x) T^a)\chi = \chi(I + i\sum \delta\lambda_a(x) T^a) ,$$

where we have made use of the antisymmetry (2.5) of the matrices T^a. The variation of the Lagrangian has the form

$$(3.3) \qquad \delta_\lambda L = - i\sum_a \chi A^\mu T^a \partial_\mu \delta\lambda_a(x) = \sum_a j^\alpha_\mu(x)\,\partial^\mu \lambda_a(x) ,$$

([8]) C. N. YANG and R. L. MILLS: *Phys. Rev.*, **96**, 191 (1954).

([9]) A. SALAM and J. C. POLKINGHORNE: *Nuovo Cimento*, **2**, 685 (1955).

([10]) B. D'ESPAGNAT and J. PRENTKI: *Nucl. Phys.*, **1**, 33 (1956).

([11]) B. D'ESPAGNAT, J. PRENTKI and A. SALAM: *Nuclear Physics*, **5**, 447 (1958). and *A Tentative Scheme for Weak Interaction*, CERN preprint by the first two authors.

(*) Cf. also S. BLUDMAN: *Nuovo Cimento*, **9**, 433 (1958). [*Note added in proof*].

(**) Essentially the same result was obtained by UTIYAMA ([2]) by means of a less elementary proof. For the special case of the 3-dimensional iso-rotation group the same result has been obtained by YANG and MILLS ([7]).

which is no longer zero, as $\lambda(x)$ does not vanish on the boundary surfaces.

However we can reestablish the invariance of the Lagrangian by introducing supplementary fields U^a_μ and a supplementary term in the Lagrangian, L_1 such that

$$\delta(L + L_1) = 0\,, \qquad L_1 = -\sum_a j^a_\mu U^\mu_a\,. \tag{3.4}$$

It is clearly insufficient to subject the field U^μ_a to the gauge transformations of the second kind known from electrodynamics

$$U^\mu_a \to U^\mu_a - \partial^\mu \lambda_a(x) \tag{3.5}$$

as in this case

$$\delta L_1(\chi, U) = -\sum_a j^a_\mu \partial^\mu \lambda_a(x) + i \sum \chi A_\mu [T^a, T^j] U^\mu_a \lambda_j(x) = \\ = -\sum j^a_\mu \partial^\mu \lambda_a(x) - \sum j^k_\mu(x)\, C^{ij}_k\, U^\mu_i(x) \lambda_j(x)\,. \tag{3.6}$$

The first term cancels with (3.3) and the second cancels only if we subject the vector fields U^μ_a to the generalized gauge transformations of the second kind

$$'U^\mu_a(x) = U^\mu_a(x) - \partial^\mu \lambda_a(x) + \sum C^{ij}_a U^\mu_i \lambda_j(x)\,. \tag{3.7}$$

In order to have a complete description of the U^μ_a-field we must investigate the possible form of the corresponding « free Lagrangian », imposing the natural conditions that it be of the general form (2.1) or reducible to that form by means of introducing suitable supplementary variables (since we are looking for first order equations), and that the Lagrangian be invariant under Lorentz transformations and extended internal transformations (here invariant means as usual, invariance up to possible appearance of expressions in the form of a four-dimensional divergence).

As well known from electrodynamics, or the theory of the Proca field, the supplementary variables needed to obtain first order equations for the vector field. are antisymmetrical tensors of the second rank, so that besides U^μ_a we introduce the f antisymmetrical tensor fields $Z^{\mu\nu}_a$ for which we suppose the following transformation law under the extended transformation

$$'Z^{\mu\nu}_a = Z^{\mu\nu}_a + i \sum_{k,l} C^{kl}_a Z^{\mu\nu}_k \lambda_l\,, \tag{3.8}$$

(there are no terms involving the derivatives of λ_i, because of the antisymmetry). This means that the internal space components of the vector U and the tensor Z transform cogrediently under our group (leaving aside the deri-

vative of λ_a, which for our present purpose can be considered as a « constant »).

Using the well-known facts from the theory of Lie groups, that the structural constants are « tensors » under the transformations of the group, and that, for fixed index a they form a matrix representation of the generators of the Lie group (one can easily verify that the identity (2.7) is just the representation of (2.6) in an f-dimensional Euclidian space with the scalar product defined by (2.16), we are able to write the equations (3.2), (3.7) and (3.8) in the form

$$(3.9)\qquad \begin{cases} {}'\chi_a = \sum_b (\delta_a^b - i \sum_c C_a^{cb}\lambda_c)\chi_b\,, \\ {}'U_a^\mu = \sum_b (\delta_a^b - i \sum_c C_a^{cb}\lambda_c) U_b^\mu - \partial^\mu \lambda_a\,, \\ {}'Z_a^{\mu\nu} = \sum_b (\delta_a^b - i \sum_c C_a^{cb}\lambda_c) Z_b^{\mu\nu}\,, \end{cases}$$

and the « metric tensor »

$$(3.10)\qquad g^{ab} = -\sum_{ij} C_i^{aj} C_j^{bc} = \sum C_i^{aj} C_j^{ib}$$

can be used for lowering or raising internal indices and for forming invariants.

Taking into account all the mentioned facts, we see that the only interesting bilinear Lorentz invariants, linear in the first derivatives of U_a^μ and $Z_a^{\mu\nu}$ are

$$(3.11)\qquad \begin{cases} I_1 = \sum_a (\partial_\mu U_\nu^a - \partial_\nu U_\mu^a) Z_a^{\mu\nu} = \sum_{ab} g^{ab}(\partial^\mu U_a^\nu - \partial^\nu U_a^\mu) Z_b^{\mu\nu}\,, \\ I_2 = \tfrac{1}{2} \sum_a Z_{\mu\nu}^a Z_a^{\mu\nu}\,, \qquad I_3 = \sum_a U_a^\mu \partial^\nu Z_{\mu\nu}^a\,, \\ I_4 = \tfrac{1}{2} \sum_{a,b,c} C_c^{ab}(U_a^\mu U_b^\nu - U_a^\nu U_b^\mu) Z_{\mu\nu}^c\,. \end{cases}$$

These forms are not invariant under the extended group, because of the derivatives of λ_a appearing in (3.9) (they are however invariant, for constant λ_a) but they can be combined so as to yield an invariant, the various terms with derivatives cancelling one another, or by using antisymmetry and neglecting terms of the form of a divergence. By these arguments we are led almost uniquely to the free Lagrangian for the U–Z- field, of the form

$$(3.12)\qquad L(U, Z) = -\tfrac{1}{2}\left[\tfrac{1}{2}\{Z_a^{\mu\nu}, (\partial_\mu U_\nu^a - \partial_\nu U_\mu^a)\} - \{U_{\nu,}^a \partial_\mu Z_a^{\mu\nu}\} - \right.$$
$$\left. - \tfrac{1}{2}\{Z_a^{\mu\nu}, Z_{\mu\nu}^a\} + \tfrac{1}{2}\{Z_{\mu\nu}^c, C_c^{ab}(U_a^\mu U_b^\nu - U_a^\nu U_b^\mu)\}\right],$$

where summation over repeated indices is understood. The first two terms in the Lagrangian can be evidently transformed into one another, up to a divergence. The form (3.12) reduces to the one used by SCHWINGER ([5]) for $C_c^{ab} = 0$.

The resulting field equations (taking into account the coupling with the χ-field through L_1 (3.4)) are non-linear generalization of the Maxwell equations of the form first proposed by YANG and MILLS ([8]).

$$Z_c^{\mu\nu} = \partial^\mu U_c^\nu - \partial^\nu U_c^\mu + \tfrac{1}{2} C_c^{ab}(U_a^\mu U_b^\nu - U_a^\nu U_b^\mu) \tag{3.13}$$

and

$$\partial^\mu Z_{\mu\nu}^a - \tfrac{1}{2} C_c^{ab} \{U_b^\lambda Z_{\lambda\nu}^c - U_\lambda^c Z_b^{\lambda\nu}\} = -j_\nu^a . \tag{3.14}$$

The non-linear character of these field equations leads to great difficulties in analysing their quantum properties, which will not be investigated here. We only want to call attention to the fact, that due to the vanishing of the rest mass of the U–Z field (a term $U_a^\mu U_\mu^a$ would lead to non-invariance of the U-Lagrangian under the extended group) and the existence of the gauge-transformation, not all the components of the U-field will be dynamical variables (the same is well known for the electromagnetic field, which, as yet, is the only U-field known to have a physical counterpart).

As already mentioned in the introduction, the only special cases of U-fields treated in the literature so far, excepting of course the electromagnetic field, are the Yang-Mills B-fields, associated with extended isotopic invariance ([7]) and the gravitational field or more exactly, the field of the Riemann affine connection, which as shown by UTIYAMA, plays the role of the U-field for « extended Lorentz transformations » *i.e.* Lorentz transformations with point-dependent coefficients ([2]) (**). UTIYAMA also called attention to the fact, that in order to obtain the invariant interaction term between the field χ and the new U-field, one has simply to replace the ordinary derivative $\partial_\mu \chi$ by the « covariant derivative »

$$\nabla_\mu \chi = \partial_\mu \chi - i T_a \chi U_\mu^a . \tag{3.15}$$

For the extended Lorentz group this coincides with the usual notion of covariant derivative, and in the case of electrodynamics it reduced to the well known recipe of introducing gauge invariant interaction terms.

(*) UTIYAMA ([2]) has proved that the free Lagrangian of the field can depend only on the combination of U and its derivatives in the r.h.s. of Eq. (3.13). It is evident that our Lagrangian (3.12) differs only by a divergence from the square of this expression. The latter would however lead to second order equations.

(**) Cf. *Note added in proof* on p. 751.

As far as the physical existence of the U-fields is concerned, it must be stressed that one cannot expect to find real particles corresponding to each of them, as not all of the considered invariance properties are strictly universal. For example isotopic rotation invariance is true only as long as electromagnetic effects are being negligible, and so one may doubt the real existence of the Yang-Mills field. On the other hand the conservation laws of baryonic and leptonic charge and the associated invariance properties of the fields are possibly rigorous laws, and should therefore lead to observable U-fields, coupled respectively to the baryons and leptons and possibly to the electromagnetic field. These two fields may in some respects resemble the Z-field, which according to SCHWINGER [5] is responsible for the weak interactions. These questions will be investigated in Part III.

From the point of view of renormalizability, the U-fields lead in general to non-renormalizable non-linear theories, which are difficult to investigate with the usual methods. However, for commutative groups, the difficulties will not be greater than in quantum electrodynamics. This question will also be investigated separately in Part III.

* * *

The author wishes to express his gratitude to Professors D. I. BLOHINČEV and N. N. BOGOLJUBOV, Directors of the Joint Institute and Theoretical Laboratory, respectively, for the kind hospitality extended to him. It is a pleasure to acknowledge the stimulating atmosphere and useful discussions with members of the staff of the J.L.N.R.

RIASSUNTO (*)

Il presente è il primo articolo di una serie in cui si esaminano le conseguenze dell'invarianza della teoria quantistica dei campi rispetto ad un gruppo di parametri f di Lie. La parte I tratta le conseguenze dell'invarianza di un lagrangiano generale rispetto a un tale gruppo. Si dimostra che l'invarianza conduce alla conservazione di f « operatori di densità di corrente », i corrispondenti operatori di carica essendo una rappresentazione del gruppo di Lie nello spazio dei vettori di stato. L'invarianza rispetto alle trasformazioni estese, cioè trasformazioni in cui i parametri sono funzioni dei punti dello spazio-tempo, porta alla necessità di introdurre f campi vettoriali non commutanti. Si determina la struttura generale del lagrangiano corrispondente a tali campi e si discute la loro entità fisica. La parte II conterrà una simile indagine nel quadro di una teoria della matrice S, e la parte III sarà dedicata a una classificazione dettagliata di possibili gruppi di trasformazioni e la corrispondente classificazione dei campi di particelle e delle loro interazioni.

(*) *Traduzione a cura della Redazione.*

IL NUOVO CIMENTO Vol. XI, N. 6 16 Marzo 1959

On K^--Hydrogen Interactions.

W. Alles, N. N. Biswas (*), M. Ceccarelli, R. Gessaroli, G. Quareni
Istituto di Fisica dell'Università - Bologna

M. Göing, K. Gottstein, W. Püschel, J. Tietge, G. T. Zorn (**)
Max-Planck-Institut für Physik und Astrophysik - München

J. Crussard, J. Hennessy
Ecole Polytechnique - Paris

G. Dascola, S. Mora
Istituto di Fisica dell'Università - Parma

(ricevuto il 27 Novembre 1958)

Summary. — Experimental data are given on the interaction of K^--mesons with hydrogen nuclei. These emulsion data do now agree with the new bubble chamber data. They indicate an essentially isotropic angular distribution, both for scattering and for absorption events, a slight decrease of the elastic scattering cross-section with energy and a larger one of the absorption cross-section.

The purpose of the present experiment was to collect further data on K^--Hydrogen interactions in nuclear emulsion, applying fixed criteria for their selection and analysis and uniformly correcting data to reduce to a minimum systematic errors. The interactions studied are elastic scatterings ($K^- + p \to K^- + p$) and absorptions ($K^- + p \to \Sigma^\pm + \pi^\mp$).

(*) At present at University of California Radiation Laboratory, Berkeley.
(**) Now at the Brookhaven National Laboratory.

Four emulsion stacks, each composed of 110 pellicles 3.5 in. $\times$ 5.5 in. $\times$ 600 μm were exposed at the Berkeley Bevatron to the separated Barkas-Heckman K^- beam. The K^- mesons of this beam had a mean energy of 80 MeV.

The scanning procedure consisted in identifying K^- tracks at 3 mm from the front edge where they had a grain density of about 2.5 times minimum and then in following them through the stack until an interaction in flight, a decay or stop in flight, or until the particle comes to rest. A total of 27 300 K^--tracks has been followed.

From those events in which the K^- interacted in flight, the K^--H elastic scatterings or absorptions were recognized by checking carefully angular correlations and consistency of ranges, with the energy balance.

In order to minimize observation biases the following selection criteria have been rigidly applied:

a) For scattering events ($K^- + p \rightarrow K^- + p$):

1) All events in which the range of the proton is $\leqslant 5$ μm irrespectively of the scattering angle have been rejected. The angular cut-off of elastic hydrogen scatterings is therefore a function of the energy of the K-particle. The reason for such a cut-off was to reject a type of event for which the scanning efficiency and the accuracy of angular measurements is low.

2) Events occurring less than 10 μm from either surface of the unprocessed emulsion have also been rejected.

3) If the energy of the K^- at the point of scattering was smaller than 10 MeV, only those events in which the K^- ended in a capture star with at least one heavily ionizing prong were considered. This restriction was introduced in order to eliminate the considerable number of K^- two prongs capture stars at rest which, for a particular range and direction of the outgoing particles may well simulate a very low energy K-p scattering.

b) For absorption events ($K^- + p \rightarrow \Sigma^{\pm} + \pi^{\mp}$).

4) Only events in which the laboratory projected angle between the Σ direction and the incident K^- is $> 10°$ have been considered. In some cases the thin pion track was overlooked during the scanning and hence the event was classified as « single scattering » of a K^--particle. Therefore all the events classified as « single scattering » by the scanner have been re-examined and a careful search for a possible π-track has been made in the angular region suggested by kinematical considerations.

5) Absorptions occurring at a K^- energy of less than 10 MeV have been rejected owing to the difficulty of discriminating them from absorption stars at rest having one thin and one heavily ionizing prong and accidentally fitting the kinematics of an absorption in flight by hydrogen.

6) Events occurring at a distance of $\leqslant 50$ μm from the surface of the unprocessed emulsions have been rejected.

For selection criteria 2) and 6) the correction is straightforward; for 3) the correction coefficient is given by the fraction of the K^- stars leading to capture stars with $N_h \geqslant 1$. This fraction has been taken equal to 22% from ref. (1).

The correction for the selection criterion 4) has been applied assuming the angular distribution in c.m.s. of the absorption events to be isotropic. The observed frequencies of absorption have finally been increased by 10% in order to take into account the loss of fast pions.

To the data collected during this experiment we have also added those previously obtained by the Göttingen group (1), after having applied the selection and correction criteria given above. We are then left with a total of 135 scattering and 47 absorption events.

In Table I we have listed the track lengths followed in different energy intervals and the corrected number of events of the two types.

The observed number of events are given in brackets.

TABLE I.

Energy interval (MeV)	Track length followed (meter)	Number of events		Cross-section (mb)	
		Elastic	Inelastic	Elastic	Inelastic
0—10	22.4	4.21 (3)	cut-off region	58.5±33.8	—
10—20	54.2	10.34 (10)	8.65 (6.5)	59.4±18.8	46.15±11.9
20—30	80.6	13.97 (13.5)	11.35 (8.5)	53.9±14.7	
				56.1±11.6	
30—40	107.2	22.76 (22)	6.65 (5)	66.0±14.1	25.7 ± 6.65
40—50	134.0	20.68 (20)	13.30 (10)	48.0±10.7	
				56.0± 8.65	
50—60	160.0	21.20 (20.5)	11.97 (9)	41.2± 9.1	18.4 ± 4.75
60—70	177.0	24.81 (24)	7.98 (6)	43.6± 9.9	
				42.4 ± 6.4	
70—80	143.5	20.69 (20)	2.00 (1.5)	44.9±10.0	5.25± 3.7
80—90	14.57	2.07 (2)	0.67 (0.5)	44.2±31.3	
				44.7 ± 9.5	

(1) W. ALLES, N. N. BISWAS, M. CECCARELLI and J. CRUSSARD: *Nuovo Cimento*, **6**, 571 (1957).

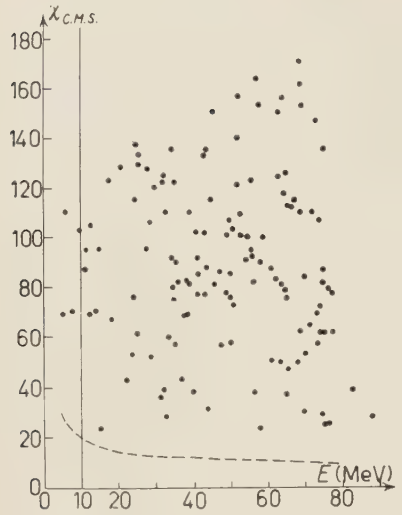

Fig. 1.

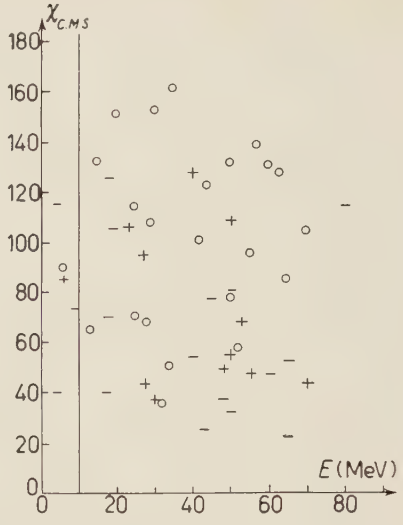

Fig. 2.

In Fig. 1 the c.m. angle and energy of the K^- for each elastic scattering on hydrogen is represented by one point. The dotted line corresponds to the 5 μm cut-off mentioned above.

Fig. 2. shows the corresponding results for K^- absorption. The angles plotted are those between the directions of motion of the K^- and the π in the c.m.s. The sign of the Σ is shown; open circles correspond to the events leading to Σ's of undetermined sign.

Fig. 3 and 4 show the cross-section versus energy for absorption and for scattering events.

In the same figures are also shown the curves calculated by DALITZ [2] fitting the low energy

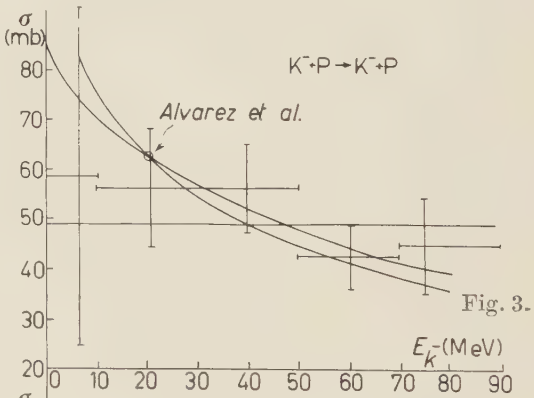

Fig. 3.

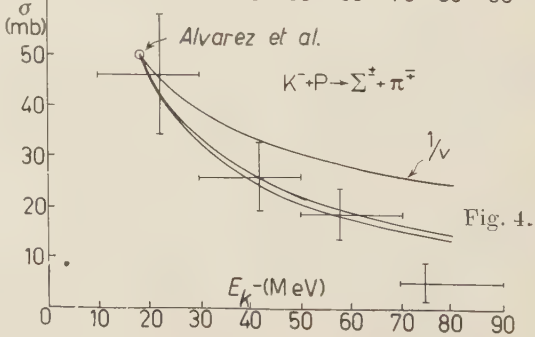

Fig. 4.

(2) R. H. DALITZ: *Report of the VIII Annual Conference on High Energy Physics*, Geneva (1958), p. 190.

bubble chamber point [3] by means of the zero range approximation treatment proposed by JACKSON *et al.* [4] for a purely S state interaction.

In Fig. 5, 6 and 7 the c.m.s. angular distributions of elastic scattering for three K^- energy intervals and in Fig. 8 the angular distribution of absorption events of all energies are represented. These results indicate:

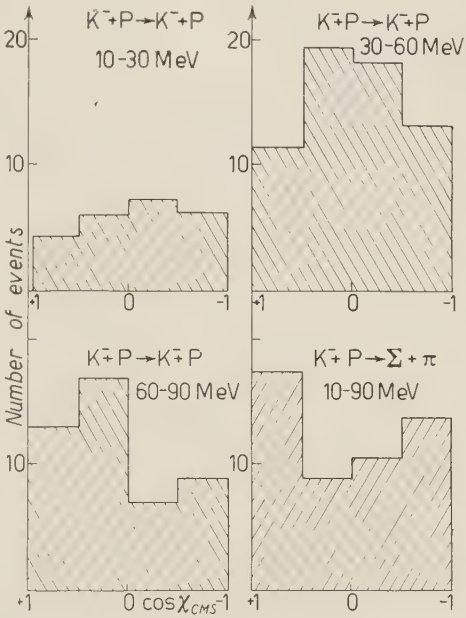

Fig. 5. Fig. 6. Fig. 7. Fig. 8.

1) A slight decrease of the scattering cross-section and a stronger than $1/v$ decrease of the absorption cross-section with increasing K^- energy; in good agreement with the calculated curves.

2) An essential isotropy of the scattering and absorption angular distributions; above 60 MeV one may notice a certain forward peaking in the scattering angular distribution.

These features seem to be also present in the collected data of other emulsion groups, and in those of the Berkeley hydrogen bubble chamber [2].

[3] *Report of the VIII Annual Conference on High Energy Physics*, Geneva (1958), p. 176-178.

[4] J. D. JACKSON, D. G. RAVENHALL and H. W. WYLD: *Nuovo Cimento*, **9**, 834 (1958).

RIASSUNTO

Si presentano risultati sperimentali sull'interazione di mesoni K negativi con nuclei di idrogeno. Questi dati, ottenuti con emulsioni nucleari, sono in accordo con i nuovi dati di camere a bolle. Essi indicano una distribuzione angolare essenzialmente isotropa sia per eventi di diffusione elastica che di assorbimento, una leggera diminuzione coll'energia della sezione d'urto di diffusione ed una più forte diminuzione della sezione d'urto d'assorbimento.

The Electric Dipole Moment of Elementary Particles.

R. L. Garwin

IBM Watson Lab. and Dept. of Physics, Columbia University - New York

L. M. Lederman (*)

CERN - Geneva

(ricevuto il 12 Dicembre 1958)

Summary. — The detection of electric dipole moments (EDM) of elementary particles is discussed and a new limit to the size of the electron EDM is presented ($\lesssim e \cdot 1.5 \cdot 10^{-15}$ cm). This result is used in a discussion of recent observations of positronium annihilation.

1. – Introduction.

It is still of considerable interest in the testing of time-reversal invariance and parity conservation to attempt to detect the electric dipole moment (EDM) of an elementary particle. The existence of an EDM implies non-invariance under time reversal and non-conservation of parity ([1-5]) and its absence under

(*) J. S. Guggenheim Fellow, 1958-59. Permanent address: Department of Physics, Columbia University, New York.

([1]) E. M. Purcell and N. F. Ramsey: *Phys. Rev.*, **78**, 807 (1950); J. Smith, E. M. Purcell and N. F. Ramsey: *Phys. Rev.*, **108**, 120 (1957).

([2]) L. Landau: *Žu. Éksper. Teor. Fiz.*, **32**, 405 (1957); *Nucl. Phys.*, **3**, 405 (1957).

([3]) T. D. Lee and C. N. Yang: *Elementary Particles and Weak Interactions*, BNL 443 (T-91) (1957), p. 17.

([4]) N. F. Ramsey: *Phys. Rev.*, **109**, 225 (1958).

([5]) D. Berley, R. L. Garwin, G. Gidal and L. M. Lederman: *Phys. Rev. Lett.*, **1**, 144 (1958).

a severe test is a sensitive indication of invariance of the particle under space reflection or time reversal (6).

SMITH, PURCELL and RAMSEY (1) in an atomic beam resonance experiment have set an upper limit to the electric dipole moment of the neutron. Their result is $D_n < 10^{-20}$ cm where D_n multiplied by the electric charge gives the dipole moment. Since we know that parity is not conserved, we may regard this measurement as showing that $|F|^2 \cdot |G|^2 < 3 \cdot 10^{-13}$, where G is the probability amplitude for parity mixing (which may be large), and F is the relative amplitude non-invariant under time reversal (*).

Motivated by the desire to find some difference between the muon and the electron other than the rest mass, a search has been made for a muon electric dipole moment with the following result (5):

$$D_\mu \lesssim 10^{-15} \text{ cm} . \tag{1}$$

A discussion (7) of the effects of a possible electron electric dipole moment in the spectroscopy of the hydrogen atom led to the results (this applies equally well to the proton):

$$D_e \lesssim 10^{-13} \text{ cm} . \tag{1}$$

Recent reports (7) of the observation of effect proportional to $\boldsymbol{\sigma} \cdot \boldsymbol{E}$ in positronium have led us to a further examination of this question. We call attention in this note to three points:

i) Many proposed experiments designed to detect the electric dipole moment of charged particles are based on the incorrect notion that it is, in practice, possible to apply an electric field to such a particle without the consequent free acceleration implied by Newton's second law.

ii) There exist in the literature, data on the behaviour of free electrons which enable a more sensitive limit than (2) to be found for the electron EDM. This type of experiment may be improved by an additional order of magnitude.

iii) The limit thus set makes it extremely unlikely that intrinsic electric moments are responsible for the « $\sigma \cdot E$ » effect observed in positronium.

---

(6) I. ZEL'DOVICH: *Journ. Exp. Theor. Phys.*, **6**, 1148 (1958). Translation. This illuminating paper discusses the connection between electric moments and asymmetric decay.

(*) Alternatively, $|E|^2 < 3 \cdot 10^{-13}$, where E is that amplitude which introduces *both* parity and time-reversal mixing.

(7) G. FEINBERG: *Phys. Rev.* (to be published).

(8) F. OBENSHAN and L. PAGE: *Phys. Rev.* (to be published).

2. – Analysis of some incorrect experiments.

Many experiments have been performed or proposed for the measurement of the EDM of charged particles. These generally run into a difficulty which does not exist for neutral particles [1]. The problem caused by the charge is simply that to measure an EDM one must apply an electric field at the particle in order to generate an interaction energy for the parameter being observed. A charged particle cannot exist unaccelerated in an electric field. However, charged particles in matter have time-averaged motions which are either rest or uniform (drift) velocity with respect to the applied electric field. Such arrangements have essentially no sensitivity to EDM. The essential reason is that all forces acting on the particle in matter are electrical. For example, the mobility of ions in liquids is well known to be of the order $\sim$ some cm/s per kV/cm of applied field. Charged particles, *e.g.* ions in the liquid, move at constant velocity in *zero average field* since the electric drag exerted by the medium exactly equals the applied field. Thus, for example, proposals to observe a shift in the resonant frequency in nuclear magnetic resonance carried out in the presence of a strong electric field, *i.e.* observing the parameter d in $(\mu \cdot H + d\sigma \cdot E)$, fail because the nucleus shifts to the new minimum in the total electric potential which it experiences. Quantum mechanical considerations do not alter the conclusion that the charged particle must be accelerated by the applied field in order to detect the EDM (*).

3. – EDM of the free electron.

It happens that an experiment has been performed for quite a different purpose which has considerable sensitivity to the electron EDM. This is the anomalous g-factor experiment of Pidd, Louisell and Crane [9]. In this experiment electrons polarized normal to a uniform magnetic field are caused to execute a large number ($\sim 10^7$) of orbital revolutions in a magnetic field. The vertical plane precession induced by the supposed EDM builds up only for a single half-period of the anomalous moment precession before decreasing again, since thereafter the spin points in the opposite sense in the orbit plane. However, no significant reduction in polarization is observed thereby setting

(*) W. Paul however notes that a second order effect may be observed in a strong electric field gradient. In this case the resultant electric field is proportional to the EDM times the field gradient.

[9] R. W. Pidd: *Bull. Am. Phys. Soc.*, **7**, 364 (1958) and private communication. See also H. R. Crane, R. W. Pidd and W. H. Louisell: *Phys. Rev.*, **91**, 475 (1953).

a limit on the electric dipole moment equal to that of the anomalous magnetic moment ($v/c \approx 1$):

$$D_e \lesssim \frac{\alpha}{2\pi}\left(\frac{\hbar}{mc}\right),$$

$$\therefore D_e \lesssim 3 \cdot 10^{-14} \text{ cm}.$$

A quite different calculation can be made using the results of this experiment. An electric dipole moment of magnitude ε times the *anomalous* magnetic moment would change the anomalous precession period by a factor $\simeq 1 + \varepsilon^2/2$. This can be seen by treating the EDM precession in the electric field $(v/c) \times H_0$ as if a rotating magnetic field of magnitude $(\alpha\varepsilon/2\pi)(v/c)H_0$ were applied and EDM $= 0$. In the CS rotating with the cyclotron frequency we observe two stationary orthogonal fields: $(\varepsilon\alpha/2\pi)(v/c)H_0$ and $H_0 - (\omega/\gamma) = (\alpha/2\pi)H_0$. Since this experiment agrees with measurements of the anomalous moment of the bound electron ([7]) and with theory to within at least 10^{-3} of the anomalous moment, we find immediately that

$$D_e \lesssim 1.5 \cdot 10^{-15} \text{ cm}. \tag{3}$$

A further increase in sensitivity can be obtained by a direct analysis by Mott scattering of the out-of-plane polarization for electrons which have been stored in the magnetic field for $\frac{1}{4}$ and $\frac{3}{4}$ periods of the anomalous precession. A measurement to 1° would yield a sensitivity $D_e \cong 10^{-16}$ cm.

4. – $\sigma \cdot E$ effect in positronium.

In this experiment, an effect is observed when positronium is formed by polarized positrons in a 15 kV/cm electric field ([8]). The effect (a change in the detected rate of 2-quantum annihilation) has the symmetry $\sigma \cdot E$. We only comment here on the impossibility of this effect being due to intrinsic EDM of the elementary particles as limited by (3) (we invoke the CPT theorem here only to similarly restrict the EDM of the positron). The argument is independent of the details of the experiment and is made as follows. The maximum interaction energy produced by the electric field is, using (3)

$$eD_eE \lesssim (5 \cdot 10^{-10})(10^{-15})(50) = 3 \cdot 10^{-23} \text{ erg}.$$

The corresponding angular frequency of the free oscillations between eigenstates of the perturbed system is thus

$$\omega \sim \frac{eD_eE}{\hbar} \lesssim 3 \cdot 10^4 \text{ s}^{-1}.$$

Since this corresponds to a period considerably longer than the lifetime of triplet positronium ($\sim 10^{-7}$ s) the maximum *amplitude* of such a presumed intrinsic EDM effect is

$$\lesssim (10^{-7})(4 \cdot 10^{4}) = 4 \cdot 10^{-3}$$

which is far from the 5% effect observed. This is certainly an absolute maximum, since detailed calculation of matrix elements, symmetry considerations, etc., can only reduce the effect. Thus, if the effect should turn out to actually have the symmetry $\boldsymbol{\sigma} \cdot \boldsymbol{E}$ (and not be a $\boldsymbol{p} \cdot \boldsymbol{E}$ effect masquerading as $\boldsymbol{\sigma} \cdot \boldsymbol{E}$ because of the $\boldsymbol{\sigma} \cdot \boldsymbol{p}$ correlation in weak interactions [8]) it would have to be attributed to the interactions involved in positronium formation and decay.

* * *

One of us (LML) would like to thank CERN for hospitality, and I. Halpern and A. Peterman for useful discussions.

RIASSUNTO (*)

Si discute la rivelazione dei momenti di dipolo elettrico (EDM) delle particelle elementari e si ottiene un nuovo limite della grandezza dell'EDM dell'elettrone ($\lesssim e \cdot 1.5 \cdot 10^{-15}$ cm). Si usa tale risultato nella discussione di recenti osservazioni dell'annichilamento del positonio.

(*) *Traduzione a cura della Redazione.*

A New Method for the Measurement of Relative Multiple Scattering on High Energy Electron Pairs.

R. Weill (*)

Laboratory of Nuclear Studies, Cornell University - Ithaca, N.Y.

(ricevuto il 12 Dicembre 1958)

Summary. — The limitation of the « dipole effect » (electron-positron screening) as a method for determining the energy of electron pairs in nuclear emulsion is discussed. It is then shown that the multiple scattering, which is mainly responsible for the separation of the trajectories at a great distance from the origin ($\sim$ 1 mm) can be evaluated from the measurement of the « geometrical effect ». This phenomenon is studied experimentally on electron pairs of energy between 0.6 and 1 GeV, for trajectory separations up to 0.6 μm.

1. – Introduction: dipole and geometrical effects.

Perkins first observed [1] that the grain density on the initial track of high energy electron pairs is less than two times the value of a plateau track and increases slowly to reach this value. He attributed this phenomenon to a screening effect of the two electrons (*Dipole effect*). The calculations by several theoreticians [2-5] of the ionization of such a dipole were found to be in agreement with the experimental observations [6-8]. The grain density

(*) On leave of absence from « Laboratoire de recherches nucléaires E.P.U.L. », Lausanne.

(1) D. H. Perkins: *Phil. Mag.*, **46**, 1146 (1955).

(2) A. E. Čudakov: *Compt. Rend. Acad. Sci. U.R.S.S.*, **19**, 651 (1955).

(3) G. Yekutieli: *Nuovo Cimento*, **5**, 1381 (1957).

(4) I. Mito and H. Ezawa: *Progr. Theor. Phys.*, **18**, 437 (1957).

(5) G. H. Burkhardt: *Nuovo Cimento*, **9**, 375 (1958).

(6) W. Wolter and M. Mięsowicz: *Nuovo Cimento*, **4**, 648 (1956).

(7) J. Idaware: *Phil. Mag.*, **3**, 680 (1958).

(8) A. A. Varfolomeev: Private communication.

starting from the value zero at the origin rises to about 1.8 times the plateau density at a point where the separation between the two trajectories is about $3 \cdot 10^{-3}$ μm. From this point on the two electrons can be considered as independent for the ionization processes.

However, it was shown ([9,10]) that another phenomenon appears then, following the dipole effect. The blob density on the electron pair track, at the point where the dipole effect stops, is only 1.5 times the plateau density and increases to two times, even though the ionization of the two electrons is now twice the plateau. The blob density is much more sensitive to this new phenomenon than the grain density. This change of the track structure was called *geometrical effect*, and is related to the fact that two electrons can cross the same grains. A part of the energy released in the grains is then lost for the photographic process. The measurement of the geometrical effect on 7 cosmic electron pairs of energies between 10 and 100 GeV gave results in agreement with the prediction of a three dimensional model of track formation ([9,10]).

2. – Measurement of the pair aperture through the dipole effect.

It has been proposed to use the dipole effect as a method for the determination of the angular aperture of high energy electron pairs. The Borsellino relation ([11]) can then give a most probable value for the energy of the photon. However, it was pointed out in a previous work ([10]) that an angular measurement cannot be performed at a distance from the origin of the pair greater than 1 mm because after such a length the separation between the two electron trajectories is due mostly to multiple scattering. This means that the use of the dipole effect for angle determination will be useless for pairs above an energy which can be calculated in the following way.

We can admit that an initial electron pair track can be recorded, provided its grain density is greater than 0.3 times the plateau density. According to the Čudakov dipole theory ([2]) this corresponds to a trajectory separation of about $2 \cdot 10^{-6}$ μm. In order that the ionization variation be measured with enough accuracy, it is necessary to record at least 200 grains on the track segment starting from the point where the separation is $2 \cdot 10^{-6}$ μm, and ending 1 mm after the (unknown) origin. In the case of normal G-5 emulsions, with about 20 blobs/100 μm for a plateau track, the integration of the Čudakov relation shows that this requirement is not fulfilled for aperture angles of

---

([9]) R. Weill, M. Gailloud and P. Rosselet: *Nuovo Cimento*, **6**, 413 (1957); **6**, 1430 (1957).

([10]) R. Weill: *Helv. Phys. Acta*, **31**, 641 (1958).

([11]) A. Borsellino: *Phys. Rev.*, **89**, 1023 (1953).

less than 10^{-6} radians. This means that the angle measurement by means of the dipole effect is *impossible for photons of more than* 10^3 GeV. The hypersensitized Bogomolov emulsions with 105 grains/100 μm at plateau ([12]) should give the possibility of reaching 10^6 GeV.)

3. – The use of the geometrical effect for the measurement of the multiple scattering.

It would then be natural to use the dipole effect for the measurement of the multiple scattering (see Sect. 4). However, this can be done more successfully with the help of the geometrical effect, which occurs for such cases in the region where the separation is due mostly to multiple scattering. The measurement of this effect will then provide a measurement of the multiple scattering. Suppose that the variation of the track structure (blob density and/or mean gap length) as a function of the separation of the trajectories is known and represented by a « calibration curve ». We can then measure the length L over which the blob density changes by a given amount for a pair of unknown energy. The calibration curve will give us the variation ΔY of the lateral separation of the trajectories over the length L. From these two data, L and ΔY, we have to estimate the energy of the photon $K = E_+ + E_-$. The relative projected lateral displacement due to multiple scattering can be considered as determined by a Gaussian distribution. The probability of having a separation between ΔY and $\Delta Y + \mathrm{d}Y$ will be

$$P(\Delta Y)\,\mathrm{d}Y = \frac{K_e}{\sqrt{2\pi} b L^{\frac{3}{2}}} \cdot \exp\left[- \frac{\Delta Y^2 K_e^2}{2 b^2 L^3} \right],$$

where

$$1/K_e = \sqrt{1/E_+^2 + 1/E_-^2},$$

b is the multiple scattering constant. The principle of « maximum likelihood » tells us that the best value K_e^* we can attribute to K_e in our measurement is that for which:

$$\frac{\partial \log P}{\partial K_e} = 0 .$$

This gives:

$$K_e^* = \frac{b L^{\frac{3}{2}}}{\Delta Y} .$$

([12]) C. Bogomolov: *Congrès International de Photographie Corpusculaire*, Montreal (August 1958).

4. – The uncertainties and the limits of the method.

The first uncertainty in the determination of K_e^* arises from the error in the blob number, caused by statistical fluctuations. This corresponds in some way to the reading error (noise) which occurs in normal multiple scattering measurements. It can be reduced to less than 5% for pairs of more than 20 GeV for which the available length is greater than 1 mm.

The « statistical inaccuracy » on K_e^* will be defined by the two intervals $\Delta' K_e$ and $\Delta'' K_e$ such that the likelihood function P drops by a factor of two for $K_e = K_e^* + \Delta' K_e$ or $K_e^* - \Delta'' K_e$. For one cell the accuracy will be characterized by $K_e^{*\,+.50K_e^*}_{\,-.70K_e^*}$. For photons of more than 10^2 GeV the rapid development of the initiated shower (appearing mostly as pseudo or real tridents on the initial track of the pair) will leave only about 1 cm for the measurements. But on such a length the geometrical effect can be studied with a maximum of 3 cells (not more, in order to keep the blob density fluctuations low enough). The statistical accuracy will then be given by $K_e^{*\,+.50K_e^*}_{\,-.41K_e^*}$; for two cells the accuracy will be given by $K_e^{*\,+.63K_e^*}_{\,-.50K_e^*}$. The statistical accuracy must of course be combined with the statistical error on blob counts, and the number of cells used (1, 2 or 3) should be adjusted to the available length in a way which minimizes the total error.

The proposed method is free of the stage and grain noise inherent in the normal multiple scattering measurements.

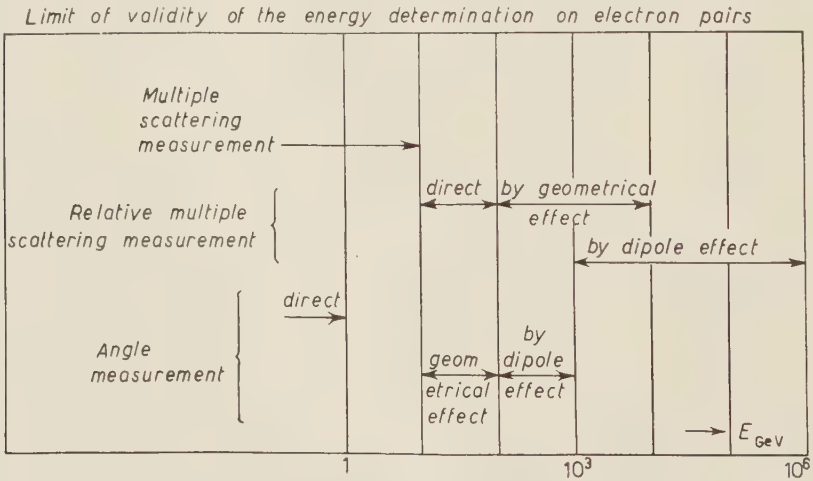

Fig. 1. – Limits of application of the different methods of electron pair energy measurement.

This method, however, is not applicable to pairs of more than 10^4 GeV. For this energy the geometrical effect will begin 1 cm after the origin. But

then the dipole effect can be used for the measurement of the multiple scattering. However, it is easy to calculate that in this case, admitting the necessity of recording at least 200 grains, the dipole method could not be useful for angles of less than 10^{-9} radians (K_e = about 10^6 GeV). The limit will be about 10^{-10} radians with Bogomolov emulsions. This value seems to be the highest electron pair energy measurement directly accessible with nuclear emulsions. We give in Fig. 1 the limits of application of the different methods of electron pair energy measurement.

5. – Measurement of the geometrical effect (calibration curve).

We have measured the geometrical effect on 76 electron pairs recorded in Ilford G-5 emulsions exposed to the photon beam of the Cornell synchrotron. The measurements were performed on electron pairs for which the initial unresolvable track was at least 90 μm in length (pairs of about 600 to 1000 MeV). For such an energy the dipole effect is effective for only about 1 μm. The tracks were divided into cells of 30 μm and the blob count was done for each cell. The projected separation of the two electron trajectories at the middle of each cell was deduced from the measured projected opening angle of each pair. (In this photon energy range the influence of the multiple scattering is negligible ([10]).) We have averaged the individual measurements, grouping the data in classes according to the trajectory separation. (The width of a class is 0.1 μm.) Fig. 2 shows the variation of the blob density of electron pairs relative to the plateau track, as a function of Y, the projected separation of the trajectories. The errors quoted are the r.m.s. deviations. We have also reported on this graph the point obtained by averaging the measurements done by VARFOLOMEEV ([8]) at the beginning of the geometrical effect on 9 pairs whose energy range was from 10^2 to $3 \cdot 10^3$ GeV. These data were obtained in NIKFI R emulsions, whose characteristics, before and after processing, are similar to those of the G-5 used in our work.

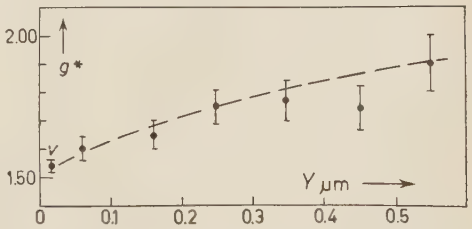

Fig. 2. – g^* (blob density relative to plateau) as a function of the projected separation Y μm of the trajectories. V is the average of Varfolomeev's measurements on 9 cosmic pairs ([8]). Errors are r.m.s. deviations.

The geometrical effect starts with a blob density relative to the plateau of 1.55. This is in fairly good agreement with the value predicted by our three

dimensional model ([9,10]) (1.55 to 1.60). Calibration against plateau tracks was done in all the plates (same batch and processing) in all the regions where the measurements were performed. All the measurements were taken in a layer situated 50 μm from the surfaces of the emulsions.

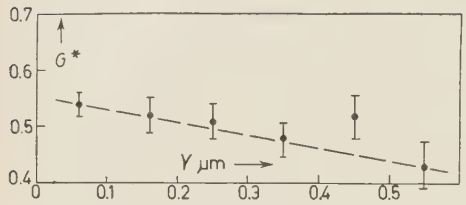

Fig. 3. – G^* (mean gap length relative to plateau) as a function of the projected separation Y μm of the trajectories. Errors are r.m.s. deviations.

We give also (as an indication) the variation of the mean gap length as a function of Y, as deduced from the measurements of 50 pairs (Fig. 3).

6. – Influence of the processing on the calibration curve.

The emulsions used for this work were Ilford G-5, with the following characteristics:

Plateau track:	Blob density:	$g = 20/100\ \mu m$
	Mean gap length:	$G = (4.35 \pm 0.08)\ \mu m$
	Mean track diameter:	$D = (0.71 \pm 0.02)\ \mu m$.

Let us call d_0 the mean grain diameter in the unprocessed emulsion. We define, according to O'Ceallaigh ([13]), a factor f which can characterize the processing by:

$$D = d_0(1 + f) .$$

The three dimensional model enables us to calculate the influence of the processing on the calibration curve. For two different processings characterized by f_1 and f_2, the ratio of the relative blob densities will be according to the relation (5) of reference ([10]):

$$g_1^*/g_2^* = \exp\left[-\alpha(P_{2d}(Y) - P_{1d}) \cdot (f_1 - f_2)\right] .$$

The definitions of the symbols are given in reference ([10]). Using the fact that $P_{2d} < 2 \cdot P_{1d}$, and the experimental value of $P_{1d} = 0.09$ we obtain:

$$g_1^*/g_2^* \cong \exp\left[-0.09\,(f_1 - f_2)\right] .$$

([13]) C. O'Ceallaigh: *Suppl. Nuovo Cimento*, **12**, 412 (1954).

For a given standard processing, f varies less than 5%. This means that the calibration curve will change by an amount less than 1%. For extreme cases, for which f goes from 1.36 to 1.79 the calibration curve would be changed by less than 3%. The three dimensional model predicts that the calibration curve for the mean gap length should be independent of the processing.

* * *

We wish to thank Professors G. Cocconi and J. Orear for many helpful discussions and Mrs. L. Van Nest for her help in the measurements.

RIASSUNTO (*)

Si discutono i limiti dell'efficacia dell'« effetto di dipolo » (schermo elettrone-positone) come mezzo per determinare in emulsione nucleare l'energia di coppie di elettroni. Si mostra quindi come lo scattering multiplo, che è la causa principale della separazione delle traiettorie a grande distanza dall'origine ($\sim$ 1 mm) possa essere calcolato dalla misura dell'effetto « geometrico ». Si studia sperimentalmente il fenomeno su coppie di elettroni di energia fra 0.6 e 1 GeV per separazioni di traiettorie fino a 0.6 μm.

(*) *Traduzione a cura della Redazione.*

On the Decay of Xenon 133.

S. Jha, H. G. Devare, M. Narayana Rao and R. M. Singru
Tata Institute of Fundamental Research - Bombay

(ricevuto il 17 Dicembre 1958)

Summary. — The γ-rays from ^{133}Xe have been studied in a scintillation spectrometer. The γ-rays have the energy of 80 keV, 160 keV, 300 keV and 380 keV with the relative intensity 1, $1.4 \cdot 10^{-2}$, $8.4 \cdot 10^{-4}$ and $4.3 \cdot 10^{-4}$. By studying the 80 keV γ-rays in coincidence, the relative intensity of the cascade and the cross-over transition from the 160 keV state has been found. Taking this into account, the log *ft* values for the β-transition to the 80 keV, 160 keV and 380 keV states have been calculated to be 5.6, 7 and 5.7 respectively.

1. – Introduction.

^{133}Xe has been known to decay from its ground state (spin $\frac{3}{2}^+$) with a half-life of 5.3 days emitting a single group of β^--rays of maximum energy of 346 keV ([1]). This decay leads to the first excited state of ^{133}Cs at 80 keV ([1,2]). The isomeric state of this isotope (spin $\frac{11}{2}^-$) decays by the emission of a 233 keV γ-ray. Recent studies of ^{133}Ba ([3-6]), the ground state of which is $\frac{1}{2}^+$, have shown that the electron capture decay of this isotope excites the levels in ^{133}Cs at 80 keV, 160 keV, 381 keV and 437 keV. The levels at 80 keV, 160 keV and

([1]) I. Beegstrom: *Ark. Fys.*, **5**, 191 (1952); **7**, 255 (1954).
([2]) D. Strominger, J. M. Hollander and G. T. Seaborg: *Rev. Mod. Phys.*, **30**, 585 (1958).
([3]) B. Crasemann J. G. Pengra and I. E. Lindstrom: *Phys. Rev.*, **108**, 1500 (1957).
([4]) R. K. Gupta, S. Jha, M. C. Joshi and B. K. Madan: *Nuovo Cimento*, **8**, 48 (1958).
([5]) S. D. Koicki *et al.*: *Bull. Inst. Nuclear Sciences « Boris Kidrich »*, **8**, No. 144, (March 1958).
([6]) M. G. Stuart, D. C. Lu and F. M. Clikeman: *Bull. Am. Phys. Soc.*, **3**, 208 (1958).

381 keV are reached also in the Coulomb excitation of ^{133}Cs. The spins and parities assigned to these states of ^{133}Cs are $\frac{5}{2}^+$, $\frac{5}{2}^+$ or $\frac{3}{2}^+$, $\frac{3}{2}^+$ and $\frac{1}{2}^+$ respectively, the ground state of ^{133}Cs being $\frac{7}{2}^+$. If the 160 keV state is $\frac{3}{2}^+$, one cannot understand the absence of a predominant electron capture decay of ^{133}Ba to this state; on the other hand, whether this state is $\frac{3}{2}^+$ or $\frac{5}{2}^+$, there should be a considerable β^--branching to this state in the β^--decay of ^{133}Xe. In order to investigate this point, the study of the γ-rays of ^{133}Xe was undertaken (*).

2. – Experimental investigations.

The ^{133}Xe source for this investigation was obtained from Harwell. The radioactive gas was sealed in a glass tube 5 cm long and 1 cm in diameter. The Harwell catalogue of isotopes states that, as the gas is collected from the iodine fraction of the fission products, approximately 0.5% of xenon activity is due to ^{131}Xe^m (half-life 12 days, γ-ray energy 163 keV and 80 keV).

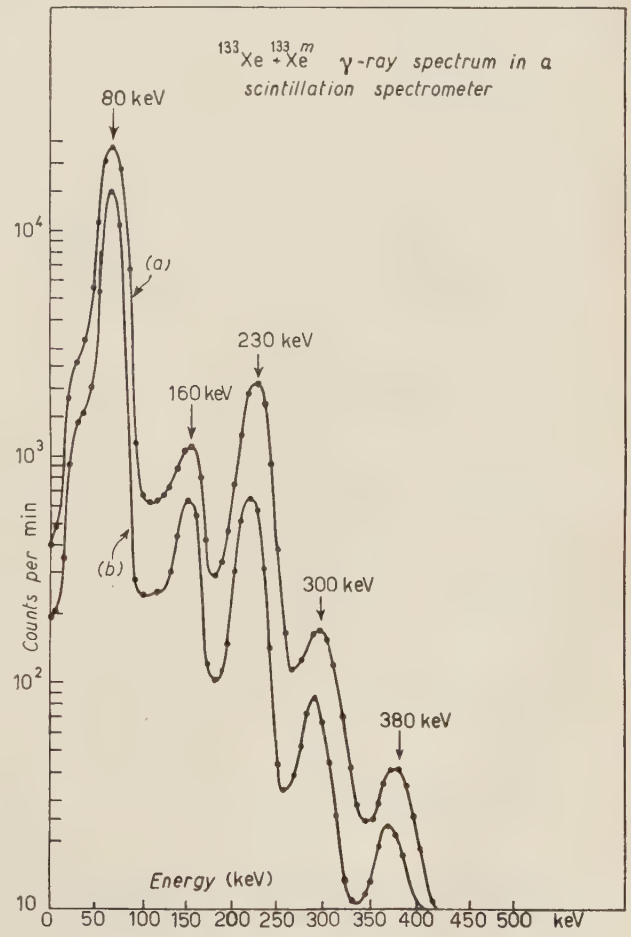

Fig. 1. – The spectrum of the γ-rays for ^{133}Xe and ^{131}Xe^m. *a*) was taken three days after the arrival of the source in Bombay. *b*) was taken 4 days later. The 230 keV γ-ray peak can be seen to have come down to nearly one fourth its previous value.

(*) This study was also suggested in a private communication by Dr. B. Crasemann of the University of Oregon, U.S.A.

The strength of the source was 200 millicuries to begin with. The tube was enclosed in a brass tube, one end of which was closed with a platinum foil (555 mg/cm²) in order to cut down the strong intensity 80 keV γ-ray and the K X-ray of Cs. The spectrum of the γ-rays was taken in a scintillation spectrometer with the NaI(Tl) crystal, $1\frac{1}{2}$ in. in diameter and 1 in. high. The activity was followed for three weeks. The spectrum of the γ-rays is reproduced in Fig. 1. One can see that γ-rays of energy 80 keV, 160 keV, 230 keV, 300 keV and 380 keV appear distinctly. It was found that the 230 keV γ-ray decayed with a half-life of about 2.3 days and could, therefore, be attributed to $^{133}Xe^{m}$, which is formed ([7]) in the decay of ^{133}I. The γ-rays of energy 80 keV, 160 keV, 300 keV and 380 keV decayed with a half-life of about 5.3 days. It was concluded that at least a very large fraction of those γ-rays originated from the same source and from ^{133}Xe.

When the activity had died down considerably, a spectrum of the γ-rays of ^{133}Xe was taken without the platinum foil covering the source. From this spectrum the intensities of the γ-rays were calculated. Corrections were made for the efficiency of detection, and the differences with energies of the ratio of the photo-peak area and total area. The relative intensity of the 80 keV, 160 keV, 300 keV and 380 keV γ-rays was found to be about 1, $1.4 \cdot 10^{-2}$, $8.4 \cdot 10^{-4}$ and $4.3 \cdot 10^{-4}$ respectively.

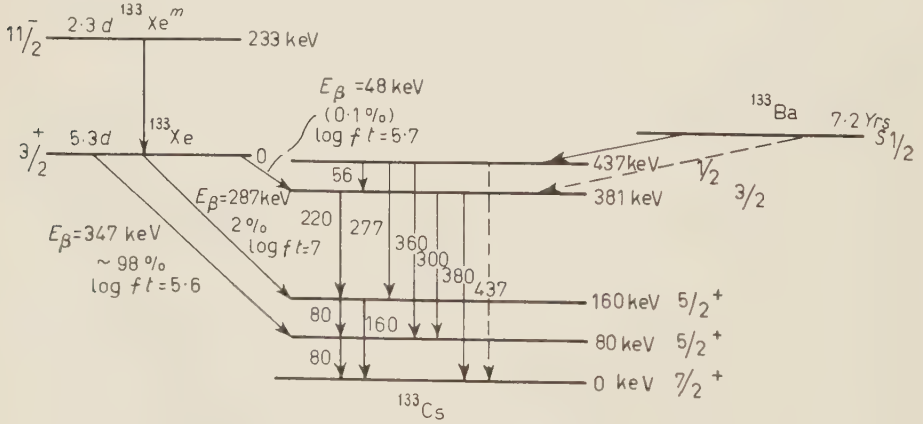

Fig. 2. – The decay scheme of ^{133}Xe and ^{133}Ba.

It is known from the studies of ^{133}Ba that the 160 keV state decays by the emission of a γ-ray of energy 160 keV and also by the cascade emission of two 80 keV γ-rays ([2,4,5]). In order to estimate the relative intensities of β^--branching it was necessary to find the intensity of the 80 keV γ-ray emitted in cascade.

([7]) A. H. SNELL and F. PLEASONTON: *Phys. Rev.*, **111**, 1338 (1958).

For this purpose, a fast-slow coincidence unit with a resolving time of $1.2 \cdot 10^{-7}$ s was used. It was found that the number of 80 keV γ-rays arising from the 160 keV state was 0.003 7 times that emitted from the 80 keV state. Taking this into account, and neglecting the contribution from the 380 keV state, the β^--branching ratios to the 80 keV state, 160 keV state, and 380 keV state were calculated to be 98%, 2% and 0.1% respectively. From the known maximum β^- energy emitted in transition to the 80 keV state, the maximum β^- energies involved in transition to the 160 keV state and the 380 keV state were calculated to be 287 keV and 48 keV respectively. From these data, the log *ft* values for the β^--transition to the 80 keV, 160 keV, and the 380 keV states were found to be 5.6, 7, and 5.7 respectively. This is illustrated in the decay scheme given in Fig. 2.

3. – Discussion.

From the occurrence of the γ-rays of energy 160 keV, 300 keV, and 380 keV in the decay of ^{133}Xe in addition to the well-known γ-ray of energy 80 keV, it is concluded that, as expected from the results of the studies of ^{133}Ba, β^--decay of ^{133}Xe leads also to the levels in ^{133}Cs at 160 keV and at 380 keV. However, the intensity of the β^--branching to the 160 keV state is rather low; consequently, the log *ft* value is much higher than what one would expect it to be if one assigns to the 160 keV state the spin and parity $\frac{5}{2}^-$ or $\frac{3}{2}^+$ as suggested from the study of the γ-rays from ^{133}Ba. It is worth noting in this connection that, as pointed out in the introduction, there is almost no electron capture decay of ^{133}Ba ($\frac{1}{2}^+$) leading to the 160 keV state of ^{133}Cs. One can see that this is consistent, so far as the decay of ^{133}Ba is concerned, with the assignment of the spin and parity of only $\frac{5}{2}^-$ to this state. The spin and parity $\frac{3}{2}^-$ assigned to the 380 keV state are consistent with the log *ft* value found here in the β^--decay of ^{133}Xe.

The relative intensities of the 300 keV and the 380 keV γ-rays, though subject to large errors in our measurements because of their low intensities, are 2:1 as found bi KOICKI *et al.* [4] in their studies of ^{133}Ba. The cascade to cross-over transition from the 160 keV state has been found here to be 1:4. The intensity of the 220 keV γ-ray emitted in the transition from the 380 keV state to the 160 keV state is rather low. It may be mentioned that there was a very low intensity γ-ray of energy about 500 keV, the origin of which was not investigated because of its low intensity. Lastly, towards the end of these investigations, the results of SNELL *et al.* [6] became available. Although they confirm the existence of these γ-rays, they found the intensity of the 300 keV γ-ray so low that they could not make the half-life measurement.

* * *

Our grateful thanks are due to Dr. P. AMMIRAJU and Miss G. C. PRAMILA for their assistance in this work.

RIASSUNTO (*)

Per mezzo di uno spettrometro a scintillazione si sono studiati i raggi γ del ^{133}Xe. I raggi γ hanno energie di 80 keV, 160 keV, 300 keV e 380 keV con intensità relative 1, $1.4 \cdot 10^{-2}$, $8.4 \cdot 10^{-4}$ e $4.3 \cdot 10^{-4}$. Studiando i raggi γ di 80 keV in coincidenza, si sono trovate l'intensità relativa della cascata e della transizione dallo stato 160 keV. Tenendo conto di queste determinazioni, si sono calcolati i log ft delle transizioni β agli stati 80 keV, 160 keV e 380 keV trovando rispettivamente i valori 5.6, 7 e 5.7.

(*) *Traduzione a cura della Redazione.*

IL NUOVO CIMENTO Vol. XI, N. 6 16 Marzo 1959

μ^--Capture in Light Nuclei.

E. G. Beltrametti

Istituto di Fisica dell'Università - Genova
Istituto Nazionale di Fisica Nucleare - Sottosezione di Genova

L. A. Radicati

Istituto di Fisica dell'Università - Pisa
Istituto Nazionale di Fisica Nucleare - Sezione di Pisa

(ricevuto il 29 Dicembre 1958)

Summary. — A shell model analysis of the μ^--capture by light nuclei without heavy particle emission, is given. Some experiments are suggested to measure the coupling constant and the relative contribution of the Gamow-Teller and Fermi interactions. A detailed study is presented of the μ^--capture in ^{3}He, ^{6}Li and ^{16}O.

---

1. – The purpose of this paper is to discuss the possibility of measuring the coupling constant g for μ^--meson capture and the relative importance of the Fermi and Gamow-Teller interactions. This problem has already been discussed for medium-heavy nuclei by Luyten and Tolhoek [1] who have used a simplified shell model description of the nucleus. However if one wants a more accurate evaluation of the coupling constant g and of the relative contribution x of the Gamow-Teller interaction one needs a situation in which the initial and final nuclear states are completely specified.

This suggests to analyze a capture in a light nucleus, possibly without emission of neutrons. The formation of the final nucleus in a bound state is not actually an unlikely process in a light nucleus. Indeed by considering the available volume in phase space one gets, for a nucleus of mass number A:

$$\frac{w_0}{w_n} \simeq \frac{1.56}{A},$$

---

[1] A. H. Tolhoek and J. R. Luyten: *Nucl. Phys.*, **3**, 679 (1957).

where w_0 and w_n are the probabilities per unit time for the two processes

$$\mu^- + (A, Z) \to (A, Z-1) + \nu\,,$$
$$\mu^- + (A, Z) \to (A-1, Z-1) + \mathrm{n} + \nu\,.$$

In Section **2** we present a formula for the matrix element for the first process (without neutron emission) valid for transitions of any order. Indeed one expects that higher order transitions should be fairly important in μ^--capture due to the high energy release. To calculate the nuclear matrix element we assume the validity of the shell model in its L-S coupling version. This seems a fairly good approximation for light nuclei and can at any rate be used as a starting point for a more refined intermediate coupling calculation. To simplify the treatment we shall assume that the proton which absorbs the μ^--meson belongs to the unfilled shell. This seems a plausible assumption at least for those processes which do not lead to neutron emission.

In Sections **3** and **4** this formula is used for discussing the capture rate by ^{6}Li, ^{3}He and ^{16}O which seem to be the simplest cases amongst the light nuclei.

Other cases are briefly discussed in Section **5**.

2. – The operator causing the transition is a tensor operator of order j which can by written in the form

$$\mathcal{H}^{(jk)}_q = \sum_{i=1}^{A} \sum_{\mu} C^{k\,a\,j}_{\mu\;q} H^{(k)}_{\mu}(i) h^{(a)}_{q-\mu}(i) t^{(1)}_{-1}(i)\,, \tag{1}$$

where $H^{(k)}_{\mu}$, $h^{(a)}_{q-\mu}$, $t^{(1)}_{-1}$ are tensor operators of order k, a and 1, operating respectively on the space, spin and isotopic-spin parts of the wave function. The magnetic quantum numbers q, μ vary from $-j$ to $+j$ or $-k$ to $+k$ respectively. k represents the order of the transition; $a = 0$ or 1 for Fermi and Gamow-Teller transitions respectively.

By using standard methods we may write the reduced matrix element of the operator (1) in the form [2]

$$\langle J \| \mathcal{H}^{(jk)} \| J' \rangle = n\sqrt{\tfrac{3}{2}} \langle l_0 \| H^{(k)} \| l_1 \rangle \langle \tfrac{1}{2} \| h^{(a)} \| \tfrac{1}{2} \rangle \cdot \tag{2}$$
$$\cdot \sum_{p} \langle \alpha \} \alpha_p \rangle \langle \alpha_p \} \alpha' \rangle K(\tfrac{1}{2}\,\tfrac{1}{2}\,TT'1T_p; -1M'_T) \begin{Bmatrix} k & L & L' \\ a & S & S' \\ j & J & J' \end{Bmatrix} \cdot$$
$$\cdot U(kl_1LL_p; l_0L')\, U(a\tfrac{1}{2}SS_p; \tfrac{1}{2}S')[(2j+1)(2L+1)(2S+1)(2J'+1)]^{\frac{1}{2}},$$

[2] See, for a similar discussion in the case of γ transitions: A. M. LANE and L. A. RADICATI: *Proc. Phys. Soc.*, A **67**, 167 (1954).

where $|J\rangle$ stands for

$$|l^{n-1} l_0 \alpha L S T M_T J\rangle$$

and represents a state with $n-1$ particles in the l-shell, one particle in the l_0-shell, coupled to orbital angular momentum L, spin S, isotopic spin T, third component M_T. J is the total angular momentum, and α stands for all the other necessary quantum numbers. In equation (2), $\langle \alpha \} \alpha_p \rangle$ are the coefficients of fractional parentage ([3]), K is the product of a Clebsh-Gordon coefficient by a Racah function:

$$K(abcdef; \varepsilon\delta) = (-1)^{e+2f-c-d+2b} C^{e\,d\,c}_{\varepsilon\,\delta} U(ebcf; ad)$$

and

$$U(abcd; ef) = [(2e+1)(2f+1)]^{\frac{1}{2}} W(abcd; ef)$$

$\begin{Bmatrix} a & b & e \\ d & e & f \\ g & h & i \end{Bmatrix}$ is the Wigner nine-j symbol ([4]). The value of the one-particle reduced matrix element $\langle \frac{1}{2} \| h^{(a)} \| \frac{1}{2} \rangle$ is 1 or 3 for Fermi ($a=0$) and Gamow-Teller ($a=1$) transitions.

To evaluate the relative importance of allowed and second forbidden transitions we shall assume that the μ^--meson wave function is a constant C over the nuclear volume.

With obvious notations the one particle space operator may be written in the form

$$H^{(k)}_\mu = \sqrt{4\pi} g i^{-k} C j_k(qr) Y^k_\mu(\theta, \varphi) ,$$

where q is the neutrino momentum. Using an infinite potential well with radius $2.54 \cdot 10^{-13}$ cm (appropriate to $A=6$) one gets for transitions between states of the $1p$-shell, and for $q = 100$ MeV/c:

$$\frac{\langle 1p \| H^{(0)} \| 1p \rangle}{\langle 1p \| H^{(2)} \| 1p \rangle} = 14 . \tag{3}$$

3. – The probability for formation of ^{6}He due to the capture of μ^--mesons by ^{6}Li ($J=1+$), can be measured by detecting the β^--activity of the target. If it should turn out that the transition to the excited state ($J=2+$;

([3]) The p-shell fractional parentage coefficients have been tabulated H. A. JAHN and H. VAN WIERINGEN: *Proc. Roy. Soc.*, A **209**, 502 (1951).

([4]) See, for example, M. E. ROSE: *Elementary Theory of Angular Momentum* (New York, 1957), Ch. XI, or A. R. EDMONDS: *Angular Momentum in Quantum Mechanics* (Princeton N.J., 1957), Ch. 6.

1.77 MeV) is unimportant, then the capture rate for the reaction

$$\mu^- + {}^6\mathrm{Li} \to {}^6\mathrm{He} + \nu$$

can be used to determine in the usual way the G.T. coupling constant.

The states of ^{6}Li and ^{6}He are, in L.S coupling, of the form

$$\begin{aligned} {}^6\mathrm{Li} \text{ ground state:} &\quad |{}^{13}S_1\rangle \\ {}^6\mathrm{He} \text{ ground state:} &\quad |{}^{31}S_0\rangle \\ {}^6\mathrm{He} \text{ first excited state:} &\quad |{}^{31}D_2\rangle . \end{aligned}$$

One can therefore easily see that in L.S coupling there is no allowed transition to the first excited state and no forbidden transitions to the ground state.

The relevant matrix elements, calculated under the assumptions that lead to equation (3), are, apart from the constant $|c|^2$, which will be consistently omitted:

(*a*) $|M_{\mathrm{GT}}|^2 = 4.70$ for the allowed transition to the ground state

(*b*) $|M_{\mathrm{GT}}|^2 = 1.38 \cdot 10^{-2}$ for the second forbidden transition to the excited state.

An intermediate coupling calculation (*) modifies (*a*) by only a few percents, ($|M_{\mathrm{F}}|^2$ still vanishes), while (*b*) becomes even smaller ($\sim 4.9 \cdot 10^{-3}$) due to interference effects, ($|M_{\mathrm{F}}|^2 \simeq 2.3 \cdot 10^{-5}$). We see from the above discussion that we can neglect the probability for the formation of ^{6}He in its excited state.

In order to determine the relative importance of the F and G.T. couplings one could use the reaction

$$\mu^- + {}^3\mathrm{He} \to \nu + {}^3\mathrm{H} . \tag{5}$$

^{3}H has no bound excited state and, as ^{6}He, undergoes β^--decay. Though this is presumably a very difficult experiment, the theoretical situation is very simple (**).

(*) For the coupling parameter we have used the values $a/K = 1.35$, $K = -1.25$ MeV and $L/K = 6$ as suggested by Inglis (*Phys. Rev.*, **87**, 915, (1952); *Rev. Mod. Phys.*, **25**, 390 (1953)) and by French (University of Pittsburg: *Technical Rep.* n. IX (1958)), to whom we refer also for the notations.

(**) The possibility of this experiment has been suggested to us by Professor M. Goldhaber (private communication) whom we wish to thank for some useful suggestions.

To evaluate the matrix element we have used for both ^{3}He and ^{3}H the space wave function suggested by IRVING (5)

$$\psi = \exp\left[-\varepsilon\sqrt{r_{12}^2 + r_{13}^2 + r_{23}^2}\right], \quad (1/\varepsilon = 1.089 \cdot 10^{-13} \text{ cm}),$$

where r_{12}, r_{13}, r_{23} are the relative co-ordinates of the three nucleons. With this function the values of the two matrix elements are

$$|M_F|^2 = 0.89 ,$$

$$|M_{GT}|^2 = 2.67 .$$

4. – The determination of g and x we have discussed depends upon the values of M_{GT} and M_F or, in others words, upon the choice of a particular nuclear model.

As in the analogous case of the β-decay, one would like to have some other independent way for determining g and x in order to check the consistency of the assumptions made about the matrix elements. A case which can be analyzed in some detail occurs in the μ^--capture by ^{16}O leading to ^{16}N. ^{16}N has only four bound states whose spins and parities are reasonably well known (6) (see Fig. 1). All the transitions to the excited states contribute, through fast γ-decay, to populate the ground state which undergoes β$^-$-decay ($\tau = 7.35$ s; $E = 10.4$ MeV). All these transitions are at least first forbidden. However, because of the higher charge of ^{16}O, the probability for formation of ^{16}N is of the same order of magnitude as the probability for the formation of ^{6}He from ^{6}Li that has been discussed before.

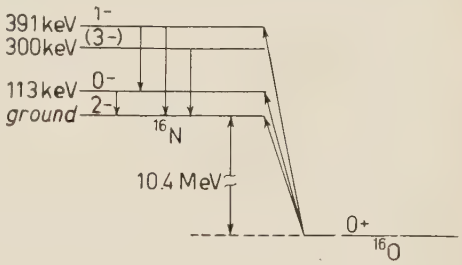

Fig. 1.

In Table I we have collected the values of the first forbidden matrix elements for the different transitions, calculated with equation (2). For this evaluation we have used the wave functions for ^{16}N calculated by ELLIOT and FLOWERS in intermediate coupling (7). The reduced single particle matrix

(5) J. IRVING: *Phil. Mag.*, **42**, 338 (1951).
(6) D. H. WILKINSON: *Phys. Rev.*, **105**, 686 (1957).
(7) J. P. ELLIOTT and H. B. FLOWERS: *Proc. Roy. Soc.*, A **242**, 57 (1957).

elements of the space operator $H^{(k)}$ (see equation (2)) have been evaluated using an infinite square well with radius $a = 3.53 \cdot 10^{-13}$ cm.

TABLE I. – $^{16}O \to {}^{16}N$ *first forbidden transitions.*

Final state (^{16}N)	First order transition	
	$\lvert M_{GT} \rvert^2$	$\lvert M_F \rvert^2$
1 — (391 keV)	$5.18 \cdot 10^{-2}$	$1.42 \cdot 10^{-2}$
0 — (113 keV)	$5.54 \cdot 10^{-2}$	0
2 — (ground)	$11.3 \cdot 10^{-2}$	0
(3 —) (300 keV)	0	0

We have neglected higher order (3-rd order) transitions to the 2 — and (3 —) levels. A rough estimation indicates that they are unimportant.

It is apparent from the above results that the measurement of the β-activity of the target can actually provide only the value of the G.T. coupling constant.

5. – If we require that the capture processes should be observed by detecting the β-activity of the daughter nucleus, then it is difficult to find any other case that could be analysed in such a complete way as ^3He, ^6Li and ^{16}O. Usually there are too many accessible excited states whose spins and parities are unknown.

The nuclei with a ground state of isotopic spin $T = \frac{3}{2}$ and third component $M_T = -\frac{3}{2}$ could be reached from the ground state of nuclei with $T = \frac{1}{2}$, $M_T = -\frac{1}{2}$. They are β-active and have presumably very few excited states. Amongst the more promising candidates in this group we suggest

$$^9Li\ (^9Be + \mu^- \to {}^9Li + \nu) \text{ and } ^{15}C\ (^{15}N + \mu^- \to {}^{15}C + \nu).$$

Another possibility would be to study the reactions which lead to the emission of one neutron; for example:

$$^7Li + \mu^- \to {}^6He + n + \nu\,,$$

$$^9Be + \mu^- \to {}^8Li + n + \nu\,.$$

In both cases the final nucleus is β-active and has few excited states.

This would probably provide a more feasible way for determining the Fermi coupling constant than the μ^--capture by ^3He that has been previously discussed. A detailed study of these cases will be given in a forthcoming paper.

Finally one could look for those transitions which lead to formation of the final nucleus in an excited state. These transitions could be observed by detecting the subsequent γ-transition.

Some examples have been studied in connection with the $^{16}O \rightarrow {}^{16}N$ transition (see Table I), and a few other cases could probably be found.

* * *

We wish to thank Professor M. GOLDHABER for a stimulating discussion, and Mr. G. FIORIO for performing some numerical calculations.

RIASSUNTO

Servendosi del modello a shell si analizza il processo di cattura dei mesoni μ^+, senza emissione di particelle pesanti, da parte di nuclei leggeri. Allo scopo di poter conoscere il contributo relativo dell'accoppiamento di Gamow-Teller e di Fermi, si suggeriscono alcune esperienze e si studia dettagliatamente la cattura μ^- in ^6Li, ^3He e ^{16}O.

On the Interaction Hamiltonian of Symmetric Pseudoscalar Meson Theory.

V. Singh

Tata Institute of Fundamental Research - Bombay

(ricevuto il 29 Dicembre 1958)

Summary. — The equivalence of the pseudoscalar and pseudovector couplings of pseudoscalar pions to nucleons has been investigated here in a straightforward manner without making any use of a canonical transformation as has been done previously (1). PS-coupling is shown to be equivalent, as far as the S-matrix is concerned, to the usual p-wave and s-wave terms along with some non-local terms whose interpretation is not yet clear.

There has been considerable work done to investigate the extent of the equivalence of pseudoscalar (PS) and pseudovector (PV) couplings of pseudoscalar pions to nucleons (1). The usual way to do this has been to perform a canonical transformation on the Hamiltonian $\mathcal{H}_{\text{PS}}$ of pseudoscalar coupling theory and approximating the transformed Hamiltonian in an appropriate way such as to get the PV-coupling term (2) $i(G/2M)\bar{\psi}\gamma^{\mu}\gamma_5\tau_i\psi(\partial\varphi_\lambda\partial x^{\mu})$ and the S wave scattering term $(G^2/2M)\bar{\psi}\psi\varphi_\lambda^2$.

The purpose of this note is to show that a similar result can be obtained more directly without the use of a canonical transformation. In fact, starting

---

(1) F. J. Dyson: *Phys. Rev.*, **73**, 929 (1948); K. M. Case: *Phys. Rev.*, **76**, 14 (1949); L. L. Foldy: *Phys. Rev.*, **84**, 168 (1951); G. Wentzel: *Phys. Rev.*, **86**, 802 (1952); L. L. Foldy, R. K. Osborn and J. M. Berger: *Phys. Rev.*, **87**, 1061 (1952); J. V. Lepore: *Phys. Rev.*, **88**, 750 (1952).

(2) We shall follow the notation used in S. S. Schweber, H. A. Bethe and F. de Hoffmann: *Mesons and fields* (New York, 1955). Also $\hbar = c = 1$.

from the PS-PS Hamiltonian $\mathcal{H}_{\mathrm{PS}}$, one can construct a « Hamiltonian » $\mathcal{H}$ which contains these two terms together with some other « non-local » terms, and which is equivalent to the original Hamiltonian as far as the scattering matrix S is concerned.

We work in the interaction representation, which has not been used for these investigations except by LEPORE ([3]). The derivation of the new « Hamiltonian » is as follows.

In the interaction representation, we have the following equations of motion for the state vector $\Psi(t)$ and the field variables $\psi(\mathbf{x})$ and $\varphi_\lambda(\mathbf{x})$ in the PS-PS theory ([4]),

$$i\frac{\partial\Psi(t)}{\partial t} = G\int_{(x^0=t)} \mathrm{d}^3x(\overline{\psi}\gamma_5\tau\cdot\varphi\psi)(\mathbf{x})\Psi(t)\,, \tag{1}$$

$$\left(-i\gamma^\mu\frac{\partial}{\partial x^\mu} + M\right)\psi(\mathbf{x}) = 0\,, \tag{2}$$

$$(\Box + \mu^2)\varphi_\lambda(\mathbf{x}) = 0 \tag{3}$$

or

$$i\frac{\partial U(t,-\infty)}{\partial t} = G\int \mathrm{d}^3x(\overline{\psi}\gamma_5\tau\cdot\varphi\psi)(\mathbf{x})\,U(t,-\infty)\,, \tag{4}$$

where

$$\Psi(t) = U(t,-\infty)\Psi(-\infty)$$

and

$$U(+\infty,-\infty) = S\,, \qquad U(-\infty,-\infty) = 1\,. \tag{5}$$

Substituting the values of $\psi(\mathbf{x})$ and $\overline{\psi}(\mathbf{x})$ obtained from (2) in (1), we get ([5])

$$\begin{aligned} i\frac{\partial U(t,-\infty)}{\partial t} &= \frac{iG}{2M}\int \mathrm{d}^3x\cdot\left\{-\frac{\partial\overline{\psi}}{\partial x^\mu}\gamma^\mu\gamma_5\tau\cdot\varphi\psi + \overline{\psi}\gamma_5\tau\cdot\varphi\gamma^\mu\frac{\partial\psi}{\partial x^\mu}\right\}U(t,-\infty) = \\ &= \frac{iG}{2M}\int \mathrm{d}^3x\left\{\frac{\partial}{\partial x^\mu}(\overline{\psi}\gamma_5\gamma^\mu\tau\cdot\varphi\psi) - \overline{\psi}\gamma_5\gamma^\mu\tau_\lambda\psi\frac{\partial\varphi_\lambda}{\partial x^\mu}\right\}U(t,-\infty)\,, \end{aligned} \tag{6}$$

([3]) J. V. LEPORE: *Phys. Rev.*, **88**, 750 (1952).

([4]) We shall use flat space-like surfaces instead of arbitrary ones for the sake of simplicity.

([5]) Only the limits of integration of the time component shall be specified, as the integration is always over the whole of allowed domain of space-components.

$$
(6)\qquad
\begin{cases}
\therefore\ U(t', -\infty) = 1 + \dfrac{G}{2M}\displaystyle\int_{-\infty}^{t'} \mathrm{d}^4x \cdot \left(\overline{\psi}\gamma^\mu\gamma_5\tau_\lambda\psi\ \frac{\partial\varphi_\lambda}{\partial x^\mu}\right) U(t, -\infty) + \\
\qquad + \dfrac{G}{2M}\displaystyle\int_{-\infty}^{t'} \mathrm{d}^4x \cdot \left\{\frac{\partial}{\partial x^\mu}\left(\overline{\psi}\gamma_5\gamma^\mu\tau\cdot\varphi\psi\right)\right\} U(t, -\infty)\,, \\
\qquad = 1 + \dfrac{G}{2M}\displaystyle\int_{-\infty}^{t'} \mathrm{d}^4x \cdot \left(\overline{\psi}\gamma^\mu\gamma_5\tau_\lambda\psi\ \frac{\partial\varphi_\lambda}{\partial x^\mu}\right) U(t, -\infty) - \\
\qquad - \dfrac{G}{2M}\displaystyle\int_{-\infty}^{t'} \mathrm{d}^4x \cdot \overline{\psi}\gamma_5\gamma^0\tau\cdot\varphi\psi\ \frac{\partial U(t, -\infty)}{\partial t} + \\
\qquad + \dfrac{G}{2M}\displaystyle\int_{-\infty}^{t'} \mathrm{d}^4x \cdot \frac{\partial}{\partial x^\mu}\left(\overline{\psi}\gamma_5\gamma^\mu\tau\cdot\varphi\psi\, U(t, -\infty)\right).
\end{cases}
$$

Substituting the value of $\partial U(t, -\infty)/\partial t$ in (6) from (4), and using the commutation relations for ψ's, we get

$$
(7)\qquad U(t', -\infty) = 1 + \frac{G}{2M}\int_{-\infty}^{t'} \mathrm{d}^4x \cdot \overline{\psi}\gamma^\mu\gamma_5\tau_\lambda\varphi\ \frac{\partial\varphi_\lambda}{\partial x^\mu}\ U(t, -\infty) -
$$

$$
- \frac{iG^2}{2M}\int_{-\infty}^{t'} \mathrm{d}^4x \cdot \overline{\psi}\psi\varphi_\lambda^2\, U(t, -\infty) + \frac{iG^2}{2M}\int_{-\infty}^{t'} \mathrm{d}^4x \left\{\sum_{\alpha\beta\gamma\delta}\int \mathrm{d}^3x_1\, \overline{\psi}_\alpha(\mathbf{x})\,(\gamma^0\gamma_5\tau\cdot\varphi)_{\alpha\beta}\cdot\right.
$$

$$
\left.\cdot\,\psi^\dagger_\nu(\boldsymbol{x}_1, t)\,\psi_\beta(\mathbf{x})\,(\gamma^0\gamma_5\tau\cdot\varphi(\boldsymbol{x}_1, t))_{\gamma\delta}\,\psi_\delta(\boldsymbol{x}_1, t)\right\} U(t, -\infty) +
$$

$$
+ \frac{G}{2M}\int_{-\infty}^{t'} \mathrm{d}^4x \cdot \frac{\partial}{\partial x^\mu}\left(\overline{\psi}\gamma_5\gamma^\mu\tau\cdot\varphi\psi\, U(t, -\infty)\right).
$$

The last term can be integrated ([6]) and (7) then becomes

$$
(8)\qquad U(t', -\infty) = 1 - i\int_{-\infty}^{t'} \mathrm{d}^4x \cdot \mathscr{H}_0(\mathbf{x})\, U(t, -\infty) +
$$

$$
\frac{G}{2M}\int \mathrm{d}^3x \cdot (\overline{\psi}\gamma_5\gamma^0\tau\cdot\varphi\psi)(\boldsymbol{x}, t')\, U(t', -\infty)\,,
$$

([6]) We make use of the adiabatic hypothesis in writing (8), that is we supply convergence factors ([7]) $\exp[-|t|/T]$ and take the limit $T \to +\infty$, after the integration has been performed. The adiabatic hypothesis is also used in writing equation (15).

([7]) F. J. Dyson: *Phys. Rev.*, **82**, 428 (1951); **83**, 608, 1207 (1951); *Proc. Roy. Soc.* (*London*), A **207**, 395 (1951).

where

$$\mathcal{H}_0(\boldsymbol{x}, t) = \frac{iG}{2M}\,\overline{\psi}\gamma''\gamma_5\tau_\lambda\psi\,\frac{\partial\varphi_\lambda}{\partial x''} + \frac{G^2}{2M}\,\overline{\psi}\psi\varphi_\lambda^2 + \int\frac{G^2}{2M}\,\mathcal{H}_R(\mathbf{x};\boldsymbol{x}_1, t)\,\mathrm{d}^3x_1\,, \tag{9}$$

$$\mathcal{H}_R(\mathbf{x};\boldsymbol{x}_1, t) = -\sum_{\alpha\beta\gamma\delta}\overline{\psi}_\alpha(\mathbf{x})\left(\gamma^0\gamma_5\tau\cdot\varphi(\mathbf{x})\right)_{\alpha\beta}\psi^\dagger_\gamma(\boldsymbol{x}_1, t)\psi_\beta(\mathbf{x})\left(\gamma^0\gamma_5'\tau\cdot\varphi(\boldsymbol{x}_1, t)\right)_{\gamma\delta}\psi_\delta(\boldsymbol{x}_1, t) \tag{10}$$

Defining

$$V(t', -\infty) = \left(1 - \frac{G}{2M}\int\mathrm{d}^3x\cdot f(\boldsymbol{x}, t')\right)U(t', -\infty)\,, \tag{11}$$

where

$$f(\boldsymbol{x}, t') = (\overline{\psi}\gamma_5\gamma^0\tau\cdot\varphi\psi)(\boldsymbol{x}, t')\,. \tag{12}$$

The equation for $V(t', -\infty)$ can be written as

$$V(t', -\infty) = 1 - i\int_{-\infty}^{t'}\mathrm{d}^4x\mathcal{H}(\boldsymbol{x}, t)\,V(t, -\infty)\,, \tag{13}$$

where

$$\mathcal{H}(\boldsymbol{x}, t) = \mathcal{H}_0(\boldsymbol{x}, t)\left\{1 - \frac{G}{2M}\int\mathrm{d}^3x_1\cdot f(\boldsymbol{x}_1, t)\right\}^{-1}. \tag{14}$$

Now (cf. footnote (6))

$$V(+\infty, -\infty) = U(+\infty, -\infty) = S\,. \tag{15}$$

Therefore as long as we are interested only in the case $t'\to+\infty$, *i.e.* S-matrix, it does not make any difference whether we use $U(t', -\infty)$ or $V(t', -\infty)$. Hence we can interpret $\mathcal{H}(\boldsymbol{x}, t)$ as a « Hamiltonian » which would give the same results for scattering problems.

We can write our new « Hamiltonian » $\mathcal{H}(\boldsymbol{x}, t)$ as

$$\mathcal{H}(\boldsymbol{x}, t) = \mathcal{H}_1(\mathbf{x}) + \mathcal{H}_2(\boldsymbol{x}, t) \tag{16}$$

with

$$\mathcal{H}_1(\mathbf{x}) = i\,\frac{G}{2M}\,\overline{\psi}\gamma^\mu\gamma_5\tau_\lambda\psi\,\frac{\partial\varphi_\lambda}{\partial x^\mu} + \frac{G^2}{2M}\,\overline{\psi}\psi\varphi_\lambda^2\,, \tag{17}$$

and

$$\mathcal{H}_2(\boldsymbol{x}, t) = \mathcal{H}_{21}(\boldsymbol{x}, t) + \mathcal{H}_{22}(\boldsymbol{x}, t) + \ldots\,, \tag{18}$$

where

$$\mathcal{H}_{21}(\boldsymbol{x},t)=\int \mathrm{d}^3x_1\left[\frac{G^2}{2M}\,\mathcal{H}_R(\mathbf{x};\,\boldsymbol{x}_1,\,t)+\frac{G}{2M}\,\mathcal{H}_1(\mathbf{x})f(\boldsymbol{x}_1,\,t)\right], \tag{19}$$

$$\mathcal{H}_{22}(\boldsymbol{x},\,t)=\int \mathrm{d}^3x_1\int \mathrm{d}^3x_2\cdot$$

$$\cdot\left[\frac{G^2}{4M^2}\,\mathcal{H}_1(\mathbf{x})f\boldsymbol{x}_1,\,t)f(\boldsymbol{x}_2,\,t)+\frac{G^3}{4M^2}\,\mathcal{H}_R(\mathbf{x};\,\boldsymbol{x}_1,\,t)f(\boldsymbol{x}_2,\,t)\right]\ldots\text{ etc.}\,.$$

Thus we see that $\mathcal{H}_2(\boldsymbol{x},\,t)$ involves implicitly the field operators at more than two space points, and is in this sense « non-local ». The local part $\mathcal{H}_1(\mathbf{x})$ of $\mathcal{H}(\boldsymbol{x},\,t)$ consists of two parts which give rise to P- and S-wave meson scattering respectively at low energies. The interpretation of the rest of the terms (the « non-local part ») is not any more clear here than in the other derivations using canonical transformation.

The new quantity $\mathcal{H}(\boldsymbol{x},\,t)$ which we call « Hamiltonian », has been shown to be equivalent to $\mathcal{H}_{\mathrm{PS}}$ only for scattering states and the two could give different results for the bound states. It appears therefore that $\mathcal{H}(\boldsymbol{x},\,t)$ cannot be derived from $\mathcal{H}_{\mathrm{PS}}$ using a canonical transformation.

* * *

The author is thankful to Shri B. M. Udgaonkar, Dr. L. K. Pandit and Dr. S. N. Biswas for helpful discussions.

RIASSUNTO (*)

L'equivalenza degli accoppiamenti pseudoscalare e pseudovettoriale dei pioni pseudo scalari ai nucleoni è stato qui esaminato in maniera diretta senza far uso di trasformazione canonica, come fatto precedentemente (1). Si dimostra che l'accoppiamento PS è equivalente, per quanto riguarda la matrice S, agli usuali termini in onde p ed s assieme ad alcuni termini non locali la cui interpretazione non è ancora chiara.

(*) *Traduzione a cura della Redazione.*

IL NUOVO CIMENTO Vol. XI, N. 6 16 Marzo 1959

Energy-Band Structure of Lithium Atoms in the Diamond Lattice.

F. Bassani and V. Celli

Istituto di Fisica dell'Università - Pavia

(ricevuto il 31 Dicembre 1958)

Summary. — A hypothetical crystal of lithium atoms in the diamond lattice is considered. The value of the energies at the special points of the reduced zone with $\boldsymbol{k} = (0, 0, 0)$, $\boldsymbol{k} = 2\pi a^{-1}(1, 0, 0)$, $\boldsymbol{k} = 2\pi a^{-1}(\frac{1}{2}, 0, 0)$ and $\boldsymbol{k} = 2\pi a^{-1}(\frac{1}{2}, \frac{1}{2}, \frac{1}{2})$ are calculated by the Orthogonalized Plane Wave method using the Wigner-Seitz crystal potential and the same electron density as in metallic lithium. The curves of energy versus $\boldsymbol{k}$ are drawn in the [1, 0, 0] and [1, 1, 1] directions. The energy bands so obtained are compared with the energy bands of diamond evaluated by F. Herman. The relative positions of the energy bands appear to be the same in the two cases and this points to the possibility that the energy-band structure is mainly determined by the symmetry of the lattice. A comparison with metallic lithium gives a higher cohesive energy in the case of the pseudolattice, when one neglects electrostatic, exchange and correlation terms.

1. – Introduction.

The idea of studying the energy bands of pseudo-crystals, *i.e.* of lattices of atoms which are known to crystallize in some other lattice, was first suggested by F. Seitz as a tool to study the influence of lattice symmetry and atomic potential on the energy-band structure.

Casella [1] estimated the energy bands of carbon atoms in the face centered cubic lattice by the Orthogonalized Plane Wave method. The results he obtained are considerably different from the results Herman [2] obtained in diamond; in particular at the point Γ ($\boldsymbol{k} = 0$) the position of the energy-

(1) R. Casella: *Phys. Rev.*, **109**, 54 (1958).

(2) F. Herman: *Phys. Rev.*, **88**, 1210 (1952); **93**, 1214 (1954).

states $\Gamma_{25'}$ and Γ_{15} are reversed. A calculation of the energy bands of sodium atoms in the diamond structure was performed by F. BASSANI [3] by the O.P.W. method and the results displayed a strict similarity with the energy bands of silicon [4].

A calculation of the energy-band structure of lithium atoms in a diamond lattice having the same atomic volume as metallic lithium is presented in this paper. The O.P.W. method is adopted because of the advantage of evaluating several energy bands and because of its successful application both to metals and to insulators.

In Section **2** an outline of the method is given in a form particularly suitable for the diamond symmetry. The energy states of the empty lattice are related to the irreducible representations of the group of the wave vector to which they belong. The crystal symmetry combinations of plane waves are also given at one of the points of interest.

The parameters which enter the actual calculations are discussed in Section **3** and numerical results for them are presented.

In Section **4** the results for the energy states of the lowest bands are given at four symmetry points of the reduced zone. A comparison is made with the energy bands in diamond and in metallic lithium in Section **5**.

2. – General method and symmetry analysis.

The method of orthogonalized plane waves was introduced by HERRING [5] and was recently discussed by many authors [6]. It is actually a variational procedure in which linear variation trial functions for valence and conduction states are formed with plane waves made orthogonal to the Bloch functions constructed from the atomic core states. For a certain value of the wave vector $\boldsymbol{k}$, inside the reduced zone, the plane waves to be considered are of the type $\exp[i(\boldsymbol{k}+\boldsymbol{h}_i)\cdot\boldsymbol{r}]$, where $\boldsymbol{h}_i$ is any vector of the reciprocal lattice. These plane waves are the eigenfunctions of the « empty lattice », *i.e.* of a lattice with a constant potential, as classified in the reduced zone scheme.

From the set of plane waves belonging to a given value of $|(\boldsymbol{k}+\boldsymbol{h}_i)|^2$, linear combinations are constructed that transform according to a given column of a certain irreducible representation of the group of the $\boldsymbol{k}$ vector. In this way the number of undetermined coefficients in the trial function is

(3) F. BASSANI: *Journ. of Chem. and Phys. of Solids* (to appear).

(4) T. O. WOODRUFF: *Phys. Rev.*, **103**, 1159 (1956); F. BASSANI: *Phys. Rev.*, **108**, 263 (1957).

(5) C. HERRING: *Phys. Rev.*, **57**, 1169 (1940).

(6) J. CALLAWAY: *Phys. Rev.*, **97**, 933 (1955); T. O. WOODRUFF: *Solid State Physics*, edited by F. SEITZ and D. TURNBULL, vol. **4**, 367 (1957).

greatly reduced and convergence is obtained to energy states that are automatically classified.

We shall estimate the energy levels at four points of the reduced zone: the point Γ with $\boldsymbol{k}=0$, the point X with $\boldsymbol{k}=(2\pi/a)\,(1,0,0)$, the point $\Delta(\frac{1}{2})$, with $\boldsymbol{k}=(2\pi/a)\,(\frac{1}{2},0,0)$ and the point L with $\boldsymbol{k}=(2\pi/a)\,(\frac{1}{2},\frac{1}{2},\frac{1}{2})$. For each of these points the lowest eigenvalues of the « empty lattice » are listed in Table I with the number of plane waves and the irreducible representations of the group of the wave vector belonging to each eigenstate. The symbols used are those introduced by BOUCKAERT, SMOLUCHOWSKY and WIGNER [7] and by HERRING [8].

TABLE I. – *Classification of the « empty lattice » eigenvalues.*

	Number of plane waves	Empty lattice eigenvalues in units $(\hbar^2/2m)(4\pi^2/a^2)$	Irreducible representations
Point $\boldsymbol{k}=0$	1	$(0,0,0)^2$	Γ_1
	8	$(1,1,1)^2$	$\Gamma_1\,\Gamma_{25'}\,\Gamma_{15}\,\Gamma_{2'}$
	6	$(2,0,0)^2$	$\Gamma_{25'}\,(\Gamma_{12'})\,\Gamma_{2'}$
	12	$(2,2,0)^2$	$\Gamma_1\;\Gamma_{25'}\Gamma_{15}\,\Gamma_{12}\,\Gamma_{25}$
Point X $\boldsymbol{k}=2\pi/a$ (1, 0, 0)	2	$(1,0,0)^2$	X_1
	4	$(0,1,1)^2$	$X_1\;X_4$
	8	$(1,2,0)^2$	$X_1\;X_2\;X_3\;X_4$
	8	$(2,1,1)^2$	$2X_1\;X_3\;X_4$
Point $\Delta(\frac{1}{2})$ $\boldsymbol{k}=2\pi/a$ $(\frac{1}{2},0,0)$	1	$(\frac{1}{2},0,0)^2$	Δ_1
	4	$(\frac{1}{2},1,1)^2$	$\Delta_1\;\Delta_{2'}\,\Delta_5$
	1	$(\frac{3}{2},0,0)^2$	$\Delta_{2'}$
	4	$(\frac{1}{2},2,0)^2$	$\Delta_{2'}\,\Delta_5\;\Delta_{1'}$
	4	$(\frac{3}{2},1,1)^2$	$\Delta_1\;\Delta_{2'}\,\Delta_5$
	4	$(\frac{3}{2},2,0)^2$	$\Delta_1\;\Delta_2\;\Delta_5$
	1	$(\frac{5}{2},0,0)^2$	$\Delta_{2'}$
Point L $\boldsymbol{k}=2\pi/a$ $(\frac{1}{2},\frac{1}{2},\frac{1}{2})$	2	$(\frac{1}{2},\frac{1}{2},\frac{1}{2})^2$	$L_1\;L_{2'}$
	6	$(\frac{3}{2},\frac{1}{2},\frac{1}{2})^2$	$L_1\;L_{2'}\,L_3\;L_{3'}$
	6	$(\frac{1}{2},\frac{3}{2},\frac{3}{2})^2$	$L_1\;L_{2'}\,L_3\;L_{3'}$
	6	$(\frac{5}{2},\frac{1}{2},\frac{1}{2})^2$	$L_1\;L_{2'}\,L_3\;L_{3'}$
	2	$(\frac{3}{2},\frac{3}{2},\frac{3}{2})^2$	$L_1\;L_{2'}$

[7] L. P. BOUCKAERT, R. SMOLUCHOWSKI and E. WIGNER: *Phys. Rev.*, **50**, 58 (1936).

[8] C. HERRING: *Journ. Franklin Inst.*, **233**, 525 (1942); see also, W. DÖRING and V. ZEHLER: *Ann. der Phys.*, VI, **13**, 214 (1953).

Linear combinations of plane waves (L.C.P.W.) belonging to a given row of any of the irreducible representations are derived from the sets of plane waves indicated in Table I by the standard method of projection operators (9). Typical crystal symmetry L.C.P.W. at the points Γ and X are given in Table II of HERMAN's paper (2). At the point L the C.S.L.C.P.W. are the same as in the face centered cubic lattice; a few of them are reported in Table V of CASELLA's paper (1). The C.S.L.C.P.W. we have used at the point $\Delta(\frac{1}{2})$ are given in Table II.

TABLE II. – *Crystal symmetry linear combinations of plane waves at the point* $\boldsymbol{k} = (2\pi/a)\ (\frac{1}{2}, 0, 0)$.

$(2\pi/a)^{-1}(\boldsymbol{k}+\boldsymbol{h})$	Δ_1	$\Delta_{2'}$	$\Delta_{1'}$	Δ_2	Δ_5^{I}	Δ_5^{II}
$(\frac{1}{2}, 0, 0)$	+1	—	—	—	—	—
$(\frac{1}{2}, 1, 1)$	+1	+1	—	—	+1	−1
$(\frac{1}{2}, \bar{1}, \bar{1})$	−1	−1	—	—	+1	−1
$(\frac{1}{2}, \bar{1}, 1)$	+1	−1	—	—	−1	−1
$(\frac{1}{2}, 1, \bar{1})$	+1	−1	—	—	+1	+1
$(\frac{3}{2}, 0, 0)$	—	+1	—	—	—	—
$(\frac{3}{2}, 1, 1)$	+1	+1	—	—	+1	−1
$(\frac{3}{2}, \bar{1}, \bar{1})$	−1	−1	—	—	+1	−1
$(\frac{3}{2}, \bar{1}, 1)$	−1	+1	—	—	+1	+1
$(\frac{3}{2}, 1, \bar{1})$	−1	+1	—	—	−1	−1
$(\frac{1}{2}, 2, 0)$	—	+1	+1	—	0	−1
$(\frac{1}{2}, \bar{2}, 0)$	—	−1	−1	—	0	−1
$(\frac{1}{2}, 0, 2)$	—	+1	−1	—	+1	0
$(\frac{1}{2}, 0, \bar{2})$	—	−1	+1	—	+1	0
$(\frac{5}{2}, 0, 0)$	—	+1	—	—	—	—
$(\frac{3}{2}, 2, 0)$	+1	—	—	+1	+1	0
$(\frac{3}{2}, \bar{2}, 0)$	−1	—	—	−1	+1	0
$(\frac{3}{2}, 0, 2)$	+1	—	—	−1	0	−1
$(\frac{3}{2}, 0, \bar{2})$	−1	—	—	+1	0	−1

In the first column the P.W.'s are indicated by the components of the vector $(2\pi/a)^{-1}(\boldsymbol{k}+\boldsymbol{h})$. The linear combination from a set of plane waves with given value of $|\boldsymbol{k}+\boldsymbol{h}|$ can be obtained from the table above multiplying each plane wave by the coefficient listed on the same row and in the column of the irreducible representation of interest. The two basis functions of the two-dimensional irreducible representation Δ_5 are indicated by Δ_5^{I} and Δ_5^{II}.

(9) L. D. LANDAU and E. M. LIFSHITZ: *Quantum Mechanics* (translated) (London, 1958), p. 336; G. F. KOSTER: *Notes on Group Theory*, in *Technical Report* No. 8-M.I.T (1956).

The problem of finding the energy eigenvalues E corresponding to every irreducible representation thus reduces to that of diagonalizing a secular determinant whose elements are sums of matrix elements of the operator $(H - E)$ between the plane waves of two C.S.L.C.P.W. orthogonalized to the core states. The order of the secular determinant is fixed by the number of C.S.L.C.P.W. used. If the crystal one-electron potential is chosen to be a sum of suitable atomic potentials V_a centered at the atomic sites, the matrix element of $(H - E)$ between the O.P.W.'s having wave vectors $\boldsymbol{k}+\boldsymbol{h}_i$ and $\boldsymbol{k}+\boldsymbol{h}_j$ for a crystal having diamond symmetry and only $(1s)$ core states has the form:

$$(1) \qquad \langle \boldsymbol{k}+\boldsymbol{h}_i | H - E | \boldsymbol{k}+\boldsymbol{h}_j \rangle = [(\boldsymbol{k}+\boldsymbol{h}_j)^2 - E]\,\delta_{ij} + \\ + \cos[(\boldsymbol{h}_i - \boldsymbol{h}_j)\cdot\boldsymbol{d}]\,[V(|\boldsymbol{h}_i - \boldsymbol{h}_j|) - (E_{1s} - E) A^*_{1s}(|\boldsymbol{k}+\boldsymbol{h}_i|) A_{1s}(|\boldsymbol{k}+\boldsymbol{h}_j|)] .$$

The vector $\boldsymbol{d}$ has components $a/4\,(1, 1, 1)$, a being the lattice constant; $V(|\boldsymbol{h}_i - \boldsymbol{h}_j|)$ is the Fourier coefficient of the potential defined by:

$$(2) \qquad V(|\boldsymbol{h}_i - \boldsymbol{h}_j|) = \Omega_0^{-1} \int V_a(\boldsymbol{r}) \exp[-i(\boldsymbol{h}_i - \boldsymbol{h}_j)\cdot\boldsymbol{r}]\,\mathrm{d}^3\boldsymbol{r} ,$$

where Ω_0 is the volume per atom; E_{1s} is the energy of the core state $(1s)$; finally the A_{1s} are the orthogonality coefficients defined by:

$$(3) \qquad A_{1s}(|\boldsymbol{k}+\boldsymbol{h}_i|) = \Omega_0^{-\frac{1}{2}} \int \varphi^*_{1s}(\boldsymbol{r}) \exp[i(\boldsymbol{k}+\boldsymbol{h}_i)\cdot\boldsymbol{r}]\,\mathrm{d}^3\boldsymbol{r} ,$$

where φ_{1s} is the atomic wave function. It is assumed that the Bloch sums for the core states are eigenfunctions of the same hamiltonian H as the valence and conduction states.

3. – Calculation of the parameters.

From Section 2 it can be seen that the parameters needed for the application of the O.P.W. method are: the lattice constant a, the core state energy E_{1s}, the orthogonality coefficients given by (3) and the Fourier coefficients of the potential given by (2). For the present calculation it is assumed that the atomic volume Ω_0 of the hypothetical lithium in the diamond structure is the same as the atomic volume of actual body-centered cubic lithium. This seemed a reasonable choice also because of the experimental evidence that allotropic transformations cause only slight density variations. The lattice constant of metallic lithium extrapolated at 0 °K is taken as 6.518 3 in atomic

units; hence the atomic volume is $\Omega_0 = 138.47$ a.u. and the lattice constant in the diamond lattice turns out to be $a = 10.347$ a.u. For the choice of the potential we have followed a recent calculation of energy levels in metallic lithium performed by GLASSER and CALLAWAY ([10]). They have used the semi-empirical free atom potential constructed by SEITZ ([11]) and have found by numerical integration a core energy $E_{1s} = -3.765$ Ry and its appropriate wave function. We have taken the same value for E_{1s} and have approximated the wave function by the sum of two exponentials $\varphi_{1s}(\boldsymbol{r}) = A \exp[-\alpha r] + B \exp[-\beta r]$; the parameters A, B, α, β were adjusted so as to obtain all the orthogonality coefficients given by GLASSER and CALLAWAY to within 1%. The error so introduced is probably less than the error involved in using atomic functions in the Bloch sum, neglecting overlap. The satisfactory values of the parameters were found to be $A = 6.422$; $B = 2.171$; $\alpha = 3.019$; $\beta = 1.907$; it was verified that with these values the approximated function φ_{1s} was automatically normalized to unity within 1%. The orthogonality coefficients obtained from formula (3) by using this analytical approximation for $\varphi_{1s}(\boldsymbol{r})$ are listed in Table III.

TABLE III. – *Orthogonality coefficients between the* 1s *core wave function and the plane waves.*

$(a^2/4\pi^2)(\boldsymbol{k}+\boldsymbol{h})^2$	$A_{1s}(\lvert\boldsymbol{k}+\boldsymbol{h}\rvert)$	$(a^2/4\pi^2)(\boldsymbol{k}+\boldsymbol{h})^2$	$A_{1s}(\lvert\boldsymbol{k}+\boldsymbol{h}\rvert)$
0	0.32901	4	0.19955
$\frac{1}{4}$	0.31701	$\frac{17}{4}$	0.19441
$\frac{3}{4}$	0.29517	$\frac{19}{4}$	0.18478
1	0.28521	5	0.18026
2	0.25059	6	0.16390
$\frac{9}{4}$	0.24305	$\frac{25}{4}$	0.16019
$\frac{11}{4}$	0.22909	$\frac{27}{4}$	0.15318
3	0.22261	8	0.13771

The crystal potential was constructed following the Wigner-Seitz method as in metallic lithium. In the diamond structure the atomic polyhedra are truncated tetrahedra rather different from spheres. In order to obtain the Fourier coefficients of the potential, however, the integral (2) has been extended over the atomic sphere of radius $r_s = (3\Omega_0/4\pi)^{\frac{1}{3}} = 3.2094$ a.u. Overlapping of nearest spheres corrects in the right way the atomic spherically symmetric

([10]) M. L. GLASSER and J. CALLAWAY: *Phys. Rev.*, **109**, 1541 (1958).

([11]) F. SEITZ: *Phys. Rev.*, **47**, 400 (1935). The potential for Lithium is correctly tabulated by W. KOHN and N. ROSTOKER: *Phys. Rev.*, **94**, 1111 (1954).

potential about each nucleus. The Fourier coefficients calculated from eq. (2) by numerical integration of the Seitz potential are listed in Table IV.

TABLE IV. – *Fourier coefficients of the crystal potential (in Rydbergs).*

$(a^2/4\pi^2)\lvert\boldsymbol{h}\rvert^2$	$V(\lvert\boldsymbol{h}\rvert)$	$(a^2/4\pi^2)\lvert\boldsymbol{h}\rvert^2$	$V(\lvert\boldsymbol{h}\rvert)$
0	— 1.0022	19	— 0.0727 7
3	— 0.3801 2	24	— 0.0685 6
8	— 0.0621 6	27	— 0.0579 9
11	— 0.0407 0	32	— 0.0381 3
16	— 0.0630 7		

4. – Results.

The values given in Section 3 for the various parameters can be substituted in the matrix elements of the secular determinant described in Section 2. The various roots of each of the resulting secular equations converge to the successive eigenvalues of the Hamiltonian as has been proven by MACDONALD [12]. The determinantal equations of third, fourth and fifth order have been solved with the electronic computer of the Engineering School in Milan. The results obtained for the lowest energy levels at different stages of approximation are given in Table V.

It can be seen from Table V that the convergence is not very good with the number of plane waves we have included. This applies particularly to the eigenstates which are automatically orthogonal to the s states by reasons of symmetry, as it was found by F. HERMAN in the case of diamond. Nevertheless we feel confident that the present approximation is sufficiently accurate to determine the energy-band structure in the reduced zone. Adding plane waves of higher energy would lower all levels with-

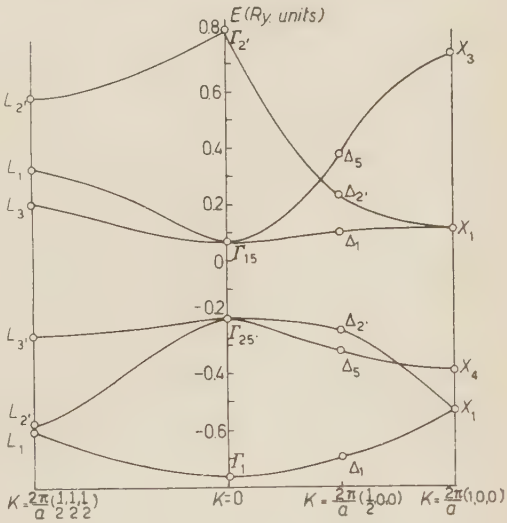

Fig. 1. – Profile of some energy bands of lithium atoms in the diamond structure in the [1, 0, 0] and [1, 1, 1] directions.

[12] J. K. L. MACDONALD: *Phys. Rev.*, **43**, 830 (1933).

out probably changing their relative positions. This was shown to be the case for the Γ point in diamond [2], silicon [4] and germanium [13].

The energy values given in Table V, the compatibility relations and the non-crossing rule allow to draw the profile of the lowest energy bands along the symmetry directions [1, 0, 0] and [1, 1, 1], which is presented in Fig. 1. Naturally this procedure leaves uncertain some of the detailed features of the energy bands such as the curvatures, but we have preferred not to use an interpolation scheme, since we are mainly interested in the sequence of the energy bands and in their qualitative features.

TABLE V. – *Energies at the points* $\boldsymbol{k}=0$ $\boldsymbol{k}=2\pi a^{-1}(1,0,0)$, $\boldsymbol{k}=2\pi a^{-1}(\frac{1}{2},0,0)$, $\boldsymbol{k}=2\pi a^{-1}(\frac{1}{2},\frac{1}{2},\frac{1}{2},)$ *(in Rydbergs).*

	Γ_1	$\Gamma_{25'}$	Γ_{15}	$\Gamma_{2'}$	—	—
E_1	— 0.667	0.166	0.166	0.828	—	—
E_2	— 0.757	— 0.163	0.068	0.825	—	—
E_3	— 0.771	— 0.206	—	—	—	—
	$X_1(1)$	X_4	$X_1(2)$	X_3	—	—
E_1	— 0.356	— 0.203	—	0.904	—	—
E_2	— 0.439	— 0.382	0.208	0.732	—	—
E_3	— 0.455	— 0.392	0.186	—	—	—
E_4	— 0.503	—	0.121	—	—	—
E_5	— 0.534	—	0.111	—	—	—
	$\Delta_1(1)$	$\Delta_5(1)$	$\Delta_{1'}(1)$	$\Delta_1(2)$	$\Delta_{2'}(2)$	$\Delta_5(2)$
E_1	— 0.591	— 0.110	0.053	—	—	—
E_2	— 0,647	— 0.243	— 0.127	0.253	0.375	0.627
E_3	— 0.688	— 0.262	— 0.142	0.138	0.316	0.385
E_4	— 0.701	— 0.320	— 0.237	0.099	0.233	0.376
E_5	—	—	— 0.250	—	—	—
	$L_1(1)$	$L_{2'}(1)$	$L_{3'}$	L_3	$L_1(2)$	$L_{2'}(2)$
E_1	— 0.370	— 0.510	— 0.166	0.314	—	—
E_2	— 0.427	— 0.551	— 0.223	0.220	0.477	0.668
E_3	— 0.565	— 0.553	— 0.268	0.204	0.476	0.666
E_4	— 0.574	— 0.569	—	—	0.385	0.662
E_5	— 0.598	— 0.589	—	—	0.327	0.577

The subscripts attached to E indicate the order of the secular determinant used in obtaining the energies.

[13] F. HERMAN: *Physica*, **20**, 801 (1954).

5. – Conclusions.

First it seems of interest to compare Fig. 1 with Fig. 1 of HERMAN's paper on the diamond energy-band calculation with the O.P.W. method. There the crystal potential is taken as a sum of carbon atomic potentials extending to infinity, furthermore the carbon atoms are more closely packed than the lithium atoms in the pseudo-crystal, the lattice constant in diamond being 6.73 a.u. to be compared with our 10.347 a.u. In spite of these differences the sequence of the energy bands at each point is the same in both cases and their relative positions at different points of the reduced zone are also preserved. The maximum of the valence bands and the minimum of the conduction bands occur at the center of the zone, the energy gap being larger in the case of diamond (0.45 Ry to 0.27 Ry). This last result is due to the smaller electron density in the pseudo-crystal than in diamond, which results in a smaller width of the energy bands consistently with the fact that in the « empty lattice » the eigenvalues are closer when the lattice constant is larger. A comparison with Herman's data also shows that in our case the states Γ_1 and $\Gamma_{2'}$ are shifted to higher energies with respect to Γ_{15} and $\Gamma_{25'}$. This can be attributed to the larger effect of the (1*s*) core state, whose wave function is more spread out in lithium than in carbon.

These results seem to point to the possibility discussed by T.O. WOODRUFF ([6]) and by J. CALLAWAY ([14]) that the sequence of the energy bands is independent of the specific atomic potential and can be predicted by the lattice symmetry and the atomic structure.

A calculation analogous to the one reported here was recently performed by F. BASSANI ([3]) on sodium atoms in the diamond lattice. The energy bands which result in that case display a strict similarity with the energy bands of silicon. They both differ from the bands in diamond and in our pseudo-crystal because the energy at Γ_{15} lies higher than at $X_1(2)$. This may be attributed to the presence of the (2*p*) core states in sodium and silicon, since they raise the energies at Γ_{15} and $\Gamma_{25'}$ more than at $X_1(2)$. In fact the leading crystal symmetry combination of plane waves which corresponds to the eigenstate $X_1(2)$ is orthogonal to the *p* states and consequently, in the perturbation approach described in Appendix A, the eigenvalue is insensitive to the effect of the *p* core states, up to the second order.

It might be of interest to compare our results with the energy bands in metallic lithium ([10,15]). In that case there is no possibility for an energy gap due to the order of appearance of the energies at the points $\boldsymbol{k} = 0$ and

---

([14]) J. CALLAWAY: *Phys. Rev.*, **103**, 1219 (1956).

$\boldsymbol{k} = 2\pi a^{-1}(1, 0, 0)$ in the b.c.c. lattice. The value of the energy at Γ_1 lies lower in our case than in lithium. The value of the effective mass obtained averaging the values calculated by fitting parabolas to the points given in Fig. 1 for the lower band is about the same as in metallic lithium ([15]).

For these reasons, if one neglects the contribution to the cohesive energy due to electrostatic interactions, exchange and correlation effects, the cohesive energy should be greater in our case than in metallic lithium by about 0.1 Ry. Very likely this means that in the diamond structure electrostatic interaction, exchange and correlation effects do not compensate as in the body centered cubic structure ([16]).

* * *

The authors are indebted to Professor F. G. FUMI for his interest and advices; they wish to thank also Dr. D. LYNCH for a reading of the manuscript.

APPENDIX

The determination of the crystal eigenstates by the O.P.W. method may be regarded approximately as a perturbation procedure on the « empty lattice » eigenstates.

A crystal eigenfunction $\psi_i^{\alpha}(\boldsymbol{k}, \boldsymbol{r})$ belonging to the α irreducible representation of the group of $\boldsymbol{k}$ can be expanded as follows:

$$\psi_i^{\alpha}(\boldsymbol{k}, \boldsymbol{r}) = S_i(\boldsymbol{k}, \boldsymbol{r}) - \sum_l \langle \Phi_l | S_i \rangle \Phi_l(\boldsymbol{k}, \boldsymbol{r}) + \tag{A.1}$$

$$+ \sum_j a_j S_j(\boldsymbol{k}, \boldsymbol{r}) - \sum_l \sum_j a_j \langle \Phi_l | S_j \rangle \Phi_l(\boldsymbol{k}, \boldsymbol{r}) + \ldots$$

Here $S_j(\boldsymbol{k}, \boldsymbol{r})$ are the linear combinations of plane waves belonging to the α irreducible representation; the unperturbed wave function $S_i(\boldsymbol{k}, \boldsymbol{r})$ belongs to an eigenstate of the « empty lattice », whose degeneracy has been fully removed by the symmetry analysis. The Bloch wave function of the l core state has been indicated by $\Phi_l(\boldsymbol{k}, \boldsymbol{r})$. The expansion coefficients a_j and the square moduli of the « orthogonality coefficients » $\langle \Phi_l | S_i \rangle$ will be considered small quantities, higher order terms having been omitted in expansion (A.1).

The crystal Hamiltonian H, in atomic units, is:

$$H = -\nabla^2 + V(0) + V_1 = H_0 + V_1 . \tag{A.2}$$

In this formula $V(0)$ is the Fourier coefficient of the crystal potential V for $\boldsymbol{h} = 0$, *i.e.* the space average of V, and $V_1 = V - V(0)$ shall be considered as

([15]) R. H. PARMENTER: *Phys. Rev.*, **86**, 552 (1952).
([16]) F. SEITZ: *Modern Theory of Solids* (New York, 1940), p. 364.

a perturbing potential. Let the eigenvalue of H_0 belonging to the eigenfunction S_j be W_j; let the first and second order corrections to the unperturbed energy W_i be W_i' and W_i''. By substituting expansion (A.1) into the equation:

$$H\psi_i^{\alpha}(\boldsymbol{k}, \boldsymbol{r}) = (W_i + W_i' + W_i'' + ...)\psi_i^{\alpha}(\boldsymbol{k}, \boldsymbol{r}) , \tag{A.3}$$

and using the techniques of perturbation theory one obtains to first order:

$$\langle S_j | V_1 | S_i \rangle - \sum_l \langle \Phi_l | S_i \rangle \langle S_j | H | \Phi_l \rangle + a_j W_j = \\ = W_i' \delta_{ij} - W_i \sum_l \langle \Phi_l | S_i \rangle \langle S_j | \Phi_l \rangle + a_j W_i . \tag{A.4}$$

As usual, one can assume for the core states:

$$H\Phi_l(\boldsymbol{k}, \boldsymbol{r}) = E_l \Phi_l(\boldsymbol{k}, \boldsymbol{r}) , \tag{A.5}$$

where E_l is the atomic value. Then from (A.4):

$$W_i' = \langle S_i | V_1 | S_i \rangle + \sum_l (W_i - E_l) | \langle \Phi_l | S_i \rangle |^2 . \tag{A.6}$$

The values of the coefficients a_j can be obtained from formula (A.4) for $i \neq j$. The value of the coefficient a_i is found to be $\frac{1}{2} \sum_l | \langle \Phi_l | S_i \rangle |$ by requiring normalization of $\psi_i'(\boldsymbol{k}, \boldsymbol{r})$ to first order.

Proceeding to second order one finds:

$$W_i'' = \sum_j (W_i - W_j)^{-1} | \langle S_j | V_1 | S_i \rangle - \sum_l (E_l - W_i) \langle \Phi_l | S_i \rangle \langle S_j | \Phi_l \rangle |^2 + \\ + \sum_l | \langle \Phi_l | S_i \rangle |^2 W_i' . \tag{A.7}$$

It can be seen from formulae (A.6) and (A.7) that the core wave function $\Phi_l(\boldsymbol{k}, \boldsymbol{r})$ has no effect on the energy when $\langle \Phi_l | S_i \rangle = 0$.

RIASSUNTO

Si considera un ipotetico cristallo costituito di atomi di litio nella struttura del diamante e avente la stessa densità di elettroni del litio metallico. Usando un potenziale del tipo di Wigner e Seitz, si calcolano col metodo delle onde piane ortogonalizzate i valori delle energie nei punti speciali della zona ridotta con $\boldsymbol{k} = (0, 0, 0)$, $\boldsymbol{k} = 2\pi a^{-1}(1, 0, 0)$, $\boldsymbol{k} = 2\pi a^{-1}(\frac{1}{2}, 0, 0)$ e $\boldsymbol{k} = 2\pi a^{-1}(\frac{1}{2}, \frac{1}{2}, \frac{1}{2})$ e si tracciano le curve dell'energia in funzione di $\boldsymbol{k}$ nelle direzioni [1, 0, 0] e [1, 1, 1]. Le bande di energia così ottenute sono paragonate con le bande di energia del diamante valutate da F. Herman. Il fatto che le posizioni relative delle bande risultino le stesse nei due casi indica la possibilità che la struttura delle bande di energia sia principalmente determinata dalla simmetria del reticolo. Dal confronto con il litio metallico, si trova che l'energia coesiva è maggiore nel caso dello pseudoreticolo, quando si trascurino i termini elettrostatici, di scambio e di correlazione.

Quadratic Lagrangians and General Relativity.

P. W. Higgs

Department of Mathematics, Imperial College - London (*)

(ricevuto il 31 Dicembre 1958)

Summary. — Two out of the three sets of field equations associated with Lagrangians quadratic in the Riemann-Christoffel tensor, which were recently discussed by Stephenson, are shown to be equivalent to the source-free Einstein equations with an arbitrary « cosmological » term.

1. – Introduction.

In a recent paper Stephenson (1) has discussed the field equations which one obtains by applying the Palatini method (independent variation of the metric tensor $g_{\mu\nu}$ and the affine connection $\Gamma^{\varkappa}_{\alpha\beta}$) to action integrals constructed from three Lagrangian densities quadratic in the Riemann-Christoffel tensor, it being assumed that both metric and connection are symmetric. The following are the action integrals and associated field equations.

Case (A). $$I_A = \int \mathrm{d}^4 x R^2 \sqrt{-g}\,;$$

(1) $$R(R_{\mu\nu} - \tfrac{1}{4} R g_{\mu\nu}) = 0\,,$$

(2) $$(R g^{\alpha\beta}\sqrt{-g})_{;\varkappa} = 0\,.$$

Case (B). $$I_B = \int \mathrm{d}^4 x R_{\lambda\mu} R^{\lambda\mu}\sqrt{-g};$$

(3) $$(R_{\mu\varrho}R_{\nu\sigma} + R_{\varrho\mu}R_{\sigma\nu})g^{\varrho\sigma} - \tfrac{1}{2} R_{\varrho\sigma} R^{\varrho\sigma} g_{\mu\nu} = 0\,,$$

(4) $$(R^{\alpha\beta}\sqrt{-g})_{;\varkappa} = 0\,.$$

(*) Now at the Department of Mathematics, University College, London.

(1) G. Stephenson: *Nuovo Cimento*, **9**, 263 (1958).

Case (C). $$I_C = \int \mathrm{d}^4 x R^{\varkappa}{}_{\lambda\mu\nu} R_{\varkappa}{}^{\lambda\mu\nu} \sqrt{-g} ;$$

(5) $$- R_{\mu\varrho\sigma\tau} R_{\nu}{}^{\varrho\sigma\tau} + R^{\pi}{}_{\mu\sigma\tau} R_{\pi\nu}{}^{\sigma\tau} + 2 R_{\pi\varrho\mu}{}^{\tau} R^{\pi\varrho}{}_{\nu\tau} - \tfrac{1}{2} R_{\pi\varrho\sigma\tau} R^{\pi\varrho\sigma\tau} g_{\mu\nu} = 0 ,$$

(6) $$(R_{\varkappa}^{\underline{\alpha\beta\gamma}} \sqrt{-g})_{;\gamma} = 0 .$$

In these equations

$$R^{\varkappa}{}_{\lambda\mu\nu} = - \Gamma^{\varkappa}{}_{\lambda\mu,\nu} + \Gamma^{\varkappa}{}_{\lambda\nu,\mu} + \Gamma^{\varkappa}{}_{\alpha\mu} \Gamma^{\alpha}{}_{\lambda\nu} - \Gamma^{\varkappa}{}_{\alpha\nu} \Gamma^{\alpha}{}_{\lambda\mu} ,$$

$$R_{\lambda\mu} = R^{\nu}{}_{\lambda\mu\nu}$$

and the remaining tensors are constructed from these with the aid of $g_{\mu\nu}$ in the usual way. A comma indicates ordinary differentiation, a semicolon covariant differentiation with respect to $\Gamma^{\varkappa}{}_{\alpha\beta}$. A bar placed under tensor indices denotes symmetrization.

Stephenson [2] has further shown that all these Lagrangian densities are invariant under the Weyl gauge transformations

(7) $$\begin{cases} g_{\mu\nu} \to \varphi g_{\mu\nu} , \\ \Gamma^{\varkappa}{}_{\alpha\beta} \to \Gamma^{\varkappa}{}_{\alpha\beta} , \end{cases}$$

where $\varphi(x)$ is an arbitrary scalar function of the co-ordinates. A direct consequence of this invariance is the vanishing of the trace of one set of equations (namely (1), (3), (5)) in each case.

The purpose of this note is to show that in cases (A) and (B) one set of equations may be transformed into field equations of the Einstein type with an *arbitrary* « cosmological constant » in terms of a new gauge-invariant metric. The other set provides algebraic relations between the old metric and the new, the solution of which contains the arbitrary gauge function. No such transformation has yet been found in case (C).

2. – Case (A).

Assuming that $R \neq 0$, we first take the trivial step of rewriting (1), (2) in the form

(1*a*) $$R_{\underline{\mu\nu}} = \lambda \psi^{-1} g_{\mu\nu} ,$$

(2*a*) $$(\psi^{-1} g^{\alpha\beta} \sqrt{-g})_{;\varkappa} = 0 ,$$

---

[2] G. Stephenson: *Quart. Journ. Math.* (*Oxford*), to be published.

where $\psi(x)$ is an arbitrary dimensionless scalar function and λ is an arbitrary constant of dimension (length)$^{-2}$. If we now introduce a new metric tensor $a_{\mu\nu}$, defined by

$$g_{\mu\nu} = \psi a_{\mu\nu} , \tag{8}$$

together with its contravariant inverse $a^{\mu\nu}$ and its determinant a, these equations become

$$R_{\underline{\mu\nu}} = \lambda a_{\mu\nu} , \tag{9}$$

$$(a^{\alpha\beta}\sqrt{-a})_{;\varkappa} = 0 . \tag{10}$$

Clearly we may regard $a_{\mu\nu}$ as a gauge scalar and write the gauge transformation (7) as $\psi \to \varphi\psi$.

The most general solution of (10) is

$$\Gamma^{\varkappa}_{\alpha\beta} = \tfrac{1}{2} a^{\varkappa\varrho}(a_{\alpha\varrho,\beta} + a_{\varrho\beta,\alpha} - a_{\alpha\beta,\varrho}) . \tag{11}$$

Consequently $R_{\mu\nu}$ is symmetric and equations (9) are of the Einstein type with an arbitrary cosmological constant λ. They are to be regarded as second-order differential equations in the gauge invariant metric $a_{\mu\nu}$. From any solution of these equations we may recover a family of metrics $g_{\mu\nu}$ by using equation (8), which contains the arbitrary gauge function ψ.

3. – Case (B).

This time we use as our definition of the new metric $b_{\mu\nu}$ the equations

$$b^{\alpha\beta}\sqrt{-b} = \lambda^{-1} R_{\underline{\mu\nu}} g^{\mu\alpha} g^{\nu\beta}\sqrt{-g} , \tag{12}$$

where again λ is an arbitrary constant of dimension (length)$^{-2}$. Equations (4) then become

$$(b^{\alpha\beta}\sqrt{-b})_{;\varkappa} = 0 , \tag{13}$$

of which the general solution is

$$\Gamma^{\varkappa}_{\alpha\beta} = \tfrac{1}{2} b^{\varkappa\varrho}(b_{\alpha\varrho,\beta} + b_{\varrho\beta,\alpha} - b_{\alpha\beta,\varrho}) . \tag{14}$$

As a consequence, $R_{\mu\nu}$ is again symmetric and we may rewrite (12) as

$$R_{\mu\nu} = \lambda\sqrt{b/g}\, g_{\mu\alpha} g_{\nu\beta} b^{\alpha\beta} . \tag{15}$$

On substituting this expression into (3) we obtain

$$g_{\mu\alpha}b^{\alpha\beta}g_{\beta\varrho}b^{\varrho\sigma}g_{\sigma\nu} = \tfrac{1}{4}\, g_{\alpha\varrho}\, g_{\beta\sigma}b^{\alpha\beta}b^{\varrho\sigma}g_{\mu\nu}$$

which may be rewritten as

$$g_{\mu\alpha}b^{\alpha\beta}g_{\beta\nu}b^{\nu\varrho} = \psi^2\delta_\mu{}^\varrho\,, \tag{16}$$

where $\psi(x)$ is an arbitrary scalar function. By combining (15) and (16) we finally obtain once more

$$R_{\mu\nu} = \lambda b_{\mu\nu}\,, \tag{17}$$

which is to be regarded as a second-order differential equation in $b_{\mu\nu}$. From any solution of (17) a family of metrics $g_{\mu\nu}$ may be constructed by solving the algebraic equations (16). These have amongst their solutions the simple relation

$$g_{\mu\nu} = \psi b_{\mu\nu}\,. \tag{18}$$

However, (16) may be written in matrix notation as

$$(\boldsymbol{g}\boldsymbol{b}^{-1})^2 = \psi^2\,\mathbf{1}\,,$$

from which it is clear that besides (18) there are other classes of solutions corresponding to various square roots of the 4×4 unit matrix. In all the classes of solutions $b_{\mu\nu}$ is to be regarded as a gauge scalar and ψ as an arbitrary gauge function transforming under (7) as $\psi \to \varphi\,\psi$.

3. – Case (C).

In both cases (A) and (B) we have been enabled to define the new metric by the fact that the second set of equations, (2), (4), has the form

$$\mathfrak{T}^{\alpha\beta}{}_{;\varkappa} = 0\,,$$

where $\mathfrak{T}^{\varkappa\beta}$ is a symmetric tensor density. This is not true in case (C), so it does not appear that equations (5) and (6) can be transformed into the Einstein equations.

4. – Remarks.

One comment should perhaps be made on the interpretation of the metric tensors in these gauge invariant theories. Presumably one wants the concept of length in such theories to be gauge invariant. Therefore it seems likely that more direct physical significance may be attached to $a_{\mu\nu}$ and $b_{\mu\nu}$ than to the original dynamic variables $g_{\mu\nu}$ which enter into the action principle. This is analogous to the situation in electrodynamics.

* * *

I am grateful to Dr. G. STEPHENSON for arousing my interest in this problem and for various helpful comments. The work was performed during the tenure of an I.C.I. Research Fellowship.

RIASSUNTO (*)

Si dimostra che due dei tre sistemi di equazioni di campo associati a lagrangiani quadratici nel tensore di Riemann-Christoffel, recentemente discussi da STEPHENSON, sono equivalenti alle equazioni di Einstein prive di sorgente con un termine « cosmologico » arbitrario.

(*) *Traduzione a cura della Redazione.*

IL NUOVO CIMENTO Vol. XI, N. 6 16 Marzo 1959

Spectral Functions in the Static Theory.

J. D. Walecka (*)

CERN - Geneva

(ricevuto il 31 Dicembre 1958)

Summary. — The spectral functions of the electromagnetic form factors of the nucleon are discussed within the framework of the static theory. $1/M$ recoil corrections are also included and it is shown that these corrections are close to those given by dispersion theory and that they profoundly alter the spectral functions indicating that the application of the static model to this problem is of doubtful validity.

1. – Introduction.

The spectral functions $G_{E,M}(\sigma^2)$ describing the electromagnetic properties of nucleons are related to the form factors $F_{E,M}(q^2)$ by

$$F_{E,M}(q^2) = \frac{1}{\pi}\int_{4\mu^2}^{\infty} \frac{G_{E,M}(\sigma^2)\,\mathrm{d}\sigma^2}{\sigma^2 + q^2}\,, \tag{1}$$

where q^2 is the four-momentum transfer occurring at the electromagnetic vertex and $\mu = m_\pi$. The spectral functions can be regarded as the quantities of fundamental theoretical interest and there have been two recent attempts at the calculation of these quantities using dispersion theory, one by Chew, Karplus, Gasiorowicz, and Zachariasen and the other by Federbush, Goldberger, and Treiman [1,2].

(*) National Science Foundation Postdoctoral Fellow.

(1) G. F. Chew, R. Karplus, S. Gasiorowicz and F. Zachiariasen: *Phys. Rev.*, **110**, 265 (1958).

(2) P. Federbusch, M. Goldberger and S. Treiman: *Phys. Rev.*, **112**, 642 (1958).

The purpose of this paper is two-fold. First it will be shown how one can calculate the spectral functions within the framework of the static theory and that the functions thus calculated agree with the static limit of the dispersion theory result. The validity of equation (1) has not yet been proved in the framework of relativistic field theory. Moreover, the computations of the spectral functions mentioned above are based on the analytic continuation of the pion-nucleon scattering amplitude for unphysical values of the angle. Therefore, it is thought useful to associate with these calculations a straightforward computation based on a simple model.

The advantage of dealing directly with the spectral functions instead of the form factors in the static theory is that in the no cut-off limit the former are finite whereas the latter are not. Now it might be hoped that the static theory would at least explain the low σ^2 part of the spectral functions, but the work of references (1) and (2) has shown that the discrepancy between dispersion theory results and their static limits are great and that they persist even down to $\sigma^2 = 4\mu^2$ (3) Therefore, the second problem dealt with here will be the result of including the $1/M$ nucleon recoil corrections into the framework of the static model and showing, that

a) the presence of these purely kinematical corrections profoundly alters the spectral function;

b) the kinematical $1/M$ corrections are in good agreement with the $1/M$ corrections calculated by dispersion theory techniques indicating that this is the main source of difference between the two theories.

The first conclusion indicates that one can have little faith in the predictions of the static theory in the electromagnetic structure problem. Also, since the partial waves of higher l value (the scattering in these states is known neither experimentally, nor theoretically), become very important in the calculation of $G_{E,M}(\sigma^2)$, there may be some doubt as to the validity of using only S and P waves in the analytic continuation of the meson-nucleon scattering amplitude as is done in the dispersion theory approach.

The calculation of the electromagnetic properties of the nucleon in the static theory has been discussed by several authors (4). In this work the notation of the last author (F) shall be used. The introduction of nucleon recoil is based on the work of Bosco, Fubini and Stanghellini (5), who use the

(3) S. Drell: *Proceedings of the 8-th Annual Conference on High Energy Physics* (Geneva, 1958).

(4) G. Salzman: *Phys. Rev.*, **99**, 973 (1955); **105**, 1076 (1957); H. Miyazawa: *Phys. Rev.*, **101**, 1564 (1956); S. Treiman and R. G. Sachs: *Phys. Rev.*, **103**, 435 (1956); F. Zachiariasen: *Phys. Rev.*, **102**, 295 (1956); S. Fubini: *Nuovo Cimento*, **3**, 1425 (1956).

(5) B. Bosco, S. Fubini and A. Stanghellini: to be published.

procedure to reproduce, up through D waves, the meson-nucleon scattering phase shifts calculated from dispersion theory.

In Section 2, the working equations are derived. In Section 3 the spectral functions are calculated and in Section 4 they are related to the corresponding quantities from the relativistic theory.

2. – Derivation of equations.

In the following, the Breit frame will be used, that is, the initial nucleon momentum is $-\boldsymbol{q}/2$ and the final nucleon momentum is $+\boldsymbol{q}/2$, where $\boldsymbol{q}$ is the momentum of the photon from the external field. In this system there is no energy transferred to the nucleon and hence $q^2 = \boldsymbol{q}^2$ and also there is only momentum vector, $\boldsymbol{q}$ for constructing invariants. Now

$$H|\pm\boldsymbol{q}/2\rangle = E_{q/2}|\pm\boldsymbol{q}/2\rangle = (M^2 + (\boldsymbol{q}/2)^2)^{\frac{1}{2}}|\pm\boldsymbol{q}/2\rangle ,$$

where H is the total meson-nucleon Hamiltonian and $|\pm\boldsymbol{q}/2\rangle$ is a physical nucleon. One thus includes the proper kinematics by replacing H by $E_{q/2}$ when acting on a physical nucleon state but then uses the static model for the dynamics and sums overs states. The reason for this is that the dynamics of the static model are relatively simple. To calculate corrections rigorously to $1/M$ one must also, of course, include $1/M$ modifications of the dynamics or H, but this complicates matters and it will be shown that the kinematical corrections alone are sufficient to give $1/M$ corrections similar to those of dispersion theory.

One starts from (F)

$$\varrho(x) = \frac{ie}{2\Omega}\sum_{\boldsymbol{k},\boldsymbol{k}'}\frac{\exp[i(\boldsymbol{k}+\boldsymbol{k}')\cdot\boldsymbol{x}]}{(\omega_k\omega_{k'})^{\frac{1}{2}}}[(\omega_k-\omega_{k'})(a_{\boldsymbol{k}'2}\,a_{\boldsymbol{k}1}-a^*_{-\boldsymbol{k}'2}a^*_{-\boldsymbol{k}1})- \\ -(\omega_k+\omega_{k'})(a^*_{-\boldsymbol{k}'1}a_{\boldsymbol{k}2}-a^*_{-\boldsymbol{k}'2}\,a_{\boldsymbol{k}1})] ,$$

$$j(x)_\mu = \frac{-ie}{2\Omega}\sum_{\boldsymbol{k},\boldsymbol{k}'}\frac{\exp[i(\boldsymbol{k}+\boldsymbol{k}')\cdot\boldsymbol{x}]}{(\omega_k\omega_{k'})^{\frac{1}{2}}}[k'_\mu-k_\mu](a^*_{-\boldsymbol{k}'2}\,a_{\boldsymbol{k}1}+ \\ +a^*_{-\boldsymbol{k}1}a_{\boldsymbol{k}'2}+a^*_{-\boldsymbol{k}'2}a^*_{-\boldsymbol{k}1}+a_{\boldsymbol{k}'2}a_{\boldsymbol{k}1}) ,$$

which are the expressions for the charge and current densities in the meson field. The subscripts 1 and 2 refer to the isotopic spin of the Hermitian charged fields. What one wants to calculate is the transition probability

$$\omega = \langle\boldsymbol{q}/2\left|\int d^3x(\varrho(x)\Phi^{\text{ext.}}(x) - j(x)\cdot\boldsymbol{A}^{\text{ext.}}(x))\right|-\boldsymbol{q}/2\rangle ,$$

where one takes

$$\Phi^{\text{ext.}}(x) = \varphi \exp[i\boldsymbol{q}\cdot\boldsymbol{x}]$$

$$\boldsymbol{A}^{\text{ext.}}(x) = \boldsymbol{a} \exp[i\boldsymbol{q}\cdot\boldsymbol{x}]$$

and defines (using invariance properties).

$$\omega = f_E(\boldsymbol{q}^2)\varphi - i\boldsymbol{\sigma}\cdot(\boldsymbol{q}\wedge\boldsymbol{a})f_M(\boldsymbol{q}^2)\,.$$

The f's are the form factors in the static theory. The procedure is to relate the expectation value of pairs of creation and annihilation operators to the meson nucleon scattering amplitudes (F). $a^*_{k\lambda}a_{k'\alpha'}$ shall be used as an example in the following and then the results given for all pairs, starting from

$$H = H_0 + H_1\,,$$

$$[H_0, a^*_{k\alpha}] = \omega_k a^*_{k\alpha}\,,$$

$$[H_1, a^*_{k\alpha}] \equiv V_{k\alpha}\,,$$

$$\langle \boldsymbol{q}/2\,|[H, a^*_{k\alpha}a_{k'\alpha'}]|-\boldsymbol{q}/2\rangle = 0\,,$$

one finds

$$\langle \boldsymbol{q}/2\,|\,a^*_{k\alpha}a_{k'\alpha'}|-\boldsymbol{q}/2\rangle = \frac{-1}{\omega_k - \omega_{k'}}\sum_n \langle \boldsymbol{q}/2\,|\,V_{k\lambda}\,|\,n\rangle\cdot$$
$$\cdot\langle n\,|\,a_{k'\alpha'}|-\boldsymbol{q}/2\rangle - \langle \boldsymbol{q}/2\,|\,a^*_{k\alpha}|\,n\rangle\langle n\,|\,V^+_{k'\alpha'}|-\boldsymbol{q}/2\rangle\,.$$

Taking matrix elements of the following relations ($\boldsymbol{p}$ is the total momentum operator)

$$[\boldsymbol{p}, a^*_{k\alpha}] = \boldsymbol{k}a^*_{k\alpha}\,,$$

$$[\boldsymbol{p}, a^*_{k\alpha}a_{k'\alpha'}] = (\boldsymbol{k}-\boldsymbol{k}')a^*_{k\alpha}a_{k'\alpha'}\,,$$

one gets

$$(\boldsymbol{p}_m - \boldsymbol{p}_n - \boldsymbol{k})\langle m\,|\,a^*_{k\alpha}\,|\,n\rangle = 0\,,$$

$$(\boldsymbol{p}_m - \boldsymbol{p}_n + \boldsymbol{k})\langle m\,|\,a_{k\alpha}\,|\,n\rangle = 0\,,$$

$$(\boldsymbol{p}_m - \boldsymbol{p}_n - \boldsymbol{k} + \boldsymbol{k}')\langle m\,|\,a^*_{k\alpha}a_{k'\alpha'}\,|\,n\rangle = 0$$

expressing the conservation of momentum.
Also from

$$[H, a_{k\alpha}]\,|\pm\boldsymbol{q}/2\rangle = (H - E_{q/2})a_{k\alpha}\,|\pm\boldsymbol{q}/2\rangle$$

one has

$$a_{k\alpha}\,|\pm q/2\rangle = \frac{-1}{H+\omega_k-E_{q/2}}\,V^+_{k\alpha}\,|\pm q/2\rangle\,.$$

Therefore

$$\langle q/2\,|\,a^*_{k\alpha}\,a_{k'\alpha'}\,|-q/2\rangle\Big|_{(q=k-k')} = \frac{1}{\omega_k-\omega_{k'}}\sum_n \frac{\langle q/2\,|\,V_{k\alpha}\,|n\rangle\langle n\,|\,V^+_{k'\alpha'}\,|-q/2\rangle}{W_n+\omega_{k'}-E_{q/2}}\Big|_{(k_n=-q/2-k')} -$$

$$-\frac{\langle q/2\,|\,V_{k\alpha}\,|n\rangle\langle n\,|\,V^+_{k'\alpha'}\,|-q/2\rangle}{W+\omega_{nk}-E_{q/2}}\Big|_{(k_m=q/2-k)},$$

W_n is the energy of the intermediate state n. Using

$$W_n = (M_n^2+k_n^2)^{\frac{1}{2}}$$

and

$$\omega_n \equiv M_n - M$$

one finds to order $1/M$ (*i.e.* if $\omega_n/M \ll 1$)

$$W_n - E_{q/2} = \omega_n + \frac{k\cdot k'}{2M}\,.$$

Until now the derivation has been rigorous.

One now uses the static model to evaluate the numerators.

Replacing $|\pm q/2\rangle \to |R\rangle$, where $|R\rangle$ denotes one of the four physical nucleon spin states one has

$$\langle q/2\,|\,a^*_{k\alpha}\,a_{k'\alpha'}\,|-q/2\rangle = \frac{-1}{\omega_k-\omega_{k'}}\sum_n \frac{\langle R\,|\,V_{k\alpha}\,|n\rangle\langle n\,|\,V^+_{k'\alpha'}\,|R\rangle}{\omega_n+\omega_k+(k\cdot k')/2M} -$$

$$-\frac{\langle R\,|\,V_{k\alpha}\,|n\rangle\langle n\,|\,V^+_{k'\alpha'}\,|R\rangle}{\omega_n+\omega_{k'}+(k\cdot k')/2M}\,,$$

$$\langle q/2\,|\,a^*_{k\alpha}\,a^*_{k'\alpha'}\,|-q/2\rangle = \frac{1}{\omega_k+\omega_{k'}}\sum_n \frac{\langle R\,|\,V_{k\alpha}\,|n\rangle\langle n\,|\,V_{k'\alpha'}\,|R\rangle}{\omega_n+\omega_k-(k\cdot k')/2M} +$$

$$+\frac{\langle R\,|\,V_{k'\alpha'}\,|n\rangle\langle n\,|\,V_{k\alpha}\,|R\rangle}{\omega_n+\omega_{k'}-(k\cdot k')/2M}\,,$$

$$\langle q/2\,|\,a_{k\alpha}\,a_{k'\alpha'}\,|-q/2\rangle = \frac{1}{\omega_k+\omega_{k'}}\sum_n \frac{\langle R\,|\,V^+_{k'\alpha'}\,|n\rangle\langle n\,|\,V^+_{k\alpha}\,|R\rangle}{\omega_n+\omega_k-(k\cdot k')/2M} +$$

$$+\frac{\langle R\,|\,V^+_{k\alpha}\,|n\rangle\langle n\,|\,V^+_{k'\alpha'}\,|R\rangle}{\omega_n+\omega_{k'}-(k\cdot k')/2M}\,,$$

where

$$V_{k\alpha} = i\left(\frac{f^0}{\mu}\right)\left(\frac{4\pi}{2\omega_k}\right)^{\frac{1}{2}} (\boldsymbol{\sigma}\cdot\boldsymbol{k})\tau_\alpha v(k) .$$

Notice that the only difference from (F) is the extra term in the denominators. Proceeding as in (F), one writes the unitarity principle

$$\frac{-3i}{2p^3v^2(p)}\langle i\alpha; r|T^\dagger - T|j\alpha'; r\rangle = \left(\frac{f^0}{\mu}\right)^2 \sum_n \delta(\omega_n-\omega_p)(R|\sigma_i\tau_\alpha|n-)(n-|\sigma_j\tau_{\alpha'}|R) ,$$

where T is defined between free meson and bare spinor states and n — is an incoming scattering state. Multiplying this equation by $1/(\omega_p+\omega_k+(\boldsymbol{k}\cdot\boldsymbol{k}'/2M))$ integrating on ω_p from μ to ∞ and noting that the sum one needs is a sum over all states and not just scattering states one finds (*)

$$\left(\frac{f^0}{\mu}\right)^2 \sum_n \frac{(R|\sigma_i\tau_\alpha|n)(n|\sigma_j\tau_{\alpha'}|R)}{\omega_n+\omega_k+(\boldsymbol{k}\cdot\boldsymbol{k}')/2M} =$$

$$= \langle i\alpha; r|\left(\frac{f}{\mu}\right)^2 \frac{(1-\boldsymbol{\sigma}\cdot\boldsymbol{l})(1-\boldsymbol{t}\cdot\boldsymbol{\tau})}{\omega_k+(\boldsymbol{k}\cdot\boldsymbol{k}')/2M} - 3\int_\mu^\infty \frac{d\omega_p}{p^3v^2(p)} \frac{\operatorname{Im} T(\omega_p)}{\omega_k+\omega_p+(\boldsymbol{k}\cdot\boldsymbol{k}')/2M}|j\alpha'; r\rangle ,$$

where f is now the renormalized coupling constant. One now takes into account the experimental evidence of the dominance of the 3-3 scattering resonance. Approximating the contribution of the resonance by a δ-function one has

$$-3\int_\mu^\infty \frac{d\omega_p}{v^2(p)p^3} \frac{\operatorname{Im} T(\omega_p)}{\omega_k+\omega_p+(\boldsymbol{k}\cdot\boldsymbol{k}')/2M} = \left(\frac{a}{\mu}\right)^2 \frac{(2+\boldsymbol{t}\cdot\boldsymbol{\tau})(2+\boldsymbol{l}\cdot\boldsymbol{\sigma})}{\omega_k+\omega_R+(\boldsymbol{k}\cdot\boldsymbol{k}')/2M} ,$$

with a^2 the effective strength ($a^2 = (4/9)f^2$ theoretically) and ω_R the resonance energy ($\omega_R \approx 2\mu$), one finds

$$(\boldsymbol{q}/2|a^*_{k\alpha}a_{-k'\alpha'}|-\boldsymbol{q}/2) = \sum_{ij}\frac{c(k,k')}{\omega_k-\omega_{k'}} k_ik'_j\langle i\alpha r|R(\omega_k)-R(\omega_{k'})|j\alpha' r\rangle ,$$

$$(\boldsymbol{q}/2|a^*_{k\alpha}a^*_{k'\alpha'}|-\boldsymbol{q}/2) = -\sum_{ij}\frac{c(k,k')}{\omega_k+\omega_{k'}} k_ik'_j\langle i\alpha r|R(\omega_k)+\overline{R(\omega_{k'})}|j\alpha' r\rangle ,$$

$$(\boldsymbol{q}/2|a_{k\alpha}a_{k'\alpha'}|-\boldsymbol{q}/2) = -\sum_{ij}\frac{c(k,k')}{\omega_k+\omega_{k'}} k_ik'_j\langle i\alpha r|\overline{R(\omega_k)}+R(\omega_{k'})|j\alpha' r\rangle ,$$

(*) Note [6]:

$$\langle i\alpha; r|1-\boldsymbol{t}\cdot\boldsymbol{\tau}|j\alpha'; r'\rangle = \delta_{ij}\langle r|\tau_\alpha\tau_{\alpha'}|r'\rangle = \langle j\alpha'; r|1+\boldsymbol{t}\cdot\boldsymbol{\tau}|i\alpha; r'\rangle ,$$
$$\langle i\alpha; r|1-\boldsymbol{l}\cdot\boldsymbol{\sigma}|j\alpha'; r'\rangle = \delta_{\alpha\alpha'}\langle r|\sigma_i\sigma_j|r'\rangle = \langle j\alpha'; r|1+\boldsymbol{l}\cdot\boldsymbol{\sigma}|i\alpha; r'\rangle .$$

[6] M. Cini and S. Fubini: *Nuovo Cimento*, **3**, 764 (1956).

with

$$c(k, k') = \frac{2\pi\, v(k)\, v(k')}{(\omega_k\, \omega_{k'})^{\frac{1}{2}}},$$

where

$$R(\omega) = R_1(\omega) + R_2(\omega)(\boldsymbol{\sigma}\cdot\boldsymbol{l} + \boldsymbol{t}\cdot\boldsymbol{\tau}) + R_3(\omega)(\boldsymbol{\sigma}\cdot\boldsymbol{l})(\boldsymbol{t}\cdot\boldsymbol{\tau})$$

$$\langle i\alpha r\,|\,\overline{R(\omega)}\,|\,j\alpha' r'\rangle \equiv \langle j\alpha' r\,|\,R(\omega)\,|\,i\alpha r'\rangle\,,$$

$$R_1(\omega_k) = \left(\frac{f}{\mu}\right)^2\left(\frac{1}{\omega_k} + \frac{\boldsymbol{k}\cdot\boldsymbol{k}'}{2M\omega_k^2}\right) + 4\left(\frac{a}{\mu}\right)^2\left(\frac{1}{\omega_k + \omega_R} + \frac{\boldsymbol{k}\cdot\boldsymbol{k}'}{2M(\omega_k + \omega_R)^2}\right),$$

$$R_2(\omega_k) = -\left(\frac{f}{\mu}\right)^2\left(\frac{1}{\omega_k} + \frac{\boldsymbol{k}\cdot\boldsymbol{k}'}{2M\omega_k^2}\right) + 2\left(\frac{a}{\mu}\right)^2\left(\frac{1}{\omega_k + \omega_R} + \frac{\boldsymbol{k}\cdot\boldsymbol{k}'}{2M(\omega_k + \omega_R)^2}\right),$$

$$R_3(\omega_k) = \left(\frac{f}{\mu}\right)^2\left(\frac{1}{\omega_k} + \frac{\boldsymbol{k}\cdot\boldsymbol{k}'}{2M\omega_k^2}\right) + \left(\frac{a}{\mu}\right)^2\left(\frac{1}{\omega_k + \omega_R} + \frac{\boldsymbol{k}\cdot\boldsymbol{k}'}{2M(\omega_k + \omega_R)^2}\right),$$

$R(\omega_{k'})$ is obtained from $R(\omega_k)$ by interchanging $\boldsymbol{k}$ and $\boldsymbol{k}'$. Substituting in the expressions for $\varrho(x)$ and $j(\boldsymbol{x})$ one has

$$f_E(\boldsymbol{q}^2) = \frac{-e\tau_3}{\pi^2}\iint \mathrm{d}^3k\,\mathrm{d}^3k'\,v(k)\,v(k')\frac{(\boldsymbol{k}\cdot\boldsymbol{k}')\,\delta(\boldsymbol{k} + \boldsymbol{k}' + \boldsymbol{q})}{k^2 - k'^2}\,[R_2(\omega_k) - R_2(\omega_{k'})]\,,$$

$$-i\boldsymbol{\sigma}\cdot(\boldsymbol{q}\wedge\boldsymbol{a})\,f_M(\boldsymbol{q}^2) = \frac{ei\tau_3}{\pi^2}\cdot$$

$$\cdot\iint \mathrm{d}^3k\,\mathrm{d}^3k'\,r(k)\,r(k')\frac{(\boldsymbol{k}\cdot\boldsymbol{a})(\boldsymbol{\sigma}\cdot(\boldsymbol{k}\wedge\boldsymbol{k}'))\,\delta(\boldsymbol{k} + \boldsymbol{k}' + \boldsymbol{q})}{k^2 - k'^2}\left[\frac{R_3(\omega_k)}{\omega_k} - \frac{R_3(\omega_{k'})}{\omega_{k'}}\right].$$

3. – The spectral function.

The problem now is to transform $f_E(\boldsymbol{q}^2)$ and $f_M(\boldsymbol{q}^2)$ to a spectral representation. To do this it is useful to have the following integral representations of the terms appearing in $R_i(\omega_k)$. These representations are derived by considering the Cauchy integral in the complex k^2 plane with cuts from $i\mu$ to $i\infty$ and $-i\mu$ to $-i\infty$ and deforming the contours to run along the cuts paying attention to the proper sign of the square root along each side of the cuts.

$$h_i(\omega_k) = \int_{\mu^2}^{\infty}\frac{\varrho_i(\alpha^2)\,\mathrm{d}\alpha^2}{\alpha^2 + k^2}\,,$$

i	$h_i(\omega_k)$	$\varrho_i(\alpha^2)$,
1	$\dfrac{1}{\omega_k + \omega_R}$	$\dfrac{1}{\pi}\dfrac{\sqrt{\alpha^2-\mu^2}}{\alpha^2-\mu^2+\omega_R^2}$,
2	$\dfrac{1}{(\omega_k+\omega_R)^2}$	$\dfrac{2\omega_R}{\pi}\dfrac{\sqrt{\alpha^2-\mu^2}}{(\alpha^2-\mu^2+\omega_R^2)^2}$,
3	$\dfrac{1}{\omega_k(\omega_k+\omega_R)}$	$\dfrac{1}{\pi}\dfrac{1}{\sqrt{\alpha^2-\mu^2}}\dfrac{\omega_R}{\omega_R^2+\alpha^2-\mu^2}$,
4	$\dfrac{1}{\omega_k(\omega_k+\omega_R)^2}$	$\dfrac{1}{\pi}\dfrac{1}{\sqrt{\alpha^2-\mu^2}}\dfrac{\omega_R^2+\mu^2-\alpha^2}{(\omega_R^2-\mu^2+\alpha^2)^2}$.

The contributions from the resonance will be calculated first and the contributions from the Born terms can easily be found by the substitutions

$$\text{in} \quad f_E(\boldsymbol{q}^2): \qquad \omega_R \to 0 \qquad -2a^2 \to f^2\,,$$

$$\text{»} \quad f_M(\boldsymbol{q}^2): \qquad \omega_R \to 0 \qquad a^2 \to f^2\,.$$

One may note in passing that since the contribution to $f_E(\boldsymbol{q}^2)$ from the Born term and resonance enter as f^2 and $-2a^2$, and since $a^2 = (4/9)f^2$, this term will be quite sensitive to assumptions about the resonance whereas $f_M(\boldsymbol{q}^2)$ will not be.

One now proceeds as follows:

a) Notice first that

$$\frac{1}{k^2-k'^2}\left[\frac{1}{\alpha^2+k^2}-\frac{1}{\alpha^2+k'^2}\right] = \frac{-1}{(\alpha^2+k^2)\,(\alpha^2+k'^2)}\,,$$

b) It is convenient to forget about the cut-off at this time. It will be needed further on to justify a partial integration but the final spectral functions, since they give the low mass behaviour, do not depend on the cut-off.

c) Introduce a change of variables

$$\boldsymbol{k}' = -\left(\boldsymbol{v}+\frac{\boldsymbol{u}}{2}\right),$$

$$\boldsymbol{k} = \boldsymbol{v}-\frac{\boldsymbol{u}}{2}\,,$$

$$\mathrm{d}^3k\,\mathrm{d}^3k' = \mathrm{d}^3u\,\mathrm{d}^3v\,.$$

This gives a $\delta(\boldsymbol{u}-\boldsymbol{q})$ and the $\boldsymbol{u}$ integration can be performed.

d) Introduce the Feynman parametrization

$$\frac{1}{ab} = \int_0^1 \mathrm{d}x \frac{1}{[ax + b(1-x)]^2},$$

and make a second change of variables to $\boldsymbol{t} = \boldsymbol{v} - (\boldsymbol{q}/2)(1-2x)$. The denominators become independent of angle and the angular integrations in the numerators can be carried out. Note that

$$\int \mathrm{d}\Omega_t \text{ (terms odd in } \boldsymbol{t}) = 0,$$

$$\int \mathrm{d}\Omega_t (\boldsymbol{a}\cdot\boldsymbol{t})(\boldsymbol{b}\cdot\boldsymbol{t}) = \frac{4\pi}{3} t^2 (\boldsymbol{a}\cdot\boldsymbol{b}).$$

The results of these four steps are

$$f_E^R(\boldsymbol{q}^2) = -\frac{8e\tau_3}{\pi}\left(\frac{a}{\mu}\right)^2 \int_0^1 \mathrm{d}x \int_{\mu^2}^\infty \mathrm{d}\alpha^2 \int_0^\infty \frac{t^2\,\mathrm{d}t}{[t^2 + A^2]^2} \cdot$$

$$\cdot \left[(t^2 - \boldsymbol{q}^2 x(1-x))\varrho_1(\alpha^2) - \frac{1}{2M}\left\{ (t^2 - \boldsymbol{q}^2 x(1-x))^2 + \frac{1}{3} t^2 \boldsymbol{q}^2 (1-2x)^2 \right\} \varrho_2(\alpha^2) \right],$$

$$f_M^R(\boldsymbol{q}^2) = \frac{4e\tau_3}{3\pi}\left(\frac{a}{\mu}\right)^2 \int_0^1 \mathrm{d}x \int_{\mu^2}^\infty \mathrm{d}\alpha^2 \int_0^\infty \frac{t^2\,\mathrm{d}t}{[t^2 + A^2]^2} \left[t^2 \varrho_3(\alpha^2) - \frac{1}{2M} t^2 (t^2 - \boldsymbol{q}^2 x(1-x))\varrho_4(\alpha^2) \right],$$

where $A^2 = \boldsymbol{q}^2 x(1-x) + \alpha^2$.

e) The $\boldsymbol{q}^2$ dependence must now be removed from the numerators. To do this use

$$t^2 - \boldsymbol{q}^2 x(1-x) = 2t^2 + \alpha^2 - (t^2 + A^2),$$

$$\boldsymbol{q}^2 = \frac{1}{x(1-x)}[(t^2 + A^2) - t^2 - \alpha^2].$$

When this is done, one finds one term in $f_E^R(\boldsymbol{q}^2)$ which has no $\boldsymbol{q}^2$ dependence. Thus one must write

$$f_E^R(\boldsymbol{q}^2) = f_E^R(\infty) + \tilde{f}_E^R(\boldsymbol{q}^2)$$

and including the Born term one has

$$f_E(\infty) = -\frac{2e\tau_3}{2\pi M} A^3 \left[\left(\frac{f}{\mu}\right)^2 - 2\left(\frac{a}{\mu}\right)^2 \right],$$

where an upper limit Λ has been put in the t integration. Since this term corresponds to $f_E(\boldsymbol{q}^2 = \infty)$, one can say nothing about it on the basis of the static theory. It can be removed by relaxing the condition that equation (1) also gives the correct charge and performing one subtraction [1]

$$F_E(q^2) - F_E(0) = \frac{-q^2}{\pi} \int_{4\mu^2}^{\infty} \frac{G_E(\sigma^2)\,\mathrm{d}\sigma^2}{\sigma^2(\sigma^2 + q^2)} .$$

Therefore it is the function $\tilde{f}_E^R(\boldsymbol{q}^2)$ which shall be investigated further.
The remaining terms in $1/[t^2+A^2]^2$ are removed by a partial integration setting

$$\mathrm{d}r = \frac{t\,\mathrm{d}t}{[t^2 + A^2]^2} , \qquad r = \frac{-1}{2(t^2 + A^2)} . \qquad s = [\text{what's left}].$$

Note two things:

1) Since there is a cut-off $sr\Big|_0^\infty = 0$.

2) Since one is interested in the spectral function for low mass behaviour, the derivative of the cut-off function may be set equal to zero. This results in

$$f_M^R(\boldsymbol{q}^2) = \frac{2e\tau_3}{3\pi}\left(\frac{a}{\mu}\right)^2 \int_0^1 \mathrm{d}x \int_{\mu^2}^{\infty} \mathrm{d}\alpha^2 \int_0^{\infty} \frac{\mathrm{d}t}{t^2 + A^2} \left[3t^2 \varrho_3(\alpha^2) - \frac{1}{2M}(8t^4 + 3t^2\alpha^2)\varrho_4(\alpha^2)\right],$$

$$\tilde{f}_E^R(\boldsymbol{q}^2) = \frac{-4e\tau_3}{\pi}\left(\frac{a}{\mu}\right)^2 \int_0^1 \mathrm{d}x \int_{\mu^2}^{\infty} \mathrm{d}\alpha^2 \int_0^{\infty} \frac{\mathrm{d}t}{t^2 + A^2} \cdot$$

$$\cdot \left[(4t^2 + \alpha^2)\varrho_1(\alpha^2) - \frac{1}{2M}\left\{(2t^2 + \alpha^2)(6t^2 + \alpha^2) - \frac{t^2(t^2 + \alpha^2)(1 - 2x)^2}{x(1 - x)}\right\}\varrho_2(\alpha^2)\right].$$

g) Consider

$$t^2 + A^2 = t^2 + \alpha^2 + \boldsymbol{q}^2 x(1 - x) =$$

$$= x(1 - x)\left[\boldsymbol{q}^2 + \frac{t^2 + \alpha^2}{x(1 - x)}\right].$$

One can write

$$\frac{1}{\boldsymbol{q}^2 + (t^2 + \alpha^2)/x(1 - x)} = \int_{4\mu^2}^{\infty} \frac{\mathrm{d}\sigma^2 \delta(\sigma^2 - (t^2 + \alpha^2)/x(1 - x))}{\boldsymbol{q}^2 + \sigma^2} ,$$

where the lower limit comes from the fact that the minimum value of

$$\frac{t^2+\alpha^2}{x(1-x)} \qquad \text{for} \left\{ \begin{array}{c} 0 \leqslant t \leqslant \infty \\ \mu^2 \leqslant \alpha^2 \leqslant \infty\,, \\ 0 \leqslant x \leqslant 1\,. \end{array} \right\} \text{is} \qquad 4\mu^2\,.$$

Putting this in and interchanging limits of integration one is left with an integrand which is just the spectral function (*)

$$g_M^R(\sigma^2) = \frac{2e\tau_3}{3}\left(\frac{a}{\mu}\right)^2 \int_0^1 \mathrm{d}x \int_{\mu^2}^{\infty} \mathrm{d}\alpha^2 \int_0^{\infty} \mathrm{d}t\, \delta(t^2+\alpha^2-\sigma^2 x(1-x)) \cdot \\ \cdot \left[3t^2\varrho_3(\alpha^2) - \frac{1}{2M}(8t^4+3t^2\alpha^2)\varrho_4(\alpha^2)\right],$$

$$g_E^R(\sigma^2) = -4e\tau_3\left(\frac{a}{\mu}\right)^2 \int_0^1 \mathrm{d}x \int_{\mu^2}^{\infty} \mathrm{d}\alpha^2 \int_0^{\infty} \mathrm{d}t\, \delta(t^2+\alpha^2-\sigma^2 x(1-x)) \cdot \\ \cdot \left[(4t^2+\alpha^2)\varrho_1(\alpha^2) - \frac{1}{2M}\left\{(2t^2+\alpha^2)(6t^2+\alpha^2) - \frac{t^2(t^2+\alpha^2)(1-2x)^2}{x(1-x)}\right\}\varrho_2(\alpha^2)\right].$$

h) Now note the following: for the δ-function to vanish one must have $\sigma^2 x(1-x) - \alpha^2 \geqslant 0$

1) since $\sigma^2 x(1-x) \leqslant \sigma^2/4$ this implies $\alpha^2 \leqslant \sigma^2/4$;

2) for given α^2, $x = \frac{1}{2}\left[1 \pm (1-(4\alpha^2/\sigma^2))^{\frac{1}{2}}\right]$

is the region of vanishing of the argument of the δ-function.

The ranges of integration thus reduce to

$$\int_{\mu^2}^{\sigma^2/4} \mathrm{d}\alpha^2 \int_{\frac{1}{2}[1-(1-(4\alpha^2/\sigma^2))^{1/2}]}^{\frac{1}{2}[1+(1-(4\alpha^2/\sigma^2))^{1/2}]} \mathrm{d}x \int_0^{\infty} \mathrm{d}t\, \frac{1}{2(\sigma^2 x(1-x)-\alpha^2)^{\frac{1}{2}}}\, \delta(t-[\sigma^2 x(1-x)-\alpha^2]^{\frac{1}{2}})[\ldots]\,.$$

The x integrations are easy to carry out since the square root in the integrand vanishes at the end points. This results in

$$g_M^R(\sigma^2) = \frac{\pi}{\sigma}\, e\tau_3 \left(\frac{a}{\mu}\right)^2 \int_{\mu^2}^{\sigma^2/4} \mathrm{d}\alpha^2 \left(\frac{\sigma^2}{4}-\alpha^2\right)\left[\frac{1}{2}\varrho_3(\alpha^2) - \frac{1}{4M}\left(\frac{\sigma^2}{2}-\alpha^2\right)\varrho_4(\alpha^2)\right],$$

$$g_E^R(\sigma^2) = -\frac{2\pi e\tau_3}{\sigma}\left(\frac{a}{\mu}\right)^2 \int_{\mu^2}^{\sigma^2/4} \mathrm{d}\alpha^2 \left(\frac{\sigma^2}{2}-\alpha^2\right)\left[\varrho_1(\alpha^2) - \frac{1}{2M}\left(\frac{\sigma^2}{2}-\alpha^2\right)\varrho_2(\alpha^2)\right].$$

(*) $\delta(\alpha x) = \dfrac{1}{a}\,\delta(x)$ and $\delta(t^2-a^2) = \dfrac{1}{2a}\,\delta(t-a)$ for $\begin{array}{l} t>0, \\ a>0. \end{array}$

The remaining integrations are elementary and yield, after the Born terms are included

$$g_M(\sigma^2)=e\tau_3\left(\frac{q_\pi^2}{\sigma}\right)\left[\frac{\pi}{2}\left(\frac{f}{\mu}\right)^2+\left(\frac{a}{\mu}\right)^2\left(-\frac{\omega_R}{q_\pi}+\frac{q_\pi^2+\omega_R^2}{q_\pi^2}\,\mathrm{tg}^{-1}\frac{q_\pi}{\omega_R}\right)-\frac{q_\pi}{M}\left\{\left(\frac{f}{\mu}\right)^2\left(\frac{2q_\pi^2+\mu^2}{q_\pi^2}\right)+\right.\right.$$
$$\left.\left.+\left(\frac{1}{3}\left(\frac{f}{\mu}\right)^2-\frac{2}{3}\left(\frac{a}{\mu}\right)^2\right)+\left(\frac{a}{\mu}\right)^2\left(\frac{3q_\pi^2+2\omega_R^2+\mu^2}{q_\pi^2}\right)\left(1-\frac{\omega_R}{q_\pi}\,\mathrm{tg}^{-1}\frac{q_\pi}{\omega_R}\right)\right\}\right],$$

$$g_E(\sigma^2)=2e\tau_3\left(\frac{q_\pi^3}{\sigma}\right)\left[\left(\frac{f}{\mu}\right)^2\left(\frac{2q_\pi^2+\mu^2}{q_\pi^2}\right)-\left(\frac{1}{3}\left(\frac{f}{\mu}\right)^2-\frac{2}{3}\left(\frac{a}{\mu}\right)^2\right)-2\left(\frac{a}{\mu}\right)^2\left(\frac{2q_\pi^2+\mu^2+\omega_R^2}{q_\pi^2}\right)\cdot\right.$$
$$\cdot\left(1-\frac{\omega_R}{q_\pi}\,\mathrm{tg}^{-1}\frac{q_\pi}{\omega_R}\right)-\frac{q_\pi}{2M}\left\{\left(\frac{f}{\mu}\right)^2\left(\frac{\pi}{2}\right)\left(\frac{2q_\pi^2+\mu^2}{q_\pi^2}\right)^2-2\left(\frac{a}{\mu}\right)^2\left[-\frac{2\omega_R}{3q_\pi}\left(\frac{11q_\pi^2+6\mu^2+5\omega_R^2}{q_\pi^2+\omega_R^2}\right)+\right.\right.$$
$$\left.\left.\left.+\frac{(2q_\pi^2+\mu^2+\omega_R^2)(2q_\pi^2+\mu^2+5\omega_R^2)}{q_\pi^2(q_\pi^2+\omega_R^2)}\left[\frac{q_\pi^2+\omega_R^2}{q_\pi^2}\,\mathrm{tg}^{-1}\frac{q_\pi}{\omega_R}-\frac{\omega_R}{q_\pi}\right]\right]\right\}\right],$$

where $q_\pi^2=(\sigma^2/4)-\mu^2$.

4. – Relation to relativistic form factors.

The S matrix for a single scattering in an external electromagnetic field is given by (*)

$$\langle p'\,|\,S\,|\,p\rangle=-\frac{1}{\Omega}\,\bar{u}(p')\Gamma_\mu(q^2)u(p)A_\mu^{\mathrm{ext}}(q)\,,$$

where $p'=p+q$, Ω is the volume of the normalization box, and $A_\mu^{\mathrm{ext}}(q)$ is the Fourier transform of $A_\mu^{\mathrm{ext}}(x)$.

Now

$$\Gamma_\mu(q^2)=F_E(q^2)\gamma_\mu-F_M(q^2)\sigma_{\mu\nu}q_\nu\,.$$

Making the non-relativistic reduction to order $1/M$ by taking

$$u(p)=\begin{pmatrix}1\\ \\ \dfrac{\boldsymbol{\sigma}\cdot\boldsymbol{p}}{2M}\end{pmatrix},$$

(*) $\gamma_\mu\gamma_\nu+\gamma_\nu\gamma_\mu=2\delta_{\mu\nu}$,

$\sigma_{\mu\nu}=\dfrac{1}{2i}(\gamma_\mu\gamma_\nu-\gamma_\nu\gamma_\mu)$,

$p_\mu=(\boldsymbol{p},\,iE)$,

one finds (in the Breit frame-note again $\boldsymbol{q}^2 = q^2$)

$$\langle \boldsymbol{q}/2 \,|\, S \,|\, -\boldsymbol{q}/2 \rangle = \frac{-(2\pi)^4 i}{\Omega}\, \delta^4(p' - p - q) \cdot$$
$$\cdot \left[\left(F_E(q^2) - \frac{q^2}{2M} F_M(q^2) \right) \varphi - i\boldsymbol{\sigma} \cdot (\boldsymbol{q} \wedge \boldsymbol{a}) \left(F_M(q^2) + \frac{F_E(q^2)}{2M} \right) \right],$$

where

$$A_\mu^{\text{ext}}(x) = a_\mu \exp[iqx] ,$$
$$a_\mu = (\boldsymbol{a}, i\varphi) .$$

The above is the full S matrix to first order in the external field. Going now to an interaction representation where the time dependence is given by the full meson nucleon Hamiltonian and $H_1 = H_{\text{electromagnetic}}$, one has

$$\langle \boldsymbol{q}/2 \,|\, S \,|\, -\boldsymbol{q}/2 \rangle = -i \langle \boldsymbol{q}/2 \,| \int H_1^{\text{ext}}(x)\, \mathrm{d}^4 x \,| -\boldsymbol{q}/2 \rangle =$$
$$= -2\pi i \delta(E_f - E_i) \langle \boldsymbol{q}/2 \,| \int H_1^{\text{ext}}(\boldsymbol{x})\, \mathrm{d}^3 \boldsymbol{x} \,| \,| -\boldsymbol{q}/2 \rangle =$$
$$= -2\pi i \delta(E_f - E_i)\omega .$$

Therefore, since

$$\frac{(2\pi)^3}{\Omega}\, \delta(\boldsymbol{p}' - \boldsymbol{p} - \boldsymbol{q}) = 1 ,$$
$$\omega = f_E(q^2)\varphi - i\sigma \cdot (\boldsymbol{q} \wedge \boldsymbol{a}) f_M(q^2) ,$$
$$f_E(q^2) = F_E(q^2) - \frac{q^2}{2M} F_M(q^2) ,$$
$$f_M(q^2) = F_M(q^2) + \frac{F_E(q^2)}{2M} .$$

For the second equation, one can add the corresponding spectral functions however, for the first equation one must write

$$f_E(q^2) = \frac{1}{\pi} \int_{4\mu^2}^{\infty} \mathrm{d}\sigma^2 \left[\frac{G_E(\sigma^2)}{\sigma^2 + q^2} - \frac{q^2}{2M} \frac{G_M(\sigma^2)}{\sigma^2 + q^2} \right] = f_E(\infty) + \tilde{f}_E(q^2) ,$$

$$f_E(\infty) = -\frac{1}{2M\pi} \int_{4\mu^2}^{\infty} G_M(\sigma^2)\, \mathrm{d}\sigma^2 ,$$

$$\tilde{f}_E(q^2) = \int_{4\mu^2}^{\infty} \mathrm{d}\sigma^2 \, \frac{G_E(\sigma^2) + (\sigma^2/2M) G_M(\sigma^2)}{\sigma^2 + q^2} .$$

Thus if one uses a superscript (1) to indicate terms up through $1/M$ and a (0) to indicate the static limit one finds for the predictions of the static theory for $G_E^{(1)}(\sigma^2)$ and $G_M^{(1)}(\sigma^2)$

$$G_M^{(1)}(\sigma^2)_{\mathrm{S.T.}} = g_M^{(1)}(\sigma^2) - \frac{g_E^{(0)}(\sigma^2)}{2M},$$

$$G_E^{(1)}(\sigma^2)_{\mathrm{S.T.}} = g_E^{(1)}(\sigma^2) - \frac{\sigma^2}{2M} g_M^{(0)}(\sigma^2),$$

$$G_M^{(1)}(\sigma^2)_{\mathrm{S.T.}} = e\tau_3\left(\frac{q_\pi^2}{\sigma}\right)\left[\frac{\pi}{2}\left(\frac{f}{\mu}\right)^2 + \left(\frac{a}{\mu}\right)^2\left(\frac{-\omega_R}{q_\pi} + \frac{q_\pi^2+\omega_R^2}{q_\pi^2}\,\mathrm{tg}^{-1}\frac{q_\pi}{\omega_R}\right) - \right.$$
$$\left. - \frac{q_\pi}{M}\left\{2\left(\frac{f}{\mu}\right)^2\left(\frac{2q_\pi^2+\mu^2}{q_\pi^2}\right) - \left(\frac{a}{\mu}\right)^2\left(\frac{q_\pi^2+\mu^2}{q_\pi^2}\right)\left(1 - \frac{\omega_R}{q_\pi}\,\mathrm{tg}^{-1}\frac{q_\pi}{\omega_R}\right)\right\}\right],$$

$$G_E^{(1)}(\sigma^2)_{\mathrm{S.T.}} = 2e\tau_3\left(\frac{q_\pi^3}{\sigma}\right)\left[\left(\frac{f}{\mu}\right)^2\left(\frac{2q_\pi^2+\mu^2}{q_\pi^2}\right) - \left(\frac{1}{3}\left(\frac{f}{\mu}\right)^2 - \frac{2}{3}\left(\frac{a}{\mu}\right)^2\right) - 2\left(\frac{a}{\mu}\right)^2\left(\frac{2q_\pi^2+\mu^2+\omega_R^2}{q_\pi^2}\right)\cdot\right.$$
$$\cdot\left(1 - \frac{\omega_R}{q_\pi}\,\mathrm{tg}^{-1}\frac{q_\pi}{\omega_R}\right) - \frac{q_\pi}{2M}\left\{\left(\frac{f}{\mu}\right)^2\left(\frac{\pi}{2}\right)\left[\left(\frac{2q_\pi^2+\mu^2}{q_\pi^2}\right)^2 + 2\left(\frac{q_\pi^2+\mu^2}{q_\pi^2}\right)\right] -$$
$$- 2\left(\frac{a}{\mu}\right)^2\left[\left(\frac{(2q_\pi^2+\mu^2+\omega_R^2)(2q_\pi^2+\mu^2+5\omega_R^2)}{q_\pi^2(q_\pi^2+\omega_R^2)} - \frac{(q_\pi^2+\mu^2)(q_\pi^2+\omega_R^2)}{q_\pi^2(q_\pi^2+\omega_R^2)}\right)\cdot\right.$$
$$\left.\left.\left.\cdot\left(\frac{q_\pi^2+\omega_R^2}{q_\pi^2}\,\mathrm{tg}^{-1}\frac{q_\pi}{\omega_R} - \frac{\omega_R}{q_\pi}\right) - \frac{2\omega_R}{3q_\pi}\left(\frac{11q_\pi^2+6\mu^2+5\omega_R^2}{q_\pi^2+\omega_R^2}\right)\right]\right\}\right].$$

The corresponding equations of dispersion theory obtained by expanding equations (15.1) to (15.7) of reference one to order $1/M$ are

$$G_M^{(1)}(\sigma^2)_{\mathrm{D.T.}} = e\tau_3\left(\frac{q_\pi^2}{\sigma}\right)\left[\frac{\pi}{2}\left(\frac{f}{\mu}\right)^2 + \left(\frac{a}{\mu}\right)^2\left(-\frac{\omega_R}{q_\pi} + \frac{q_\pi^2+\omega_R^2}{q_\pi^2}\,\mathrm{tg}^{-1}\frac{q_\pi}{\omega_R}\right) - \frac{q_\pi}{M}\cdot\right.$$
$$\left.\cdot\left\{2\left(\frac{f}{\mu}\right)^2\left(\frac{2q_\pi^2+\mu^2}{q_\pi^2}\right) - \left(\frac{a}{\mu}\right)^2\left(\frac{2q_\pi^2+\mu^2+\omega_R^2}{q_\pi^2}\right)\left(1 - \frac{\omega_R}{q_\pi}\,\mathrm{tg}^{-1}\frac{q_\pi}{\omega_R}\right)\right\}\right],$$

$$G_E^{(1)}(\sigma^2)_{\mathrm{D.T.}} = 2e\tau_3\left(\frac{q_\pi^3}{\sigma}\right)\left[\left(\frac{f}{\mu}\right)^2\left(\frac{2q_\pi^2+\mu^2}{q_\pi^2}\right) - 2\left(\frac{a}{\mu}\right)^2\left(\frac{2q_\pi^2+\mu^2+\omega_R^2}{q_\pi^2}\right)\cdot\right.$$
$$\cdot\left(1 - \frac{\omega_R}{q_\pi}\,\mathrm{tg}^{-1}\frac{q_\pi}{\omega_\pi}\right) - \frac{q_\pi}{2M}\left\{\left(\frac{f}{\mu}\right)^2\frac{\pi}{2}\left[\left(\frac{2q_\pi^2+\mu^2}{q_\pi^2}\right)^2 + 2\left(\frac{q_\pi^2+\mu^2}{q_\pi^2}\right)\right] -$$
$$- 2\left(\frac{a}{\mu}\right)^2\left[\left(\frac{(2q_\pi^2+\omega_R^2+\mu^2)^2 - (q_\pi^2+3\omega_R^2)(q_\pi^2+\mu^2)}{q_\pi^2(q_\pi^2+\omega_R^2)}\right)\cdot\right.$$
$$\left.\left.\left.\cdot\left(\frac{q_\pi^2+\omega_R^2}{q_\pi^2}\,\mathrm{tg}^{-1}\frac{q_\pi}{\omega_R} - \frac{\omega_R}{q_\pi}\right) + \frac{2\omega_R}{q_\pi}\left(\frac{q_\pi^2+\mu^2}{q_\pi^2+\omega_R^2}\right)\right\}\right].$$

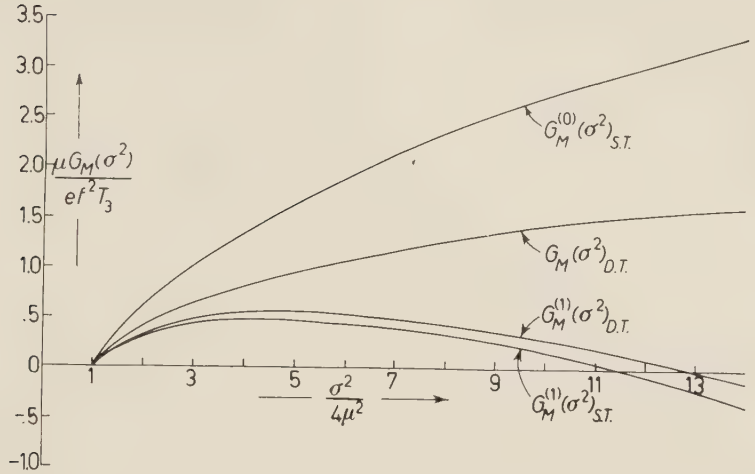

Fig. 1. – Spectral functions for the magnetic form factors calculated from dispersion theory (D.T.) and the static theory (S.T.). (0) indicates the static limit and (1) indicates first order in $1/M$.

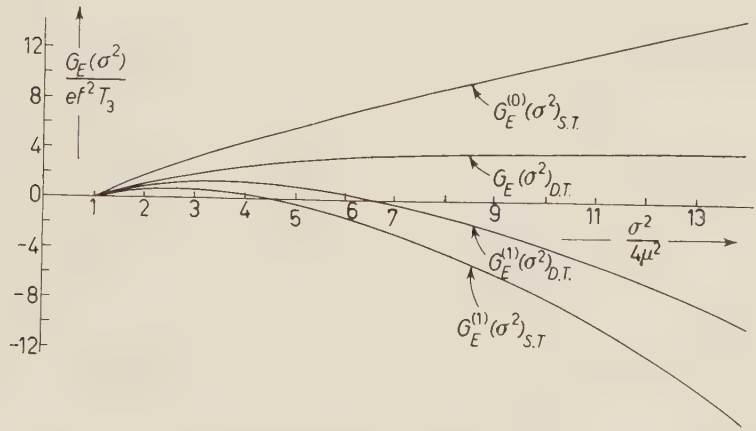

Fig. 2. - Spectral functions for the charge form factor calculated from dispersion theory (D.T.) and the static theory (S.T.). (0) indicates the static limit and (1) indicates first order in $1/M$.

In Figs. 1 and 2 are plotted $G^{(0)}_{M,E}(\sigma^2)_{\text{S.T.}}$, $G^{(1)}_{M,E}(\sigma^2)_{\text{S.T.}}$, $G^{(1)}_{M,E}(\sigma^2)_{\text{D.T.}}$ and also $G_{M,E}(\sigma^2)_{\text{D.T.}}$ obtained from the equations of reference [1].

5. – Summary and discussion of results.

To summarize the results.

a) One can calculate spectral functions within the framework of the static theory by a direct transformation of the form factors.

b) The results obtained agree with the static limit of the results obtained from dispersion theory (except for the term proportional to $\frac{1}{3}(f/\mu)^2 - \frac{2}{3}(a/\mu)^2$ in $g_E(\sigma^2)$ in the static theory which must come from the neglect of pair effects; it happens to be almost zero).

c) The $1/M$ corrections coming solely from the addition of the kinematics of nucleon recoil are very nearly equal (*) to the corresponding corrections in the dispersion theory and the fact that they are so large raises serious doubts as to the applicability of the static model to the study of the electromagnetic structure of the nucleon.

The physics of the situation is this, the nucleon likes to emit and absorb P-wave mesons, and indeed, if it is infinitely heavy can only do so. After the meson picks up a photon from the external fields it is no longer a P state relative to the nucleon, but has a great probability of being in a higher angular momentum state. If now one allows the nucleon to move and hence interact with mesons of higher angular momentum, even though the interaction is small, the amplitude of such a wave may be large enough so that the result may compete with P wave absorption. This is what was found above.

* * *

The author would like to express his great indebtness to Prof. S. Fubini for suggesting the problem and for his assistance throughout. He would also like to acknowledge a stimulating correspondence with Prof. S. Drell and to thank Prof. B. Ferretti and the theoretical division at CERN for the hospitality extended to him during his stay.

(*) Notice that the $1/M$ Born terms are given exactly.

RIASSUNTO (*)

Le funzioni spettrali dei fattori di forma del nucleone si discutono nel quadro della teoria statica. Si includono anche correzioni per il rinculo $1/M$ e si mostra che tali correzioni sono prossime a quelle date dalla teoria dispersiva e che alterano profondamente le funzioni spettrali indicando che l'applicazione del modello statico a questo problema è di dubbia validità.

(*) *Traduzione a cura della Redazione.*

IL NUOVO CIMENTO Vol. XI, N. 6 16 Marzo 1959

On the Radiative Decay of Charged π-Mesons.

N. Cabibbo

Istituto di Fisica dell'Università - Roma
Istituto Nazionale di Fisica Nucleare - Sezione di Roma

(ricevuto il 7 Gennaio 1959)

Summary. — The radiative decay $\pi^+ \to \mu^+ + \nu + \gamma$ is examined in the frame of the $A-V$ theory of weak interactions. The modifications of the spectrum of μ^+ emitted due to the structure of the μ-meson are in part related to the process $\pi^0 \to \gamma + \gamma$. These modifications turn out to be negligible.

A recent experiment by C. Castagnoli and M. Muchnik [1] has shown the possibility of measuring the spectrum of μ^+ coming from the radiative pion decay:

$$\pi^+ \to \mu^+ + \nu + \gamma \ .$$

In the present paper we shall attempt a detailed analysis of this process in the $A-V$ theory suggested by Feynmann, Gell-Mann and Marshak-Sudarshan.

If one deals with e.m. and weak interactions only to the first order, Lorentz invariance and gauge invariance impose strong limits on the form of the relevant S-matrix elements [2]. Assuming universal Fermi interaction in the form:

$$(1) \qquad H_{\text{wi}} = \sqrt{8}\, G(\bar{\mu}\gamma_\varrho a \nu)(\bar{n}\gamma_\varrho a p) \ ; \qquad a = \tfrac{1}{2}(1+\gamma_5) \quad [3]$$

[1] C. Castagnoli and M. Muchnik: to be published in *Physical Review*.

[2] S. Kamefuchi and S. Oneda: *Nuclear Physics*, **6**, 114 (1958).

[3] According to the hypothesis of non renormalization of the vector part in weak interactions, this part shall be written: $G(\bar{\mu}(x)\gamma_\mu a \nu(x))J_\mu^{(-)}(x)$ with the condition: $\partial_\mu J_\mu^{(-)}(x) = 0$.

the matrix element will be a combination with coefficients depending on (pk) of the following terms

$$(2)\qquad \begin{cases} \mathcal{M}_A = \dfrac{im}{2(qk)}\,(\overline{u}^{(\mu)}\{\boldsymbol{\epsilon k} + 2(q\varepsilon)\}au^{(\nu)})\,, \\ \mathcal{M}'_A = (pk)\,(\overline{u}^{(\mu)}\boldsymbol{\epsilon} au^{(\nu)})\,, \\ \mathcal{M}_V = (\overline{u}^{(\mu)}\gamma_\varrho a u^{(\nu)})\varepsilon^{\varrho\mu\nu\sigma}\varepsilon_\mu p_\nu k_\sigma = (\overline{u}^{(\mu)}\{\boldsymbol{k\epsilon p} + \boldsymbol{\epsilon}(pk)\}au^{(\nu)})\,, \end{cases}$$

k and ε are momentum and polarization vector of the photon emitted, p is the four-momentum of the π-meson, q and h the momenta respectively of the μ-meson and of the neutrino, M is the mass of the π, m the mass of the μ; (pk) is the scalar product $p_\mu k_\mu$, $\boldsymbol{\epsilon} = \varepsilon_\mu \gamma_\mu$. We use units in which $\hbar = c = 1$.

Neglecting effects due to the internal structure of the π, the actual (weak and strong) interactions can be substituted by a simple derivative coupling between mesons and leptons [4]. In this simple theory the only term which appears in the S-matrix is $\mathcal{M}_A$.

$$(3)\qquad S = \left(\frac{e}{\sqrt{4\pi}}\right)\frac{1}{2\pi\sqrt{k_0}}A\mathcal{M}_A\,,$$

the constant A is defined in terms of the matrix element for the normal mode $\pi^+ \to \mu^+ + \nu$

$$(4)\qquad S^0 = A(\overline{u}^{(\mu)}\boldsymbol{p}au^{(\nu)})\,.$$

In order to evaluate the structure effects on the μ^+ spectrum, we made a perturbation calculation of the S-matrix to the lowest order, making use of standard Feynmann-Dyson techniques, with the following interaction Hamiltonian:

$$(5)\qquad H' = H_{\text{wi}} + H_{\text{e.m.}} + g(\overline{n}\gamma_5 p)\varphi_\pi + \dots\,.$$

The result is an addition of $\mathcal{M}'_A$ and $\mathcal{M}_V$ terms to the principal $\mathcal{M}_A$ term:

$$(6)\qquad S = \left(\frac{e}{\sqrt{4\pi}}\right)\frac{1}{2\pi\sqrt{k_0}}A\{\mathcal{M}_A + R[\mathcal{M}'_A + \mathcal{M}_V]\}\,.$$

---

[4] G. E. Fialho and J. Tiomno: *Anais Acad. Brasil. Cienc.*, **24**, 245 (1952); B. Ioffe and A. Rudik: *Dokl. Akad. Nauk SSSR*, **87**, 359 (1952). S. A. Bludman and M. A. Ruderman: *Phys. Rev.*, **101**, 910 (1956).

The constant A is the same that appears in eq. (3) and (4), while R is defined as

$$(7) \qquad R = \int \frac{\mathrm{d}^4 r}{(r^2+N^2)(s^2+N^2)(t^2+N^2)} \Big/ \int \frac{\mathrm{d}^4 r}{(r^2+N^2)(s^2+N^2)} ; \quad \begin{matrix} s_\mu = p_\mu + r_\mu, \\ t_\mu = k_\mu + r_\mu. \end{matrix}$$

where N is the nucleon mass. If we do not use a cut-off in the evaluation of the integrals, R turns out to be zero, and we fall back to the case of equations (3) and (4).

From equations (6) and (2) we get the following expression for the differential probability, integrated to give the spectrum of μ^+

$$(8) \qquad W(E)\,\mathrm{d}E = \left(\frac{e^2}{4\pi}\right) \frac{W^0}{2\pi} \frac{1}{P_0^2} \left\{ (E_0 - E) f(E) + \frac{4EP_0}{E_0 - E}\left(g(E) - \frac{P}{E}\right) + \right.$$

$$+ RM(E_0 - E)[2(M-E)f(E) - Mg(E)] +$$

$$\left. + R^2 \frac{4M^3}{m^2} P(E_0 - E)\left[ME_0 - E^2 - \frac{M}{2}(M-E)\right]\right\} \mathrm{d}E ,$$

$f(E)$ and $g(E)$ are the following functions:

$$(8') \qquad \begin{cases} f(E) = \log \dfrac{(E+P)M - m^2}{(E-P)M - m^2}, \\ \\ g(E) = \log \dfrac{E+P}{m}. \end{cases}$$

Here W^0 is the probability of the normal decay $\pi^+ \to \mu^+ + \nu$; $P_0 = (M^2 - m^2)/2M$ and $E_0 = (M^2 + m^2)/2M$, are the maximum values of the momentum P, and of the total energy E of the μ. The coefficient of $\mathcal{M}_A'$ in equation (6) is equal to the coefficient of $\mathcal{M}_V$; this result rests only on the perturbation treatment. The coefficient of $\mathcal{M}_V$, on the contrary, can be related by the following equation (5) to the lifetime of the neutral π^0-meson under the hypothesis of non-renormalization of the vector part

$$(9) \qquad |R| = \frac{P_0 m}{\pi\sqrt{8}M^2}\left(\frac{4\pi}{e^2}\right) 4 \sqrt{\frac{\tau^+}{\tau^0}} = 0.3 \cdot 10^{-10} \sqrt{\frac{\tau^+}{\tau^0}}\ \mathrm{MeV}^{-2},$$

(5) V. G. VAKS and B. L. IOFFE: *Nuovo Cimento*, **10**, 342 (1958).

In the Appendix we give a new derivation of a result due to VAKS and IOFFE, based on straightforward application of reduction formulae, in which the role played by the different approximations is clearly exhibited.

τ^+ and τ^0 are in the lifetimes respectively of π^+ and π^0-mesons. The sign of R cannot be determined in this way, but we assume it to be positive, as in a cut-off evaluation of eq. (7). At present we have only an upper experimental limit for τ^0: 10^{-15} s [6], while the most reliable theoretical evaluation gives $5 \cdot 10^{-17}$ s [7]. The correspondent values of R are $R = 0.14 \cdot 10^{-6}$ MeV^{-2} and $R = 0.64 \cdot 10^{-6}$ MeV^{-2}; from eq. (7), with a cut-off equal to the nucleon mass N: $R = 0.38 \cdot 10^{-6}$ MeV^{-2}.

An experimental determination of the μ^+ spectrum could give some information on the value of R, and hence, through eq. (9), on τ^0. However, assuming $R = 10^{-6}$ MeV^{-2}, the terms in eq. (8) proportional to R and R^2 turn out to be negligible: the contribution of the term proportional to R^2 to the total probability of radiative decay is of order of $10^{-10} W^0$. If we consider the coefficients of $f(E)$ and $g(E)$ in the R term, they turn out to be smaller by a factor 10^{-2} and 10^{-5} respectively than the coefficients of the same functions in the first term, even for the more favorable values of E. Of course the coefficient of $\mathcal{M}_V$ may actually be different from that of $\mathcal{M}'_A$, but we think that our estimate will still give the right order of magnitude.

Moreover the coefficients of $f(E)$ in the first term and in the R term have nearly the same energy dependence.

* * *

I am grateful to Prof. R. Gatto who suggested this problem and has given constant advice, to Prof. M. Cini for useful suggestions, and to Prof. C. Castagnoli for his interest in this work.

I am also grateful to Dr. Francesco Calogero for his active collaboration in the early stages of the work.

Appendix

The vector part of the matrix element $\langle \gamma \mu^+ \nu_{\text{out}} | \pi^+_{\text{in}} \rangle$ is related to the matrix element $\langle \gamma\gamma_{\text{out}} | \pi^0_{\text{in}} \rangle$ [5]: from invariance arguments these matrix elements can be written in similar form:

$$\langle k \mu^+ \nu_{\text{out}} | \pi^+_{\text{in}} \rangle = \frac{Ge}{(2\pi)^{\frac{3}{2}}} B^1 \delta(p - q - h - k) \varepsilon^{\nu\lambda\varrho\sigma} l_\nu \varepsilon_\lambda p_\varrho \Delta_\sigma \,, \tag{10}$$

$$\langle \gamma\gamma_{\text{out}} | \pi^0_{\text{in}} \rangle = 2e^2 B^2 \delta(p - k - k^1) \varepsilon^{\nu\lambda\varrho\sigma} \varepsilon^1_\nu \varepsilon_\lambda p_\varrho \Delta_\sigma \,, \qquad l_\nu = (\bar{u}^{(\mu)} \gamma_\nu a u^{(\nu)}) \,. \tag{10'}$$

[6] G. Harris, J. Orear and S. Taylor: *Phys. Rev.*, **106**, 327 (1958).
[7] M. L. Goldberger and S. B. Treiman: *Nuovo Cimento*, **9**, 451 (1958).

In the following we will show that the factors B^1 and B^2 are the same function $B(pk)$.

In (10): k^1 is the total momentum $q+h$ of the leptons emitted.

In (10′): ε^1 and k^1 are the polarization vector and the momentum of one of the photons, ε and k those of the other. In both (10) and (10′), $\Delta = \frac{1}{2}(k - k^1)$. All other notations have already been used in the text.

The tensor form of (10) is equivalent to that of $\mathcal{M}_1$ in equation (2), as is easily seen using the energy-momentum conservation: $k + k^1 = p$.

B will be a function of the number $\xi = (pk)/\Lambda^2$, where Λ has the dimension of a mass, and plays the role of a cut-off parameter. If we assume $\Lambda = N$, the values of ξ are in both cases very small, and we can assume $B(\xi) = B(0) = B$.

In the Heisenberg representation the μ^+-meson field $\mu(x)$ and the e.m. potentials A_μ satisfy in our approximation:

$$(\partial + m)\mu(x) = G(\gamma_\mu a\nu(x))\, J_\mu^{(-)}(x)\,, \tag{11}$$

$$\Box^2 A_\mu(x) = eJ_\mu(x) = e(J_\mu^{(3)}(x) + J_\mu^s(x))\,. \tag{11′}$$

The e.m. current is divided in an isovector part $J^{(3)}$, and an isoscalar part $J^{(s)}$. In the derivation we use the following equations, which are true only in the lowest order of the constants e and G:

$$[A_\mu, J_\nu^s] = [A_\mu, J_\nu^{(i)}] = 0\,, \tag{12}$$

$$\nu(x) = \nu_{\text{out}}(x)\,. \tag{13}$$

By repeated application of reduction formulae to the matrix element $\langle \gamma\mu^+\nu_{\text{out}} | \pi^+_{\text{in}} \rangle$, we get:

$$\begin{aligned}
\langle \gamma\mu\nu_{\text{out}} | \pi^+_{\text{in}} \rangle &= \frac{iG}{(2\pi)^{\frac{3}{2}}}\, \bar{u}_\varrho^{(\mu)} \int \mathrm{d}^4x\, \langle \gamma\nu_{\text{out}} | \,(\gamma_\nu a\nu(x))_\varrho J_\nu^{(-)}(x) \,| \pi^+ \rangle \exp[-iqx] = \\
&= \frac{iG}{(2\pi)^3}\, l_\nu \int \mathrm{d}^4x\, \langle \gamma | J_\nu^{(-)}(x) | \pi^+ \rangle \exp[-i(q+h)x] = \\
&= -\frac{Ge}{(2\pi)^{\frac{9}{2}}}\, l_\nu \varepsilon_\lambda \int \mathrm{d}^4x\, \mathrm{d}^4y\, \langle 0 | J_\lambda(y) J_\nu^{(-)}(x) | \pi^+ \rangle \exp[-ik^1x - iky] = \\
&= -\frac{Ge}{(2\pi)^{\frac{3}{2}}}\, 2\pi\delta(p - k - k^1) l_\nu \varepsilon_\lambda \int \mathrm{d}^4x\, \langle 0 | J_\lambda\left(\frac{x}{2}\right) J_\nu^{(-)}\left(-\frac{x}{2}\right) | \pi^+ \rangle \exp[-ix\Delta]\,.
\end{aligned} \tag{14}$$

Here equation (13) was used to take the neutrino out of the state, and equation (12) allows us to reduce a T product to a simple product. Moreover equation (14) is still satisfied if we commute $J_\lambda(x/2)$ and $J_\nu^{(-)}(-x/2)$:

$$\begin{aligned}
\langle \gamma\mu\nu_{\text{out}} | \pi^+_{\text{in}} \rangle = &-\frac{Ge}{(2\pi)^{\frac{3}{2}}}\, 2\pi\delta(p - k - k^1) l_\nu \varepsilon_\lambda \cdot \\
&\cdot \int \mathrm{d}^4x \langle 0 | J_\nu^{(-)}\left(-\frac{x}{2}\right) J_\lambda\left(\frac{x}{2}\right) | \pi^+ \rangle \exp[-ix\Delta]\,.
\end{aligned} \tag{14′}$$

The same procedure can be applied to the matrix element $\langle \gamma\gamma'_{\text{out}} | \pi^0_{\text{in}} \rangle$, and we get:

$$\langle \gamma\gamma'_{\text{out}} | \pi^0_{\text{in}} \rangle = -e^2 2\pi\delta(p-k-k^1)\,\varepsilon^1_\nu \varepsilon_\lambda \cdot \int \mathrm{d}^4x \langle 0 | J_\lambda\left(\frac{x}{2}\right) J_\nu\left(\frac{-x}{2}\right) | \pi^0 \rangle \exp[-ix\Delta] \,. \tag{15}$$

Now, as in equation (11), we divide the current J_λ in an isoscalar current J^S, and the third component of an isovector current $J^{(i)}$, of which $J^{(-)}$ is the (—) component.

Under the generalized charge conjugation $G = C \exp[i\pi T_2/2]$ these currents, and the vacuum and one meson states transform as follows:

$$\begin{cases} G J^{(i)} G^{-1} = -J^{(i)}\,, & G|\pi\rangle = -|\pi\rangle\,, \\ G J^S G^{-1} = J^S\,, & G|0\rangle = |0\rangle\,. \end{cases} \tag{16}$$

Therefore it is easily seen that the only non vanishing terms are those of the form $\langle 0 | J^S J^{(i)} | \pi \rangle$ and $\langle 0 | J^{(i)} J^S | \pi \rangle$. From charge independence we get the following identities:

$$\begin{cases} \langle 0 | J^S_\lambda\left(\frac{x}{2}\right) J^3_\nu\left(-\frac{x}{2}\right) | \pi^0 \rangle = \langle 0 | J^S_\lambda\left(\frac{x}{2}\right) J^{(-)}_\nu\left(-\frac{x}{2}\right) | \pi^+ \rangle\,, \\ \langle 0 | J^3_\lambda\left(\frac{x}{2}\right) J^S_\nu\left(-\frac{x}{2}\right) | \pi^0 \rangle = \langle 0 | J^{(-)}_\lambda\left(\frac{x}{2}\right) J^S_\nu\left(-\frac{x}{2}\right) | \pi^+ \rangle\,. \end{cases} \tag{17}$$

Comparing equations (14) and (14′), with equation (10), we get:

$$-2\pi \int \mathrm{d}^4x \langle 0 | J_\lambda\left(\frac{x}{2}\right) J^{(-)}_\nu\left(-\frac{x}{2}\right) | \pi^+ \rangle \exp[-ix\Delta] = \tag{18}$$

$$= -2\pi \int \mathrm{d}^4x \langle 0 | J^{(-)}_\nu\left(-\frac{x}{2}\right) J_\lambda\left(\frac{x}{2}\right) | \pi^+ \rangle \exp[-ix\Delta] = \varepsilon^{\nu\lambda\varrho\sigma} p_\varrho \Delta_\sigma B^1(\xi)\,.$$

From (15) and (17) we get:

$$2\varepsilon^{\nu\lambda\varrho\sigma} p_\varrho \Delta_\sigma B^2 = \{\varepsilon^{\nu\lambda\varrho\sigma} p_\varrho \Delta_\sigma + \varepsilon^{\lambda\nu\varrho\sigma} p_\varrho (-\Delta_\sigma)\} B^1\,. \tag{19}$$

Therefore $B^1 = B^2$.

In order to derive equation (9) we need the lifetime of π^+- and π^0-mesons in terms of A and B:

$$\tau^+ = (W^0)^{-1} = 2M(mP_0A)^{-2}\,, \qquad \tau^0 = 16M(e^2BM^2)^{-2}\,. \tag{20}$$

RIASSUNTO

Si esamina il decadimento radiativo $\pi^+ \to \mu^+ + \nu + \gamma$ nello schema della teoria A—V per le interazioni deboli. Le modificazioni dello spettro dei μ^+ emessi, dovute alla struttura del mesone π sono in parte messe in relazione col decadimento $\pi^0 \to \gamma + \gamma$. Queste modificazioni risultano trascurabili.

L/K-Capture Ratio in ^{195}Au.

A. Bisi, E. Germagnoli (*) and L. Zappa

Istituto di Fisica del Politecnico - Milano

(ricevuto il 14 Gennaio 1959)

Summary. — The L/K-capture ratio in orbital electron capture decay of ^{195}Au was investigated by using a measurement procedure based on coincidence techniques. It was found for the transition to the 128 keV level of ^{195}Pt: $P_L/P_K = 5.5 \pm 0.9$ which corresponds to a transition energy of 106 keV. In addition a determination of the half-life of ^{195}Au and of the K conversion coefficient of the 97 keV transition was made. It was obtained $T_{\frac{1}{2}} = (192 \pm 5)$ d and $\alpha_K = 8.4 \pm 0.5$. The proposed decay scheme agrees quite well with previous results.

1. – Introduction.

The decay of ^{195}Au to the excited levels of ^{195}Pt has been investigated by several authors (1), and so the γ-ray energies and the orbitals of the excited levels (Fig. 3) are well known. The obtained level pattern is in agreement with that deduced from the decay of ^{195}Pt^m, while there is only a partial agreement with the results of Coulomb excitation of ^{195}Pt, which suggest that the 97 and 30 keV transitions are interchanged.

A few uncertainties still remain on the conversion coefficients and relative transition rates of the excited levels of ^{195}Pt. Moreover the currently listed value of the half-life of ^{195}Au ($T_{\frac{1}{2}} = 185$ d) appears to be in contrast with the value ($T_{\frac{1}{2}} = 90 \pm 10$ d) recently obtained by Cressman and Wilkinson (2).

As far as concerns the L/K-capture ratio and the disintegration energy of ^{195}Au no further progress has been made after the investigation carried out

(*) Laboratori C.I.S.E. e Istituto di Fisica del Politecnico di Milano.

(1) D. Strominger, J. M. Hollander and G. T. Seaborg: *Rev. Mod. Phys.*, **30**, 585 (1958).

(2) D. J. Cressman and R. G. Wilkinson: *Phys. Rev.*, **109**, 872 (1958).

by some of us [3] a few years ago. It is worthy of mention that in the above investigation the L/K-capture ratio was deduced from the measurement of L and K X-rays intensity.

Errors in the result may have arisen from the fact that the L fluorescence yield values are rather uncertain, that in the decay scheme are present low energy γ transitions which are highly converted in the L-shell and whose conversion coefficients are not well known, and that the procedure was rather indirect.

The present work was intended to determinate once again the L/K capture ratio by using a direct measurement procedure based on coincidence techniques already employed in analogous investigations [4]. As a by-product of this research some data on the decay of ^{195}Au and its half-life were obtained.

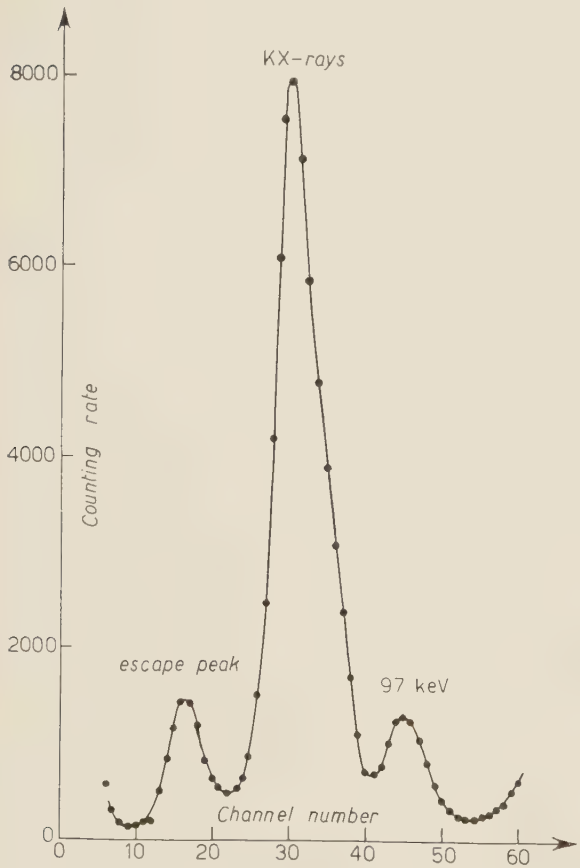

2. – Experimental results.

^{195}Au was obtained after irradiation of Pt with deuterons in the Amsterdam cyclotron and supplied as carrier-free $AuCl_3$. It can be mentioned that the decay of ^{195}Au was observed over a period of about 250 days and that its half-life resulted to be (192 ± 5) d; moreover it was observed that the relative intensities of K X and γ peaks did not noticeably change in the same time interval. This fact points out that no other important activities are present within the examined active specimens.

Fig. 1. – K X- and γ-ray spectrum from ^{195}Au.

(3) A. BISI and L. ZAPPA: *Nuovo Cimento*, **12**, 539 (1954).

(4) A. BISI, E. GERMAGNOLI and L. ZAPPA: *Nuclear Physics*, **1**, 593 (1956); *Nuovo Cimento*, **4**, 764 (1956); **6**, 299 (1957).

2'1. – Fig. 1 shows the γ and KX spectrum, which was obtained with the help of a single crystal spectrometer (NaI(Tl) crystal, of 3.75 cm diameter, 2.50 cm high, optically coupled to a Dumont 6292 photomultiplier): during the present measurements the spectra were examined by means of a ten channel fast pulse analyzer. An intense peak whose energy (about 67 keV) corresponds to characteristic K X-rays of Pt and a γ line at 97 keV can be easily noticed: the weaker peak at about 130 keV is a composite one and is mainly due to the fact that two K X quanta, which are emitted in the same disintegration, can both be detected by the crystal spectrometer, the resulting peak actually being at about 130 keV. Another consequence of the integrating features of the γ spectrometer is the presence of a very weak peak noticed at about 165 keV: this is due to coincidence between a KX quantum and a 97 keV γ-ray. However the intensity of this peak is so low that no quantitative conclusions could be drawn in this case.

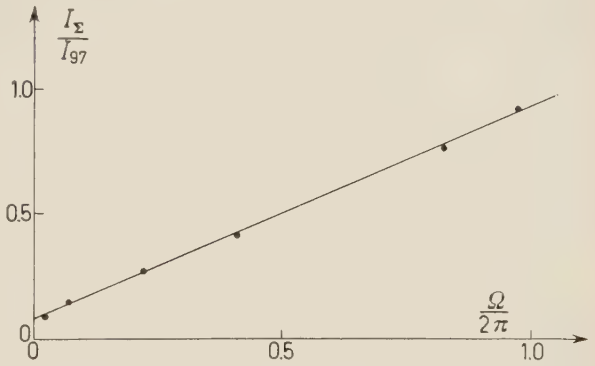

Fig. 2. – Determination of the I_{128}/I_{97} ratio by the summation method.

The ratio between the intensities of the summation peak at 130 keV and the γ line at 97 keV was measured after locating a point source of ^{195}Au at different distances from the surface of the detector. The obtained results are given in Fig. 2. The ratio decreases linearly if the source-detector solid angle is decreased and becomes constant at distances greater than 15 cm. This procedure allows the conclusions that a weak γ line at about 128 keV is present within the summation peak.

Table I gives the results concerning the relative intensities of K X and γ lines which where observed: the efficiencies of the detector and the escape probabilities of I K X-rays from the crystal were taken into account.

TABLE I.

Energy	Relative intensity
K X-rays	100
97 keV	9.61
128 keV	0.71

2·2. – All the peaks which are listed in Table I were used in coincidence measurements. In any case, only pulses belonging to one definite photopeak were allowed to trigger the coincidence circuit (2 μs resolving time). In coincidence work with the 97 keV γ-ray the triggering peak was filtered by means of Ag absorbers to eliminate the contribution of the tail of the intense K X peak: an analogous method was used when the triggering pulses belonged to the 128 keV line: in this way the above mentioned summation peak was completely cut down. Table II summarizes the results which were obtained in coincidence measurements; corrections for the probability of escape of I K X-rays from the crystal are included.

TABLE II.

Triggering peak	Coincidence intensity/intensity of triggering peak		
	K X-rays	97 keV	128 keV
128 keV	$(6.8 \pm 1.0)\cdot 10^{-2}$	—	—
97 keV	0.141 ± 0.010	—	—
K X-rays	0.227 ± 0.018	$(1.42 \pm 0.12)\cdot 10^{-2}$	weak

According to the decay scheme given in Fig. 3 the L/K-capture ratio for the orbital electron capture transition between the ground level of ^{195}Au and the 128 keV excited level of ^{195}Pt can be deduced from the coincidence measurements with the 128 keV line used as triggering peak:

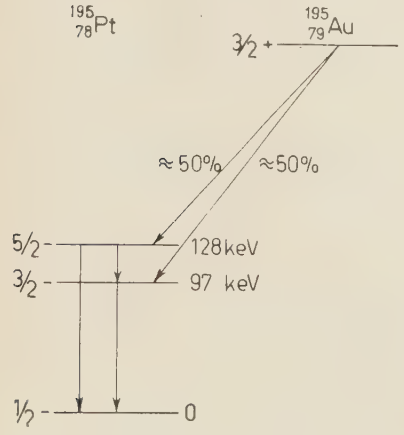

Fig. 3. – Decay scheme of ^{195}Au.

$$(1) \qquad \frac{I_{128,K}}{I_{128}} = \varepsilon_K \omega_K \frac{P_K}{P_L + P_K} .$$

Here P_L and P_K are the electron capture probabilities for the L- and K-shells, ω_K is the fluorescence yield for the K-shell in Pt ($\omega_K = 0.95$) and ε_K is the counter efficiency for K X-rays ($\varepsilon_K = 0.461$ for our experimental arrangement). From the data of Table II we obtain

$$\frac{P_L}{P_K} = 5.5 \pm 0.9 ,$$

which according to the calculations by BRYSK and ROSE [5] corresponds to a transition energy of 106 keV, if the transition itself is either allowed or first forbidden ($\Delta I < 2$).

As far as the 97 keV γ transition is concerned, the K-shell internal conversion coefficient α_K can be readily obtained from the coincidence measurements with the K X peak used as triggering peak. Actually we get

$$\frac{I_{K,K}}{I_{K,97}} = 2\alpha_K \frac{\omega_K \varepsilon_K}{\varepsilon_{97}}, \tag{2}$$

where ε_{97} is the counter efficiency for 97 keV γ-rays. For a thick NaI crystal, ε_{97} can be regarded as equal to ε_K and consequently from $I_{K,K}/I_{K,97} = 16 \pm 1$ we obtain

$$\alpha_K = 8.4 \pm 0.5 .$$

Finally, if the 97 keV γ line is used to trigger the coincidence circuit,

$$\frac{I_{97,K}}{I_{97}} = \varepsilon_K \omega_K \left[\mu \left(\frac{P_K}{P_L + P_K} \right)_1 + (1-\mu) \left(\frac{P_K}{P_L + P_K} \right)_2 \right], \tag{3}$$

where μ is the branching probability towards the 120 keV excited state of ^{195}Pt, $(1-\mu)$ is the branching probability towards the 97 keV excited state of ^{195}Pt and the indexes 1 and 2 refer to the two considered transitions. The relationship (3) shows that the L/K-capture ratio for the orbital electron capture transition between the ground level of ^{195}Au and the 97 keV excited level of ^{195}Pt cannot be directly deduced. Nevertheless if the experimental result $I_{97,K}/I_{97} = 0.141$ is inserted in (3) we get

$$0.322 = \mu \left(\frac{P_K}{P_L + P_K} \right)_1 + (1-\mu) \left(\frac{P_K}{P_L + P_K} \right)_2 .$$

Taking $(P_K/(P_L+P_K))_1 = 0.154$, which was deduced above, and $(P_K/(P_L+P_K))_2 = 0.49$, which was calculated from the results by BRYSK and ROSE for an allowed or first forbidden transition ($\Delta I < 2$) whose energy is about $(106 + 128 - 97)$ keV $= 137$ keV, we find

$$\mu \simeq 0.5 .$$

It may be concluded that the two considered electron capture transitions take place with approximately the same probabiliy. It has been assumed that

---

[5] H. BRYSK and M. E. ROSE: *Rev. Mod. Phys.*, **30**, 1169 (1958).

there is no appreciable branching between the ground states of ^{195}Au and ^{195}Pt: this was suggested by the fact that the observed intensity of K X-rays is completely accounted for by the contributions due to the K internal conversion of the 97 keV γ-ray and to the 106 keV and 137 keV K electron capture processes.

2·3. – The internal consistency of the above conclusions was checked by the results obtained from the observed intensity of K X-K X coincidence pulses. If the probability of the 128 keV γ-transition is supposed to be so small, that its contribution to K X emission can be neglected, we get

$$(4) \quad \frac{I_{K,K}}{I_K} = 2\omega_K \varepsilon_K \frac{\alpha_K}{1+\alpha} \frac{1}{1+\alpha_K/(1+\alpha)\left[\mu(P_K/(P_L+P_K))_1+(1-\mu)(P_K/(P_L+P_K))_2\right]^{-1}} .$$

The total conversion coefficient α of the 97 keV γ transition was considered equal to 9.9, in accordance with the results by DE SHALIT *et al.* [6]; if this value of α and the above experimental results are used, we have

$$\frac{I_{K,K}}{I_K} \simeq 0.20 ,$$

which is in satisfactory agreement with the value $I_{K,K}/I_K = 0.227 \pm 0.018$, obtained from coincidence measurements.

3. – Conclusion.

Fig. 3 shows the decay scheme of ^{195}Au as suggested by the results of Section 2; it appears to agree completely with previous results. The disintegration energy to the 128 keV level is slightly different from that given in ref. [3], although the new P_L/P_K value (5.5) is much greater than the old one (0.58). This is because in the low energy region the transition energy varies very slowly against P_L/P_K. The disagreement between the new P_L/P_K value and the old one can be explained by recalling that measurements involving L X-rays are made difficult from the necessity of estimating the counter efficiency and L fluorescence yields; moreover the old value was obtained from the difference of two near terms.

By assembling the obtained information on disintegration energy, branching ratio and half-life, the log ft values for the transitions to the 128 keV and 97 keV levels were found respectively equal to 5.7 and 6.3.

---

[6] A. DE SHALIT, O. HUBER and H. SCHNEIDER: *Helv. Phys. Acta*, **25**, 279 (1952).

These values are typical of allowed ($\Delta I = 0.1$; no) or first forbidden ($\Delta I = 0.1$; yes) transitions, and together with the K conversion coefficient value for the 97 keV transition obtained in Section 2, represent a set of results consistent with the orbital assignement to the levels involved in the decay, made by previous authors and included in Fig. 3.

An additional information can be deduced after combination of data given in the previous paper ([3]) and of the present results. The intensity of unconverted 30 keV γ-rays, measured by means of a proportional A+CH_4 counter, was equal to 1.42, taking the K X intensity equal to 100. If the probabilities of the two electron capture transitions towards the 97 and 128 keV levels are supposed to be equal, as suggested from the present data, from $I_{97}/I_{30} = 6.8$ one gets that the total conversion coefficient of the 30 keV γ transition is $\simeq 30$. This is consistent with the assumption of a $M1$ transition.

RIASSUNTO

Viene studiato il rapporto tra cattura L e cattura K nel decadimento dell'^{195}Au usando un procedimento di misura basato su tecniche di coincidenza. Si è ottenuto: $P_L/P_K = 5.5 \pm 0.9$ per la transizione che conduce al livello di 128 keV del ^{195}Pt. A questo valore corrisponde una energia di transizione pari a 106 keV. Sono stati, inoltre, misurati il periodo di dimezzamento dell' ^{195}Au $\left(T_{\frac{1}{2}} = (192 \pm 5)\ \mathrm{d}\right)$ ed il coefficiente di conversione K della transizione da 97 keV ($\alpha_K = 8.5 \pm 0.5$). Lo schema di decadimento proposto è in accordo con i risultati di precedenti ricerche.

NOTE TECNICHE

Performance of a Large Area non Focusing Čerenkov Counter and Absolute Yield of Čerenkov Light.

G. Caglioti (*), R. Cervellati (*) and L. Mezzetti

Istituto di Fisica dell'Università - Roma
Istituto Nazionale di Fisica Nucleare - Sezione di Roma

(ricevuto il 23 Febbraio 1959)

Summary. — The design and the performance of a large area, comparatively thin toluene Čerenkov counter are described. The velocity resolution of non focusing Čerenkov counters and its basic limitation, due to the Landau fluctuations in the emission of fast knock-on electrons, are discussed and compared with those of scintillation counters. The absolute yield of the Čerenkov light is evaluated from the measurements and found to be in good agreement with the theoretical yield.

1. – Introduction.

In the last few years focusing and non-focusing Čerenkov counters have been extensively used for the detection of fast charged particles [1].

The measurement of the velocity β of a charged particle can be performed with great precision with a focusing counter, when the incident beam has a very small cross-sectional area and angular divergence [2].

Non focusing counters can be used also when these conditions are not fulfilled, using the total amount of light produced as a measurement of β [3-5]. A further advantage of a counter of this type is that it can be converted into

(*) Now at the Comitato Nazionale Ricerche Nucleari, Roma.

(1) J. V. Jelley: *Čerenkov radiation and its applications* (London, 1958).

(2) R. L. Mather: *Phys. Rev.*, **84**, 181 (1951).

(3) P. Bassi, A. M. Bianchi and C. Manduchi: *Nuovo Cimento*, **9**, 861 (1952).

(4) M. Mandò: *Nuovo Cimento*, **12**, 5 (1954).

(5) J. R. Winckler, E. N. Mitchell, K. A. Anderson and L. Peterson: *Phys. Rev.*, **98**, 1411 (1955).

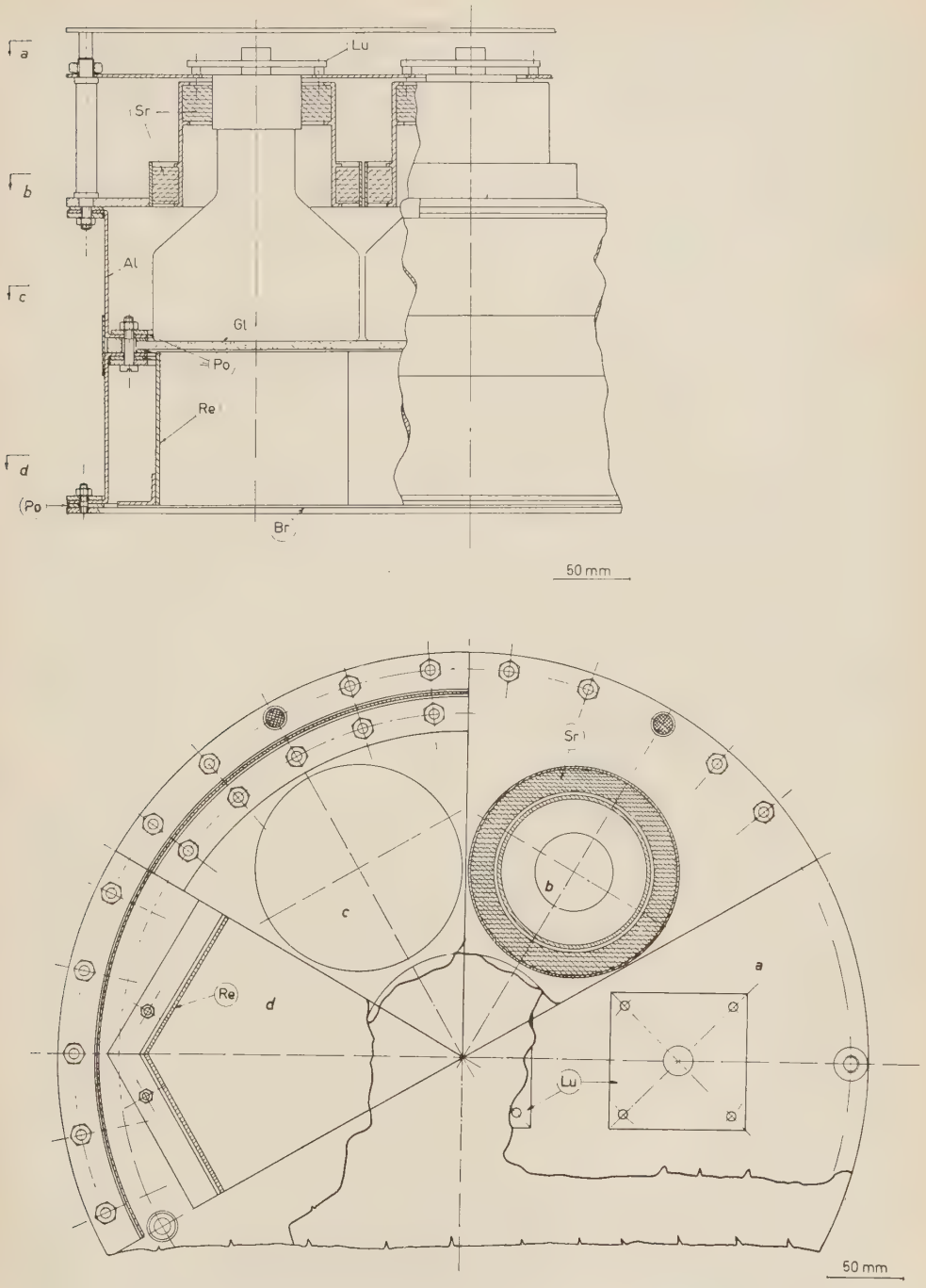

Fig. 1. – Schematic arrangement of the Čerenkov counter. Some of the materials are indicated: Gl = Glass, Al = Aluminum, Re = Reflector (polished Aluminum or white coating), Po = Polyethylene, Br = Brass, Sr = Soft rubber, Lu = Lucite.

a multichannel velocity selector by applying conventional pulse height analysis. Serious drawbacks, however, are represented by the relatively small amount of light usually available, which gives rise to poor photomultiplier statistics, and the fundamental limitation set by the Landau fluctuations.

In this paper we want to discuss quantitatively such possibilities and limitations on the basis of a few results obtained with a comparatively thin, large area Čerenkov counter built in this laboratory for measurements on Cosmic Ray particles. The counter was originally designed to select fast Cosmic Ray secondaries travelling upwards, from a very large cross-sectional area.

2. – Experimental apparatus.

The Čerenkov counter (C) is shown in Fig. 1; it is enclosed in two cylindrical Aluminium boxes 47 cm in diameter, separated by a 5 mm thick circular glass window.

One of the two boxes hides seven Dumont 6364 photomultipliers (PM). The PM are mounted in a close-packed hexagonal arrangement; their cathodes are kept in optical contact with the glass window by the spring action of the silvered steel contacts providing the electrode voltages, mounted on a lucite frame.

The other box is completely filled, to a thickness of 10 cm, with about 12 liters of pure toluene.

The choice of the Čerenkov material was based on the requirement of maximum light output for a given energy loss. For ultrarelativistic singly charged particles one can use as figure of merit M the quantity:

$$M = \frac{436}{\varrho Z/A}\left(1 - \frac{1}{n^2}\right) \text{ photons g}^{-1}\,\text{cm}^2\,,$$

which gives the number of photons between 3 000 and 7 000 Å generated in a material of density ϱ, index of refraction n, and effective mass to atomic number ratio A/Z. For lower energies, the calculated light yields for a few transparent materials are plotted in Fig. 2. Good light transmission and weak scintillation [6] were obviously also required and checked.

The sensitive region of the liquid is limited laterally by a hexagonal reflector whose cross-section matches the array of the seven photocathodes.

The seven PM anodes are connected to an open ring of heavy wire which forms a line of approximately 200 Ω impedance correctly matched at one end (« fast » output). A « slow » output, more suitable for accurate pulse height analysis, is obtained by mixing the dynode signals at the common plate of seven preamplifiers.

The anode supply voltages of the seven PM were chosen so as to give equal pulse for equal amount of light collected by the photocathode. Standard light pulses were obtained from a small plastic scintillator with a weak Polonium α-source, placed in turn near the center of each photocathode.

---

[6] R. Madey and L. Leipuner: *Nucleonics*, **14**, no. 4, 51 (1956).

The « slow » signal was fed either to a threshold discriminator or to a nine channel differential discriminator through a linear amplifier ($T_R = 0.08$ μs, maximum gain = 80 db).

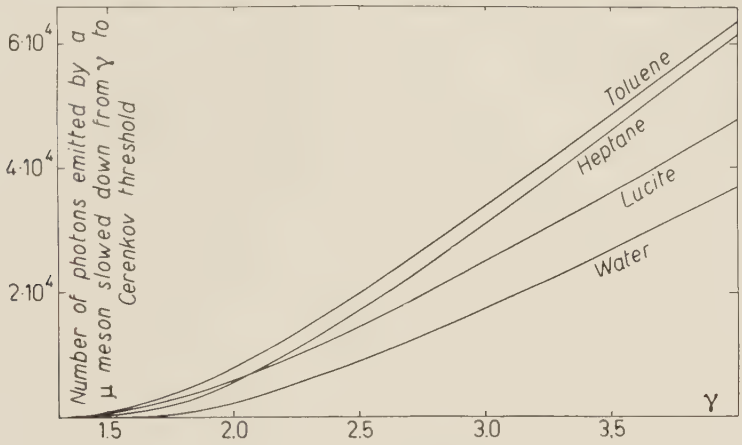

Fig. 2. – Calculated number of photons (between 3 000 and 7 000 Å) emitted by a μ-meson slowed down, in various transparent materials, from initial energy $E = m_0c^2\gamma$ to Čerenkov threshold, *vs.* γ.

In both cases the discriminator was gated by the twofold (or threefold) coincidence of a Cosmic Ray μ-meson vertical telescope AB (or ABD).

Two kinds of measurements have been performed.

In the first series of measurements we tested the counter for its « anti-directionality » ([4]): to this end, the bottom plate was covered with black velvet, and the lateral reflector consisted of a mirror polished sheet of aluminum alloy.

In the second series of measurements we tested the counter for optimum pulse height resolution: to this end, the lateral walls and the bottom plate were covered with a white coating of TiO_2 dispersed in water glass on a white enamel background. The Čerenkov counter was usually operated with the photomultipliers *looking down* (C_{down}). This arrangement, in which the light undergoes at least one diffusion before reaching the photocathodes, was found to be the most convenient, because of the greatly improved uniformity of light collection, in spite of the loss of light involved.

3. – Results.

3·1. *Antidirectionality tests.* – The results of the antidirectionality test are summarized in the plots of Figs. 3 and 4.

The main features of the curves in Fig. 3 are in agreement with what one expects. We would only like to emphasize that a high efficiency and a good antidirectionality can both be obtained with a comparatively thin radiator (8.7 g/cm² in our case).

To investigate the origin of distributions III and IV we performed the measurement indicated in Fig. 4 (curve V).

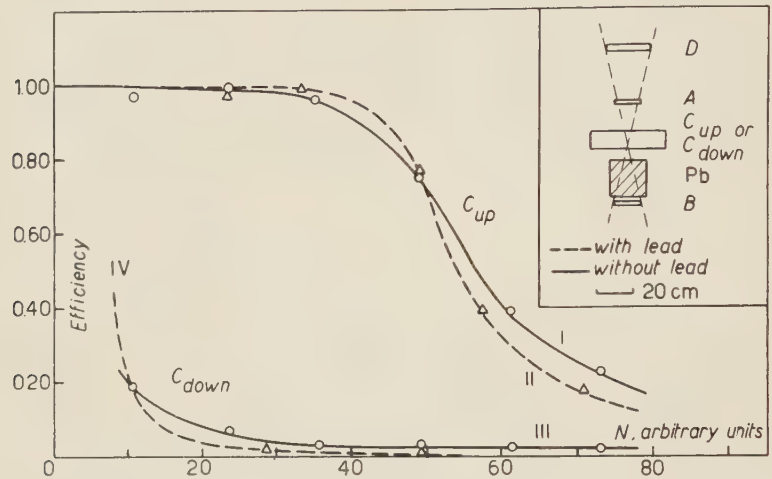

Fig. 3. – Efficiencies of the antidirectional Čerenkov counter *vs.* minimum pulse height N accepted by the integral discriminator, for the telescope shown in the inset.

A glance at curves IV and V shows that approximately equal amounts of light going upwards are somehow produced in the toluene and in the glass window.

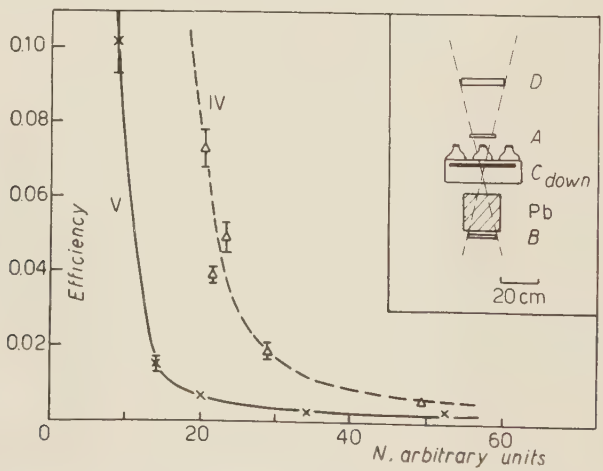

Fig. 4. – Efficiency *vs.* minimum pulse height N. Curve V was obtained with the arrangement shown in the inset, *i.e.* with counter emptied and with a black lucite plate in optical contact with the glass window so as to absorb completely the Čerenkov light produced in the glass. Curve IV of Fig. 3 is reproduced for comparison.

Actually it is a known fact [6] that most of the substances used for Čerenkov counters do scintillate when they are crossed by ionizing particles.

D.C. measurements performed in this laboratory indicate that our toluene and our glass have a scintillation efficiency, for 5 MeV α-particles, about 10^{-2} and $5 \cdot 10^{-2}$ times that of a standard p-terphenyl in toluene solution. This explains the relative positions of curve IV and V. The long tails towards the larger pulse heights can be qualitatively accounted for in terms of small knock-on showers.

3·2. *Pulse height resolution measurements.* – Fig. 5 shows an overall C_{down} distribution obtained by combining measurements performed with a narrow beam of μ-mesons over a period of several weeks (*). The individual distri-

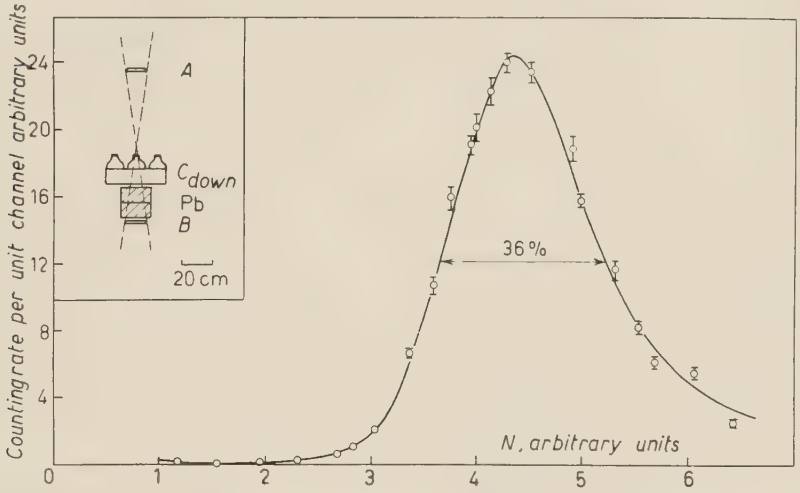

Fig. 5. – Overall differential pulse height distribution obtained with the « white » Čerenkov counter and the telescope shown in the inset.

butions were not exactly reproducible because of a slight long-range instability of the electronics, including the calibration equipment. For this reason the spread of the combined distribution is somewhat larger than that of the individual runs.

In Fig. 6 are plotted two typical distributions obtained with the white Čerenkov counter looking up and down and a lead filter 20 cm thick.

As expected, the most probable pulse height is larger for the disposition C_{up} than for C_{down}, while the relative width of the C_{down} distribution is smaller than that of C_{up}. From the ratio of the most probable pulse heights we obtain a value of about 0.7 for the average light diffusion coefficient in agreement with direct spectrophotometric measurements.

(*) The lead filter used was sometimes 10 and sometimes 20 cm thick, but its thickness did not appreciably affect the results.

The counter was tested also for uniformity of response over its large area, by shifting it horizontally up to about 10 cm with respect to the telescope. The C_{down} response was found to be uniform within the limits set by the mentioned instability of the electronics, *i.e.* better than $\pm 5\%$.

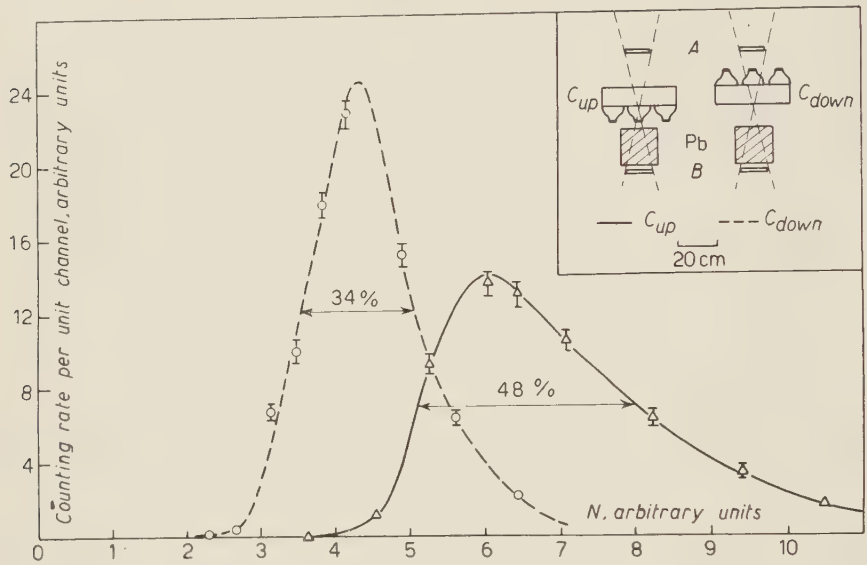

Fig. 6. – Differential pulse height distributions obtained with the « white » Čerenkov counter and the telescope shown in the inset.

4. – Landau type fluctuations and resolution.

The velocity resolution of a non focusing Čerenkov counter is limited by many effects, and ultimately by the Landau fluctuations in the emission of fast knock-on electrons.

The latter have been discussed qualitatively by LINSLEY and HORWITZ (7) who showed that for a sufficiently thin Čerenkov counter the « theoretical » resolution is better than that of a scintillator of the same thickness, because of the existence of a threshold in the Čerenkov emission.

According to LINSLEY and HORWITZ's criterion our counter cannot be considered « thin » and its behaviour is therefore expected to be similar to that of a scintillator; this is in agreement with the shape of our experimental distributions, showing the typical Landau asymmetry. The contribution of this type of fluctuations to the fractional total width at half maximum can therefore be estimated directly from Landau's treatment (8), giving, for the average

(7) J. LINSLEY and N. HORWITZ: *Rev. Sci. Instr.*, **26**, 557 (1955).
(8) L. LANDAU: *Journ. Phys.* (*USSR*), **8**, 201 (1944).

μ-meson crossing our telescope (see eq. (4)):

$$\left(\frac{A_{\frac{1}{2}}}{H}\right)_d = 0.185 \quad (*) . \tag{1}$$

One may notice that the relation between the error in the measurement, for example, of the quantity $\gamma = E_{\text{tot}}/m_0c^2$ and the fractional error $\Delta H/H$ in the measurement of the light yield is in favour of the Čerenkov counter, in a range of γ-values depending on the index of refraction, as indicated in Fig. 7.

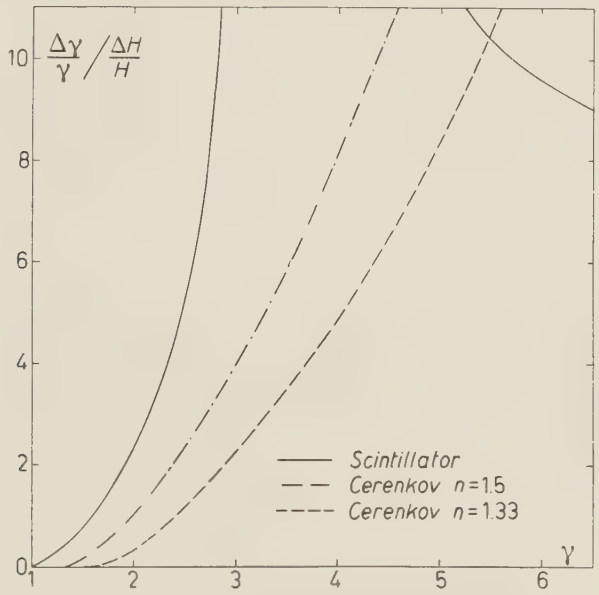

Fig. 7. – Calculated fractional error $\Delta\gamma/\gamma$ due to a fractional error $\Delta H/H$ in pulse height, *vs.* $\gamma = (1-\beta^2)^{-\frac{1}{2}}$ for a scintillator and for typical Čerenkov counters. The scintillation pulse is assumed to be proportional to the specific energy loss; the slowing down of the particle within the counters is neglected.

To exploit this fact it is of course necessary to reduce the fluctuations due to photoelectron statistics to a sufficiently small amount, by improving the collection and photomultiplier conversion efficiency. Such improvements do not seem beyond the reach of foreseeable technological developments.

(*) A calculation using the gaussian approximation [9] leads to

$$\left(\frac{A_{\frac{1}{2}}}{H}\right)_{\text{Čerenkov}} = 0.24 , \qquad \left(\frac{A_{\frac{1}{2}}}{H}\right)_{\text{Scintillator}} = 0.26 .$$

[9] B. Rossi: *High Energy Particles* (New York, 1952), p. 31.

5. – Absolute yield of Čerenkov light.

It is interesting to try to evaluate from our results the absolute yield of the Čerenkov light per particle, in order to compare it with the theoretical yield given by the Frank and Tamm formula. Estimates of this kind were performed firstly by Čerenkov himself ([10]) (luminescence of a strong β-source in benzene), and later, through a somewhat indirect method, by BELCHER ([11]) (again with β-rays in water), and by ASCOLI-BALZANELLI and ASCOLI ([12]) (with Cosmic Ray μ-mesons in gases and vapours).

To do this we have estimated the absolute average number q of photoelectrons per particle in two ways:

A) From the measured size of the most probable voltage pulse height.

B) From the relative width of the pulse height distribution.

A) The first method consists obviously in applying the equation

$$q = \frac{CH}{eG_p G_c}, \tag{2}$$

where C is the average output capacitance, G_p is the PM gain, G_c is the total gain of the amplification chain, and H is the most probable pulse height as measured (in volts) by the discriminator.

For G_p we took the average gain of the seven PM computed from the nominal tube characteristics; G_c was calibrated by means of a mercury switch pulse generator.

Inserting the numerical values we obtained:

$$q = 135 \text{ photoelectrons/particle} .$$

To obtain the number of Čerenkov photoelectrons we must subtract the contribution due to the scintillation of our radiator, evaluated from the curves of Fig. 3. The final result is

$$q_{\text{Čerenkov}} = 106 \text{ photoelectrons/particle} . \tag{3}$$

B) The second method requires that the contribution *a*) to the measured total spread due to the PM statistics be isolated from the other contributions, such as: *b*) energy and *c*) angular spreads of the impinging particles; *d*) Landau-type fluctuations of Čerenkov light; *e*) non-uniformity of the light collection efficiency and photocathode sensitivity; *f*) statistical fluctuations in the number of photons collected.

We assume that the relative width of the pulse height distribution (full width at half-maximum $A_{\frac{1}{2}}$ divided by the most probable pulse height H) is

([10]) P. A. ČERENKOV: *Compt. Rend. Acad. Sci. USSR*, **21**, 116 (1938).
([11]) E. M. BELCHER: *Proc. Roy. Soc.*, A **216**, 90 (1953).
([12]) A. ASCOLI-BALZANELLI and R. ASCOLI: *Nuovo Cimento*, **6**, 1392 (1957).

made up by partial widths due to the above effects:

$$\left(\frac{A_{\frac{1}{2}}}{H}\right)_a^2 = \left(\frac{A_{\frac{1}{2}}}{H}\right)^2 - \left\{\left(\frac{A_{\frac{1}{2}}}{H}\right)_b^2 + \ldots + \left(\frac{A_{\frac{1}{2}}}{H}\right)_f^2\right\} . \tag{4}$$

The most important partial width in the sum at the right hand side of eq. (4) is that due to the Landau-type fluctuations, and has been discussed in the preceding section. The second important is the contribution *f*) which can be calculated as a correction with a successive approximation procedure assuming an average cathode efficiency of 11%. Taking into account also the other small contributions we obtained

$$\left(\frac{A_{\frac{1}{2}}}{H}\right)_a^2 = (0.34)^2 - (0.21)^2 = 0.072 .$$

The effect of photomultiplier statistics can be represented with the formula (*)

$$\left(\frac{A_{\frac{1}{2}}}{H}\right)_a^2 = \frac{(2.36)^2}{q}\left[1 - f + \frac{\varepsilon\delta}{\delta_1(\delta - 1)}\right] , \tag{5}$$

where q is the number of useful photoelectrons, f is the ratio of q to the number of impinging photons, δ is the average dynode multiplication factor times the electron collection efficiency, δ_1 is the analogous quantity for the first dynode (which is usually operated at a higher voltage than the others), and ε is a parameter connected with the supernormality of the statistics of the multiplication process, ranging, according to the various authors, from 1.0 to 1.5; for the latter we take the value 1.3 (*).

Inserting the appropriate numerical values and correcting as before for the scintillation photoelectrons, we obtained:

$$q_{\text{Čerenkov}} = 79 \text{ photoelectrons/particle} . \tag{6}$$

It should be emphasized that this result is affected by a rather large uncertainty (and is probably too low) because of its critical dependence on the estimates of the individual partial widths and specially on the value of the measured total spread. For example, a change of the latter from 0.34 to 0.33 would increase the value of q by about 10%; furthermore the spreads due to instability of the electronics and to non-uniformity of light collection and photomultiplier cathode efficiency, which have been disregarded, could easily account for an increase of several percent each in the final result.

On the other hand, the number of Čerenkov photoelectrons to be expected can be calculated starting from the Frank and Tamm formula. The procedure is straightforward, but requires the knowledge of the optical properties of the whole apparatus used as a function of wavelength. We write approximately:

$$q_{\text{Čerenkov}} = \frac{2\pi}{137}\left(1 - \frac{1}{\beta^2 n^2}\right) Lg \int \frac{hc}{\lambda^3}\, t(\lambda) R(\lambda)\, \mathrm{d}\lambda , \tag{7}$$

(*) For a complete discussion see U. Amaldi, jr.: *Thesis* (Rome, 1957).

where β is the velocity of the impinging particle, n is the (constant) index of refraction of our radiator, L is the radiator thickness in cm, and $g = 0.53$ is the geometrical collection efficiency for the Čerenkov photons. In the integral $t(\lambda)$ is the attenuation suffered by light of wavelength λ along its average path through the toluene and the glass up to the photocathodes, $R(\lambda)$ is the absolute spectral sensitivity of the PM used (S4) as given by the manufacturer (*), and hc/λ^3 is the energy spectrum of the Čerenkov light. $t(\lambda)$ has been obtained by spectrophotometric measurements; g has been calculated taking into account in an approximate way the multiple diffusion of the light on the white walls of the counter. To this end, the diffusion coefficient was estimated as mentioned in Section 3.

In this way we obtained

$$q_{\text{Čerenkov}} = 102 \text{ photoelectrons/particle} . \tag{8}$$

Disregarding the factor $t(\lambda)$ one would obtain, instead, 265 photoelectrons/particle. Considering the uncertainties involved in the evaluations of $q_{\text{Čerenkov}}$ the agreement between the three values obtained is remarkably good, and may be considered as a further check of the absolute intensity of the Čerenkov light as given by FRANK and TAMM.

6. – Conclusions.

In conclusion, we would like to stress the following points:

1) The Čerenkov counter described in this paper can be used as a high efficiency antidirectional detector, or as a good resolution non focusing device; in both cases good uniformity of response over its large area was obtained.

2) The contribution of the Landau-type fluctuations to the overall spread of the pulse height distribution is found to be comparable with that of photoelectron statistics.

3) The absolute yield of the Čerenkov light is experimentally found to be in good agreement with the theoretical one.

(*) Differences between individual phototubes are at least partially compensated by the fact that the light is distributed among seven photocathodes.

RIASSUNTO

Vengono illustrati la costruzione e le prestazioni di un contatore di Čerenkov a toluolo di spessore relativamente piccolo. Viene discussa la risoluzione in velocità dei contatori di Čerenkov non focheggiati e la sua limitazione essenziale dovuta alle fluttuazioni di Landau nell'emissione di elettroni knock-on veloci. Viene effettuato un confronto fra l'intensità assoluta della luce di Čerenkov ottenuta sperimentalmente e quella calcolata a partire dalla formula di Frank e Tamm. L'accordo fra i valori teorici e sperimentali è buono.

IL NUOVO CIMENTO Vol. XI, N. 6 16 Marzo 1959

Experiments on a Ion Source for an Electromagnetic Isotope Separator.

F. Bisi and B. De Michelis

Istituto di Fisica Sperimentale del Politecnico - Milano

(ricevuto il 24 Febbraio 1959)

Summary. — The paper describes a hot cathode, magnetic ion source for an electromagnetic isotope separator. The source, useful both for gaseous and solid charge materials, gives a total ion output of about 20 mA. Measurements on discharge characteristics, extracted currents and source efficiency are reported and the effects of introducing reflecting electrodes in the discharge chamber are discussed.

1. – Introduction.

We have developed a ion source to operate in an electromagnetic isotope separator. The choice of the type of source was determined by the usual requirements:

1) maximum ion output not lower than 10 mA;

2) low operating pressure;

3) good performance both for gaseous and solid charge materials.

To satisfy these requirements we studied a hot cathode, magnetic ion source with radial ion extraction ([1-3]). The behaviour of our source is satisfactory for good efficiency and high ion output: in particular, a considerable increase in efficiency has been obtained by the introduction of two reflecting electrodes in the discharge chamber, as is described in Sect. **6**.

([1]) H. Heil: *Zeits. Phys.*, **120**, 212 (1943).

([2]) R. Bernas: *Journ. Phys. et Rad.*, **14**, 34 (1953).

([3]) J. Kistemaker, P. K. Rol, J. Schutten and C. De Vries, in M. L. Smith: *Electromagnetically Enriched Isotopes and Mass Spectrometry* (London, 1955), p. 10.

2. – The source.

The discharge chamber is cut from a block of graphite and supported by a stainless steel tube (Fig. 1). Two copper rods support the tungsten filament (diameter = 1 mm) and serve the current supply. The filament is connected to the conical extremities of the copper rods by two invar nuts: the negligible

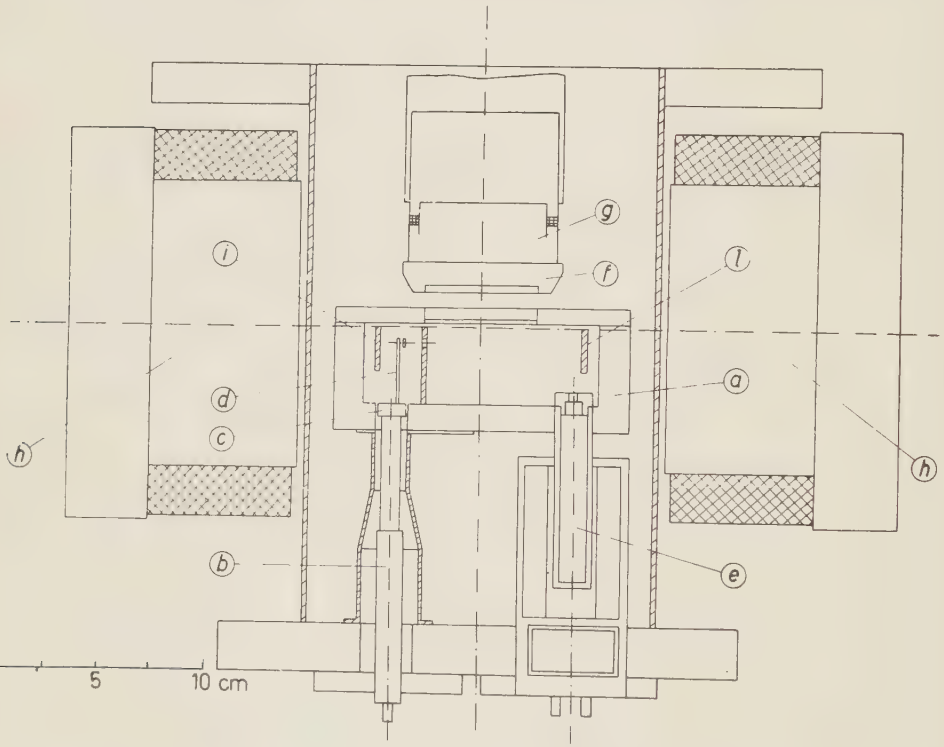

Fig. 1. – Ion source: *a*) graphite box; *b*) copper rods; *c*) invar nut; *d*) filament; *e*) graphite furnace; *f*) extraction electrode; *g*) ion collector; *h*) magnet; *i*, *l*) reflecting electrodes at cathode potential.

thermal dilatation coefficient of invar assures a good electrical contact between rods and filament, even at high temperatures. The exit slit on the front plate of the chamber was shaped as a Pierce electrode ([4]).

The graphite furnace for evaporation of solid charge materials is electrically heated and can be easily replaced by a system for introducing gas in the

([4]) J. R. PIERCE: *Journ. Appl. Phys.*, **11**, 548 (1940).

discharge chamber. When solid charge materials are used, it is convenient to maintain the discharge chamber at a higher temperature than that of the furnace, in order to prevent material from being deposited in the source: to obtain this condition an electric resistance (200 W) is inserted in the walls of the chamber. Some parts of the system are water-cooled to maintain the *O* ring seals at low temperature, while the source is operating.

The graphite extraction electrode is shaped as a Pierce surface for a collimated ion beam. The dimensions of the slits are respectively 2×50 mm for the exit slit on the front plate and 4×55 mm for the extraction slit. The distance between the two slits can be varied: most measurements were taken at a distance of 8 mm. The ions are collected in a Faraday cage which is always at a positive potential with respect to the extraction electrode, so as to avoid errors in current measurements due to secondary electrons from the collector. The magnet for the alignement of electrons emitted from the filament gives a maximum induction of 800 G; the gap is 170 mm.

The operating conditions used during the measurements are reported in the following Table:

TABLE I.

Arc voltage	$(50 \div 200)$ V
Arc current	$(0.1 \div 5)$ A
Filament heating current	$(40 \div 60)$ A
Magnetic field	$(100 \div 800)$ G
Extraction potential	$(2 \div 7)$ kV
Furnace heating power	500 W

The study of the characteristics of the ion source was made with argon. We were interested to know the pressure in the discharge chamber; therefore the system for gas introduction was supplied with a Pirani gauge head or a ionization gauge head for different ranges of pressure. In experiments with argon the source ran continuously for several hours with great stability, good efficiency and high ion output. Periodical dismounting and cleaning of the source was necessary; the operation is very easy due to the simplicity of assembly. Some preliminary experiments with zinc gave satisfactory results.

3. – Measurements on the discharge.

In Fig. 2 are reported some current-voltage characteristics of a discharge in argon at different pressures. At low discharge currents the arc voltage is generally less than 40 V and the arc current is mostly carried by primary electrons emitted from the filament. When the arc current exceeds the saturation current from the cathode, higher arc potentials are necessary to increase the current, to which the secondary electrons in plasma contribute. The curves show a decrease of arc voltage at low currents when pressure is increased;

this fact may be due to the higher collision probability that allows the same values of arc current with lower accelerating potential for electrons being reached.

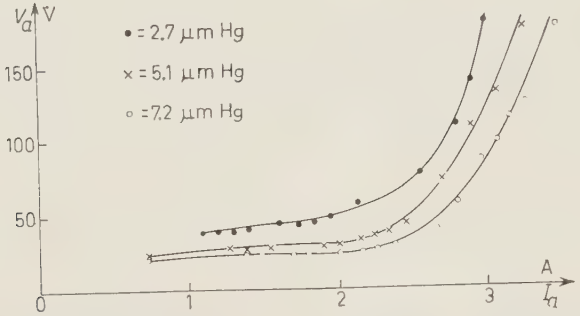

Fig. 2. Current-voltage characteristics of a discharge in argon for different pressures (magnetic induction = 630 G; filament heating current = 58 A).

Fig. 3 shows the effect of increasing pressure on arc current: the curves, at a constant arc voltage and different values of filament heating power, show the existence of a minimum pressure ([5]) required to maintain the discharge; that for our source is about 10^{-3} mm Hg.

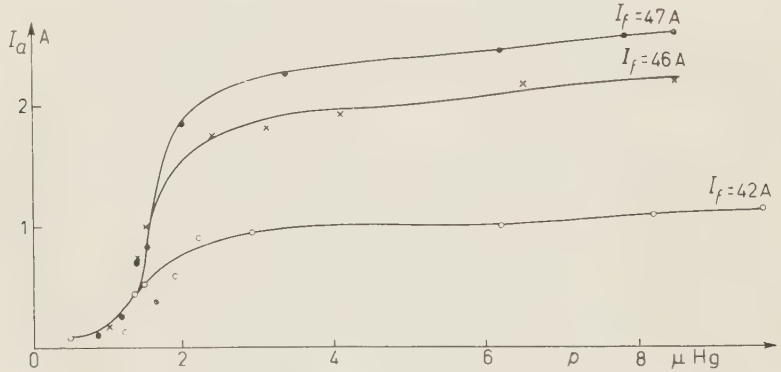

Fig. 3. – Arc current as a function of discharge pressure for different filament heating currents (magnetic induction = 630 G; anode voltage = 170 V).

4. – Measurements on ion current.

Due to the low extraction potentials, the ion currents collected on the Faraday cage are low. However the total ion current, including the current collected on the extraction electrode, can exceed 10 mA. Fig. 4 shows

([5]) W. WALCHER in J. KOCH: *Electromagnetic isotope separators and applications of electromagnetically enriched isotopes* (Amsterdam, 1958), ch. XIII.

that the collected saturation current increases at increasing extraction potentials: this means that measured currents are space charge limited. With an extraction potential of 6 kV at an extraction distance of 8 mm we obtained

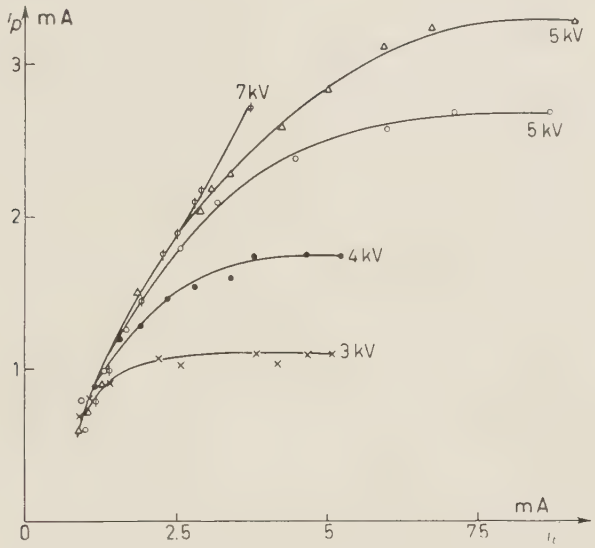

Fig. 4. – Ion currents at collector as a function of total extracted current for different extraction voltages (magnetic induction = 630 G; distance between the electrodes = 8 mm).

a ion current of about 8 mA with a ratio 1 : 1 between the collimated current and the current collected on the extraction electrode. Obviously the value of collimated current and the extraction ratio can be greatly improved with higher accelerating potentials valuable in the electromagnetic separator operation.

In Fig. 5 the saturation values of collected currents are plotted as function of extraction potential; the data fit well the Langmuir formula [6]

$$i_p = G \sqrt{\frac{U^3}{M}} \cdot \frac{A_m}{d^2},$$

where U is the extraction potential, A_m the area of the emitting electrode, d the distance between emitting and accelerating electrode and M the mass number of ions. G is a constant depending on the geometric configuration of the extraction system.

---

[6] I. Langmuir e K. T. Compton: *Rev. Mod. Phys.*, **3**, 327 (1937).

In measurements of collected currents as function of the distance d between the electrodes, the Langmuir formula was well verified except in case of short distance, probably due to the deformation of the plasma meniscus at strong electric fields.

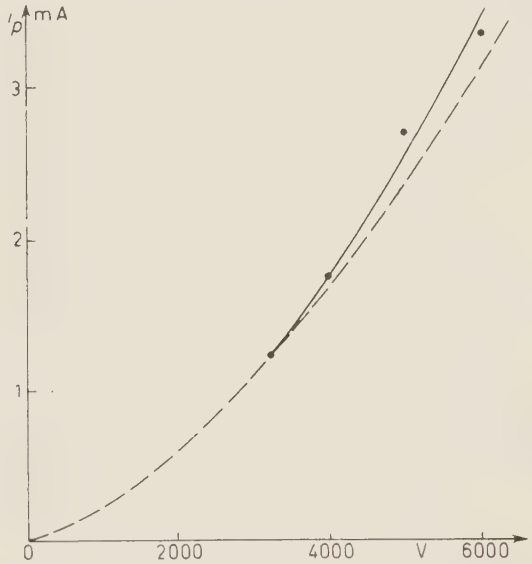

Fig. 5. Collected current at saturation as a function of extraction potential (magnetic induction = 630 G; distance between electrodes = 8 mm); ● experimental data; – – – theoretical curve.

5. – Measurements on efficiency of the source.

It is of interest to operate a high efficiency source, chiefly in separating radioactive or rare substances. We have therefore measured the efficiency of the source, usually defined as

$$\varepsilon = \frac{\eta}{1+\eta},$$

where η is the ratio of the number of ions per second emitted from the source to the number of neutral atoms per second emerging through the exit hole. This last term can be calculated when pressure p and temperature T_g in the discharge chamber, and the area A_0 of the exit slit are known [5]. Then for a gas of atomic weight M and an extracted current i, we have:

$$\eta = 1.79 \cdot 10^{-1} \frac{\sqrt{T_g M}}{p A_0} \cdot i .$$

From the data for our source, when operating with argon, we obtain:

$$\eta = 29.8 \frac{i}{p},$$

where i is expressed in ampere and p in μm Hg. In the calculation we have used a discharge temperature T_g of 700 °K.

With regard to the total current i emitted from the source slit, the theory [5] enables us to calculate the total efficiency of the source as:

$$\eta_t \propto j_e \sigma \frac{V}{A} \sqrt{\frac{M}{T_g}} \cdot \frac{A_m}{A_0},$$

where j_e is the electron current density, σ the ionization cross section for the gas, V the volume of plasma, A the total limiting area of plasma, and A_m the area of the ion extraction meniscus. This relation is independent, at first approximation, of pressure in the source. If we consider only the current i_p of the collimated beam, we have:

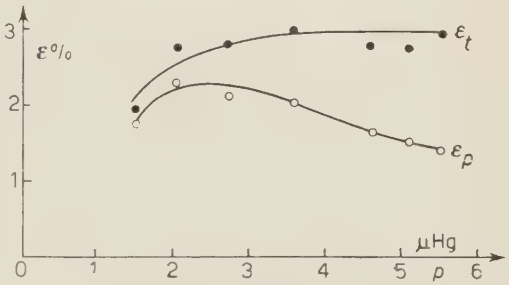

Fig. 6. – Total source efficiency ε_t and source efficiency for collimated beam ε_p as a function of pressure (magnetic induction 800 G; extraction potential = 5 kV; distance between electrodes = 8 mm).

$$\eta_p \propto \frac{\sqrt{U^3 T_g}}{pd^2} \cdot \frac{A_m}{A_0},$$

the efficiency of the source then decreases with pressure.

The experimental curves for ε_t and ε_p in our sources are reported in Fig. 6 as a function of pressure. The total efficiency of the source can reach the value of about 4.5%.

6. – Effect of reflecting electrodes.

To increase the efficiency we introduced two reflecting electrodes i and l (Fig. 1) at the same potential as the cathode [2,3]; the electrode just behind the filament increases the primary electron current that enters the main discharge chamber, while the other electrode compels the electrons to oscillate, and so lengthening their path in gas and enhancing collision probability. With such an arrangement we obtained an overall efficiency higher than 25%: the total extracted currents can reach (20÷25) mA.

Total efficiency curves ε_t for different operating conditions are reported in Fig. 7: the effect of introducing reflecting electrodes is clearly visible. When

the source is operating with reflecting electrodes, efficiency over 25% can be obtained by increasing the filament heating power: however the curves show a marked dependence on pressure, which can probably be attributed to the variation of plasma meniscus area A_m, at increasing arc current, and to the variation of electron primary current, due to the ion bombardment of filament.

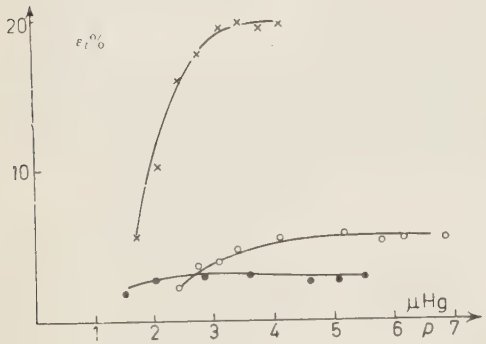

Fig. 7. – Effect of reflecting electrodes on total source efficiency: x both electrodes at cathode potential; • without reflecting electrodes; o electrode *l* at cathode potential; electrode *i* at ground potential.

At high arc currents an intense effect of filament sputtering takes place, which shortens the filament's life and causes the metal vapours to be deposited on insulators. To obviate this inconvenience we have used a different type of filament, whose coils have a diameter just greater than the diameter of the electron collimating hole. Such a disposition greatly reduces the sputtering as well as the efficiency, though the latter has still a tolerable value.

Naturally an effective evaluation of the optimum operating conditions of the source is related to a study of the beams at the collector of the separator.

* * *

Thanks are due to prof. G. Bolla for his kind interest in this work.

RIASSUNTO

Viene descritta una sorgente di ioni a campo magnetico e catodo caldo per un separatore elettromagnetico di isotopi. La sorgente, progettata sia per sostanze solide che sostanze gassose, può fornire una corrente totale di ioni di circa 20 mA. Vengono riportate misure sulle caratteristiche di scarica, sulle correnti estratte e sul rendimento della sorgente e viene discusso l'effetto di elettrodi riflettori, posti nella camera di scarica, sul funzionamento della sorgente.

LETTERE ALLA REDAZIONE

(La responsabilità scientifica degli scritti inseriti in questa rubrica è completamente lasciata dalla Direzione del periodico ai singoli autori).

The $\Sigma \to p + \gamma$ Decay Induced by Heavy Vector Mesons (*) (**).

P. Prakash

Centro Brasileiro de Pesquisas Físicas - Rio de Janeiro

A. H. Zimerman

Instituto de Física Teórica - São Paulo

(ricevuto il 27 Dicembre 1958)

A Universal Vector minus Axial Vector coupling for the Fermi interaction among four fermions was proposed by several authors (1). It was suggested by Feynman and Gell-Mann that such Universal interaction may arise from the exchange of « electrically charged » vector mesons of very high mass between the two currents formed by the two pairs of fermions. Leite Lopes (2) suggested the possibility of including the neutral counterpart of the vector meson in the theory also, provided that we assume that the neutral meson enters the coupling with the fermion field in such a way that the current which creates the neutral meson is conserved. The neutral meson then leads to an effective non-electromagnetic potential between neutron (or neutrino) and electron.

In a theory which allows only direct four fermion interaction the radiative decays of the type $\mu \to e + \gamma$, $\Sigma \to p + \gamma$ etc. involve at least the square of the Fermi coupling constant G in the matrix element and consequently are very slow. However, if the interaction is due to the existence of vector mesons (3) these decays are possible with only the first power of the coupling constant (or rather eG) in the matrix element. These decays may not be then very small compared to the corresponding other modes of decays known experimentally and involving the first power of the coupling constant G. Feinberg (4) has shown that, through the vector

(*) Supported in part by the Conselho Nacional de Pesquísas of Brasil.

(**) Presentato al XLIV Congresso della Società Italiana di Fisica, Palermo, 6-11 Novembre 1958.

(1) R. P. Feynman and M. Gell-Mann: *Phys. Rev.*, **109**, 193 (1958); E. C. G. Sudarshan and R. E. Marshak: *Padua-Venice Conference on Mesons and Recently Discovered Particles* (September 1957); J. J. Sakurai: *Nuovo Cimento*, **8**, 649 (1958).

(2) J. Leite Lopes: *Nucl. Phys.*, **8**, 234 (1958).

(3) The vector meson must be of very high mass in order to be unstable for the decay into known particles [reference (2)]. This is also implied by the close agreement of the experiments with the predictions of the local Fermi interaction theory.

(4) G. Feinberg: *Phys. Rev.*, **110**, 1482 1958).

meson, the branching ratio of $\mu \to e + \gamma$ to $\mu \to e + \nu + \bar{\nu}$ is $\sim 10^{-4}$ while that for $\mu^+ \to e^+ + e^+ + e^-$ arising from the internal conversion of the photon is $\sim 10^{-6}$.

In this note we have calculated the branching ratios for the decay $\Sigma^+ \to p + \gamma$ which is also possible through the intermediate vector meson. The Σ^+ decays virtually into a charged vector meson and a neutral baryon which then recombines to create a proton. The photon may be emitted due to the interaction of the electromagnetic field with the charged meson or with the ingoing or the outgoing charged particles ([5]).

The interaction Hamiltonian for the coupling of fermion fields with the vector meson field is given by ([6])

$$\mathcal{H}_I(x) = g\bar{\psi}_n\gamma_\rho(1+\gamma_5)\psi_\Sigma\varphi_\rho + g\bar{\psi}_p\gamma_\rho(1+\gamma_5)\psi_n\varphi_\rho + \text{h.c.}\,.$$

The quadratically divergent terms as well as the non-gauge invariant terms disappear when the contributions from the three diagrams are summed and the final result is only logarithmically divergent. The matrix element $\mathcal{M}$ is given by

$$\mathcal{M} \simeq e\frac{g^2}{M_x^2}\bar{u}^P(p_1)\left\{\frac{i\pi^2}{2}D[(1-\gamma_5)m_2 + (1+\gamma_5)m_1]\,\sigma_{\mu\nu}(\varepsilon_\mu k_\nu - \varepsilon_\nu k_\mu) + F\right\}u^\Sigma(p_2).$$

Here p_1 and p_2 are the four momenta of the proton and the Σ of masses m_1 and m_2 respectively and k is the four momentum of the photon of the polarization four vector ε. $D = (1/i\pi^2)\int d^4q/(q^2 + M_x^2)^2$ is the logarithmically divergent integral and F is the finite term. When the mass of the vector meson is assumed high (say ten proton masses) F can be shown to be proportional to the inverse of the square of the vector meson mass and can be neglected.

For the branching ratios we obtain (summing over the various intermediate baryons), for a cut-off of the order of the mass of the vector meson:

$$\frac{P(\Sigma \to p + \gamma)_{\text{theo.}}}{P(\Sigma \to p + \pi^0)_{\text{exp.}}} = 1.4 \cdot 10^{-4},$$

and ([7])

$$\frac{P(\Sigma \to p + \gamma)_{\text{theo.}}}{P(\Sigma \to n + \mu^+ + \nu)_{\text{theo}}} = 4.3 \cdot 10^{-3}.$$

([5]) For a similar decay of Λ^0 into a neutron and a photon, the photon may be emitted by the intermediate charged meson or the baryon only. The decay $\Sigma^0 \to \Lambda^0 + \gamma$ should be treated differently since it conserves strangeness and is known to be very fast.

([6]) The coupling constant g is related to the coupling constant G involved in the direct Fermi interaction written in the form

$$\mathcal{H}_I(x) = \frac{G}{\sqrt{2}}[\bar{\psi}_a\gamma_\rho(1+\gamma_5)\psi_b][\bar{\psi}_c\gamma_\rho(1+\gamma_5)\psi_d] + \text{h.c.}$$

by $g^2/M_x^2 = G/\sqrt{2}$. Here M_x is the mass of the vector meson [see reference ([1])].

([7]) The leptonic decay of Λ^0 ($\Lambda^0 \to p + e^- + \bar{\nu}$) has recently been confirmed experimentally. Similar leptonic modes of decay are expected for Σ with the branching ratios to the known pionic modes of the order 10^{-2}, [J. LEITE LOPES: *Ann. Acad. Bras. Ci.*, **29**, 521 (1957); see also FEYNMAN and GELL-MANN: reference ([1])].

It may be remarked that for the muon decay ($\mu \to e + \nu + \bar{\nu}$) the hypothesis of the non-locality in ($V-A$) Fermi interaction (with $G_V = G_A = G$) from the exchange of vector meson leads to an effective increase in the Michel parameter ϱ while the life time of the decay is decreased. In fact we have

$$\varrho \simeq \frac{3}{4}\left(1 + \frac{m_\mu^2}{M_x^2} - 4\frac{m_e^2}{m_\mu^2}\right)$$

and

$$\tau = (2.26 \cdot 10^{-6}) \Big/ \left(1 + \frac{3}{5}\frac{m_\mu^2}{M_x^2} - 4\frac{m_e^2}{m_\mu^2}\right) \text{ s} .$$

Hence it is suggested that the vector meson should have a mass higher than about ten proton masses (see also reference [2]).

* * *

The authors are grateful to Professor J. Leite Lopes for the suggestion of the problem and the continued aid in its completion. One of us (A.H.Z.) wishes to express his gratitude to the Instituto de Física Teórica for the grant which made this work possible at the Centro Brasileiro de Pesquísas Físicas. We are grateful to the Centro Brasileiro de Pesquísas Físicas for the hospitality.

* * *

Note. - An event which, as suggested by M. Goldhaber, could be interpreted as the decay $\Sigma \to p + \gamma$ was found by E. P. George, A. J. Herz, J. H. Noon and N. Solntseff: *Nuovo Cimento*, **3**, 94 (1955); see R. E. Behrends: *Phy. Rev.*, **111**, 1691 (1958), footnote [4])

IL NUOVO CIMENTO Vol. XI, N. 6. 16 Marzo 1959

On the Possibility of Neutrons Producing Secondary Interactions in High Energy Showers.

P. K. Aditya (*)

Physics Honours School, Panjab University - Chandigarh
Institute for Theoretical Physics, University of Copenhagen

(ricevuto il 14 Gennaio 1959)

For nuclear disintegrations initiated by cosmic ray particles of great energy (E per nucleon $\gtrsim 10^{12}$ eV), there exists at present no satisfactory method of estimating the relative proportion of π-mesons, K-mesons, hyperons, and nucleon-antinucleon pairs produced amongst shower particles. Since direct mass measurements of secondary particles are impossible at such high energies, several attempts by indirect methods have been made.

A method due to Brisbout *et al* (1), and later used by other workers (2), of determining the proportion of neutral rather than charged K-mesons, hyperons, and nucleon-antinucleon pairs (hereafter called x-particles) amongst shower particles, involves the following assumptions:

a) because of their very short lifetime, π^0-mesons cannot contribute to nuclear interactions;

b) secondary interactions produced by neutral particles are due to x^0-particles or ejected nucleons;

c) the mean free path of x-particles, nucleons, and π-mesons is the same;

d) nucleons and (or) heavy mesons ($K^{\pm}$, θ^0, $\bar{\theta}^0$) with isotopic spin, $I = \frac{1}{2}$, are produced in a charge-independent way, so that if one assumes that it is true also for the hyperons, then unlike pions for which $n_{\pi^{\pm}} = 2n_{\pi^0}$, $n_{x^{\pm}} = n_{x^0}$.

Using N^0, the number of secondary interactions produced by neutral particles and $N^{\pm}$, the corresponding number of interactions produced by charged particles all observed within the same angular interval (defined by a strip of width 720 μm and length ~ 10 cm) within the narrow cone of high-energy showers initiated by singly and doubly charged particles of energy $\gtrsim 10^{12}$ eV, Brisbout *et al.* (1) obtained the ratio $N^0/N^{\pm}$ as $Q = 0.25$. Because of assumption (*c*) above, $Q = n_{s^0}/n_{s^{\pm}}$ or $\simeq n_{x^0}/(n_{x^{\pm}} + n_{\pi^{\pm}})$, where n_{π}, n_x and n_s refer to the numbers of π-mesons, x-particles, and the total number of charged shower particles,

(*) Formerly known as P. Kumar.

(1) F. A. Brisbout, C. Dahanayake, A. Engler, Y. Fujimoto and D. H. Perkins: *Phil. Mag.*, **1**, 605 (1956).

(2) B. Edwards, J. Losty, D. H. Perkins, K. Pinkau and J. Reynolds: *Phil. Mag.*, **3**, 237 (1958).

respectively. While considering the possibility that the large proportion of observed non-pions could be due to nucleon contamination, they ([1]) discussed the probability that nucleons produced from the target nucleus as a result of multiple collisions within it, would be found in the region of the narrow forward cone, but in view of the high multiplicity involved at such high energies, estimated that such a contribution from the nucleons would be negligible. No account seems to have been taken of the nucleons of the primary, which as we shall see would continue undeviated or only slightly affected in a collision even with a single nucleon of the target. It is our aim to consider presently the processes by which high-energy neutrons of the projectile enter the forward cone and to see whether such considerations affect the result. Since charged secondary interactions are produced by both $\pi^{\pm}$ and $x^{\pm}$ while the neutral interactions are due only to the x^0-particles (π^0-mesons being excluded because of assumption *a*) above) the relative proportion of x-particles is much more sensitive to the presence of a few neutrons than it would be if an equal number of protons were present.

There are two ways by which neutrons can enter the forward cone of high-energy interactions. These are:

i) If the primary is a complex nucleus, an α-particle or a heavy singly charged particle (deuteron or triton), only a part of the constituent nucleons may participate in the first interaction and the remainder proceed in the shower with the same energy per nucleon as that of the primary.

ii) The primary nucleon may participate in the collision and emerge from it with an energy still higher than that of any of the nucleons from the target.

We are at present not particularly interested in heavy primary interactions for which it follows naturally that during collisions with nuclei only a fraction of the incident nucleons take part in the interaction. For α-particle interactions within a wide range of primary energies ([3-5]), it is known that, during collisions with emulsion nuclei, on the average only half of the incident nucleons contribute to meson production. In collisions with lighter elements or peripheral collisions with heavy targets (*i.e.*, events of smaller number of heavy prongs), one would expect a still smaller fraction to take part in the collision. It is reasonable to assume that all such nucleons which do not take part in the first interaction would appear within an angle α to the primary direction where $\alpha \sim (\frac{1}{3})^{\frac{1}{2}} p_i/p_0$ (p_i is the internal momentum of the nucleons within the nucleus and p_0 is the external momentum per nucleon of the primary). For p_i corresponding to the average binding energy per nucleon (~ 8 MeV) and p_0 corresponding to the energy per nucleon of the incident α-particle, E (in eV), the angle α (in radians) is given by the relation $\alpha \simeq 10^8/E$. For α-particles of energy from 300 MeV to $\geqslant 10$ GeV per nucleon, several workers ([3-5]) have experimentally obtained the angular distribution of singly charged particles. From these data it is possible to find the energy dependence of the maximum angle within which are found most of the nucleons of an α-particle which presumably do not take part in the first event. We find this energy dependence to be in agreement with the relation for α derived above. Consequently, this relation may be used also for the energy region we are interested in at present, and one concludes that the nucleons of the projectile, which do not take part in the primary event, would be able to contri-

([3]) M. Ceccarelli, G. Quareni and G. T. Zorn: *Nuovo Cimento*, **1**, 669 (1955).

([4]) G. Quareni and G. T. Zorn: *Nuovo Cimento*, **1**, 1282 (1955).

([5]) M. V. K. Appa Rao, R. R. Daniel and K. A. Neelakantan: *Proc. Ind. Acad. Sci.*, **43**, 181 (1956).

bute to secondary neutral interactions in the region under investigation. On account of the secondary processes occurring in the uppermost layers of the atmosphere, it seems reasonable to assume that some fraction of the high-energy interactions initiated by singly charged particles in the stratosphere may in fact be due to deuterons or tritons (*). Similarly as for multiply charged primary events, the nucleon which does not participate in the primary collision is likely to produce secondary interactions. The calculation of this contribution is not straightforward and so we shall not enter into more detail here.

As to process ii), the nucleons that have participated in the primary collision can produce secondary interactions only if they appear in the angular interval defined by the scanned volume. A number of factors, such as the nature of the primary and target nuclei involved in the collision, inelasticity of the interaction, and primary energy determine this probability. In the first approximation, let us consider for example an elastic nucleon-nucleon collision. At relativistic velocities, the angle between the two departing nucleons is given by $2\gamma_c/(\gamma_c^2-1) < \operatorname{tg}\theta < \infty$, where γ_c is related to the velocity β_c of the c.m. system by the relation $\gamma_c=[1-\beta_c^2]^{-\frac{1}{2}}$. (It may be seen that the factor $2\gamma_c/(\gamma_c^2-1)$ reduces in the non-relativistic case to $\approx 4/W$, where W is the kinetic energy of the nucleon in terms of its rest mass, so that the angle θ is always about 90°, as is well known). The minimum angle between the two nucleons is $\sim 2/\gamma_c$, so that both the nucleons will only rarely appear together within the narrow core. It also means that, if one of the nucleons makes an angle between $1/\gamma_c$ and zero, the other nucleon will appear correspondingly between angles from $1/\gamma_c$ and 90°. In actual practice, the collisions are no longer elastic, but since at very high energies the primary particle does not lose more than a small fraction of its energy in meson production, the likelihood of the primary nucleon appearing in the narrow cone of half-angle $1/\gamma_c$ is very high. On the same grounds, the struck nucleon of the target is not likely to appear in the scanned volume unless there are multiple collisions. If one makes further the reasonable assumption that in half of the cases the interacting nucleon would suffer a charge exchange, then both, protons undergoing charge exchange and neutrons which leave the interaction after suffering only energy loss, would contribute to secondary neutral interactions.

Concluding that the nucleons from the projectile (whether or not they have participated in the primary collision) can contribute to secondary interactions, let us look at the data of Brisbout *et al.* [1] for which some experimental details are available. 9 neutral interactions were observed while following 166.2 cm of axial length along showers produced by singly charged particles and 82.1 cm of the shower axis for α-particle stars. In the same region, 36 charged interactions were also observed. If it is assumed *a*) that one neutron is present for a fraction F of the length 166.2 cm, *b*) that two neutrons are present along 82.1 cm, and *c*) that the interaction mean free path of the neutron is the same as that of the proton, *i.e.*, $\lambda_n = 34$ cm, one finds that even for $F = 0.5$ (which corresponds to the presence of an exchange neutron in half of the cases and takes no account of the possible contribution of neutrons resulting from heavier singly charged primaries) 7.3 interactions out

(*) In such a case the stripped off nucleon would proceed without deviation or loss of energy, so that if it interacted, the second interaction would have similar characteristics as the first event. An event of this type observed in an earlier work [6] led us to some interesting conslusions, which we shall describe separately while considering the probability of the presence of deuterons and tritons in the stratosphere.

of the 9 can be attributed to neutrons, thereby reducing the proportion of x-particles to about 5% of the shower particles. This value may further be modified if account is taken of the possibility of deuteron and triton primaries. In view of the limited statistics such detailed considerations may not be meaningful, but it appears that the proportion of x-particles determined from the ratio of neutral to charged secondary interactions is highly sensitive to the presence of nucleons amongst the shower particles.

* * *

Some of the arguments presented here are based upon an earlier work [6] done at the Panjab University, Chandigarh, India.

Thanks are due Professor B. M. ANAND for encouragement and to the Government of India, Department of Atomic Energy, for financial assistance.

The author is indebted to Professor B. PETERS for the facilities afforded at the Tata Institute of Fundamental Research, Bombay, and for many stimulating discussions at the Institute for Theoretical Physics in Copenhagen. It is a pleasure to thank Professor NIELS BOHR for the hospitality of this Institute.

Note added in proof.

Since this paper was written, the results of an investigation by LOHRMANN and TEUCHER (*Phys. Rev.*, **112**, 587 (1958)) have come to our attention. Amongst secondary particles produced at an average energy of $\sim 10^{13}$ eV, they obtained the ratio of interactions produced by neutral to charged particles as $(16 \pm 6)\%$. Their procedure of correcting for the presence of nucleons has been different from ours, and has yielded a value of $(9^{+8}_{-6})\%$ for the proportion of strange particles and anti-particles among charged secondary products. This result is in agreement with our present considerations.

[6] P. KUMAR: *Proc. 45-th Ind. Sci. Cong.*, III-3, Abs. n. **9**, Jan. 1958.

IL NUOVO CIMENTO Vol. XI, N. 6 16 Marzo 1959

Zur leitfähigen Haut des Titanoxyds.

S. Yamaguchi

The Institute of Physical and Chemical Research - Tokyo

(ricevuto il 2 Febbraio 1959)

Auf eine Glasfläche wurde Titan durch Vakuumverdampfung niedergeschlagen. Der erhaltene Titanfilm ließ sich mit der ozonhaltigen Luft auf Zimmertemperatur oxydieren. Die auf diese Weise hergestellte Haut (Dicke: ca. 300 AE) lieferte ein in Fig. 1 wiedergegebenes Beugungsbild. Sowohl die Beugungsflecken als auch die Ringe in diesem Bild entsprechen dem Titan-Oxyd (TiO_2) des Rutiltyps. Die den Flecken entsprechenden Kristalle sind regelmäßig orientiert, indem die (110)-Ebenen derselben der Substratfläche parallel liegen. Dieser Oxydfilm war elektrisch leitfähig. In der Tat erkannte man keine Elektronenaufladung beim Beugungsversuch. Die betreffende Oxydhaut wies eine bemerkenswerte Adhäsion für das Substrat auf. Dies spricht dafür, daß sich die in der Haut befindlichen TiO_2-Kristalle auf dem Substrat orientieren.

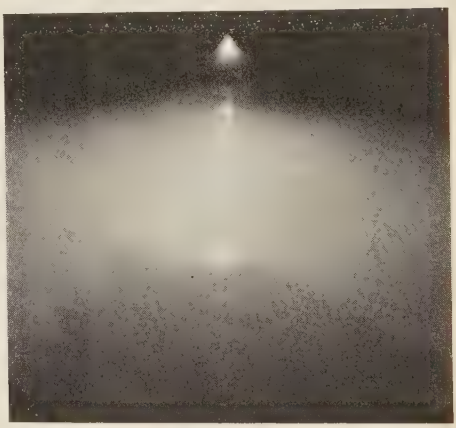

Fig. 1. – Reflektionsbild der leitfähigen TiO_2-Haut. Wellenlänge: 0.032 3 AE. Kameralänge: 495 mm. Positiv in 2.3 facher Vergrößerung.

IL NUOVO CIMENTO Vol. XI, N. 6 16 Marzo 1959

A Remark on One-Dimensional Quantum Electrodynamics.

V. Glaser and B. Jakšić (*)

Theoretical Study Division CERN - Geneva

(ricevuto l'11 Febbraio 1959)

In a recent note, I. Bialynicki-Birula (1) has shown that the one-dimensional quantum electrodynamics with zero mass electrons can be solved exactly. In what follows we would like to show that this one-dimensional model is essentially equivalent to the Thirring model (2).

The field-equations in this model are as follows:

$$\boldsymbol{p}\psi = e\gamma^\mu, A_\mu\psi \,. \tag{1a}$$

$$(\Box - \mu^2)A^\mu = -j^\mu \equiv -e\overline{\psi}\gamma^\mu\psi \,, \tag{1b}$$

where $\boldsymbol{p} = -i\gamma^\mu\partial_\mu$;, $\gamma^1 = i\sigma_1$, $\gamma^2 = \sigma_2$ (2), and μ is the mass of the « photons ». It will turn out that the case $\mu = 0$ has no physical solution due to the fact that the Coulomb force in the one-dimensional case does not vanish at infinity. (1 *a*, *b*) should be supplemented with the usual (non-renormalized) canonical commutation relations and the subsidiary condition $\chi^{(+)}(x)\,|a\rangle = 0$, $\chi = \partial_\mu A^\mu$, $|a\rangle$ being a physically allowed state.

From (1*a*) there follow the conservation laws:

$$\partial_\mu s^\mu = 0 \,, \qquad \partial_\mu t^\mu = 0 \,,$$

where

$$s^\mu = \frac{1}{e} j^\mu = \overline{\psi}\gamma^\mu\psi = (\varrho_1 - \varrho_2,\ \varrho_1 + \varrho_2) \,,$$

$$t^\mu = \overline{\psi}\gamma^\mu\gamma\psi = (\varrho_1 + \varrho_2,\ \varrho_1 - \varrho_2) \,, \qquad \varrho_\alpha = \psi_\alpha^* \psi_\alpha \,, \qquad \gamma = \gamma^2\gamma^1 = \sigma_3 \,.$$

(*) On leave of absence from the Institute « Ruder Bošković », Zagreb, and the University of Zagreb.

(1) We are indebted to the author for sending us a preprint of his letter to the *Nuovo Cimento*.

(2) W. E. Thirring: *Ann. Phys.*, **9**, 91 (1958); *Nuovo Cimento*, **9**, 1007 (1958); V. Glaser: *Nuovo Cimento*, **9**, 990 (1958).

With the introduction of new variables $u = t+x$, $v = t-x$, the conservation laws lead to

$$\left.\begin{aligned} \varrho_1 &= \varrho_1(v) = \psi_1^*(x-t,0)\psi_1(x-t,0)\,, \\ \varrho_2 &= \varrho_2(u) = \psi_2^*(x+t,0)\psi_2(x+t,0)\,. \end{aligned}\right\} \tag{2}$$

This means $\Box s^\mu = \Box t^\mu = 0$, and

$$[j^\mu(x), j^\nu(x')] = 0 \quad \text{for all } x \text{ and } x'. \tag{3}$$

The last fact follows from (2) and the canonical commutation relations.

From this basic result we see that $(1/\mu^2)j^\mu(x)$ is a solution of (1*b*). The most general solution of (1*b*) will be

$$A^\mu(x) = A_0^\mu(x) + \frac{1}{\mu^2} j^\mu(x)\,, \tag{4}$$

where $A_0^\mu(x)$ satisfies the homogeneous equation $(\Box - \mu^2)A_0^\mu(x) = 0$. From (3) and the canonical commutation relations it follows furthermore

$$[A^\mu(x), j^\nu(x')] = [A_0^\mu(x), j^\nu(x')] = 0\,, \tag{5}$$

and

$$[A^\mu(x), A^\nu(x')] = [A_0^\mu(x), A_0^\nu(x')] = i\,g^{\mu\nu}\Delta(x-x', \mu^2)\,. \tag{6}$$

This all implies $A_0^\mu = A_{\text{in}}^\mu = A_{\text{out}}^\mu$, so that the model does not give rise to any creation or scattering of « photons ».

Inserting (4) into (1a) we obtain

$$\boldsymbol{p}\psi = eA_{0\mu}\gamma^\mu\psi + \frac{e^2}{\mu^2}(\overline{\psi}\gamma^\mu\psi)\gamma_\mu\psi\,. \tag{7}$$

We introduce now the « Ansatz »

$$\psi(x) = \exp\left\{i\,\frac{e}{\mu^2}\,\Lambda(x)\right\}\psi_T(x)\,, \tag{8}$$

where

$$\Lambda(x) = \partial_\mu A_0^\mu + \gamma\varepsilon^{\mu\nu}\partial_\mu A_{0\nu} = -i\boldsymbol{p}\gamma^\mu A_{0\mu}\,,$$

$$\varepsilon^{\mu\nu} = -\varepsilon^{\nu\mu}, \qquad \varepsilon^{12} = +1, \qquad [\Lambda(x), \Lambda(x')] = 0\,,$$

for all x and x' by virtue of (6). One sees immediately that $\overline{\psi}\gamma^\mu\psi = \overline{\psi}_T\gamma^\mu\psi_T$ and the equation (7) leads to

$$\boldsymbol{p}\psi_T = \frac{e^2}{\mu^2}(\overline{\psi}_T\gamma_\mu\psi_T)\gamma^\mu\psi_T = 2\,\frac{e^2}{\mu^2}(\overline{\psi}_T\psi_T)\psi_T\,. \tag{9}$$

This is exactly the Thirring equation for ψ_T with the coupling constant $g_T = -e^2/\mu^2$, compare (2).

The « gauge transformation» (8) leading to the Thirring model means that the S-matrix, defined by $\psi_{\text{out}} = S^{-1}\psi_{\text{in}}S$, $A_{\text{out}} = S^{-1}A_{\text{in}}S = A_{\text{in}}$, is identical with the S-matrix of the Thirring model: $S = \exp\{ig_T Q_1 Q_2\}$, compare (2). It is a unit matrix with respect to the « photons ».

In the case $\mu = 0$ equation (1b) can be written in the form $\Box A_{\pm} = -e\varrho_{1,2}$ with $A_{\pm} = \frac{1}{2}(A^2 \pm A^1)$. The formal solution

$$A_+ = \frac{eu}{4}\int_{v_0}^{v} \varrho_1(v')\,\mathrm{d}v' + A_+(u, v_0)\,,$$

contains a factor which increases linearly with time, so that the asymptotic conditions cannot be satisfied. The physical reason for this behaviour has already been mentioned before.

The study of the Green's functions and the Wightman functions in this model does not seem to reveal anything essentially new as compared to the Thirring model.

* * *

In conclusion, we would like to thank Dr. W. Thirring and Dr. F. L. Scarf for discussions, which led to the clarification of the physical content of this model.

The Attractive K^--Meson Proton Interaction (*).

E. M. Ferreira (**)

Department of Mathematics, Imperial College - London

(ricevuto il 12 Febbraio 1959)

Experiments [1,2] seem to indicate the K^--proton interaction to be attractive. However it is known that the lowest (2nd) order perturbation theory matrix element $K^-p \to Y \to K^-p$, where Y represent Λ or Σ (virtual) hyperons, has a sign that corresponds to a repulsive potential between K^- and proton for either parity of Λ and Σ hyperons. The question then arises whether or not the higher order matrix elements give contributions of the correct sign and large enough to make agreement with experiment possible.

We have calculated one of these higher order diagrams, that obtained from the lowest order one by adding the exchange of a π-meson between the incident and the outgoing proton. We specialized to the case of forward and threshold (zero kinetic energy) scattering. The ratios $M^{(4)}/M^{(2)}$ of this fourth order matrix element to the second order one for the several possible parities of the Λ and Σ hyperons are indicated in the Table below.

$\Gamma_{K\Lambda N}$	$\Gamma_{K\Sigma N}$	$M^{(4)}/M^{(2)}$
1	1	$-\frac{G_\pi^2}{4\pi\hbar c}\,0.06\,\frac{G_{K\Lambda N}^2+5G_{K\Sigma N}^2}{G_{K\Lambda N}^2+G_{K\Sigma N}^2}$
1	γ_5	$-\frac{G_\pi^2}{4\pi\hbar c}\,0.06\,\frac{G_{K\Lambda N}^2+4.24G_{K\Sigma N}^2}{G_{K\Lambda N}^2+0.125G_{K\Sigma N}^2}$
γ_5	1	$-\frac{G_\pi^2}{4\pi\hbar c}\,0.41\,\frac{G_{K\Lambda N}^2+5.9G_{K\Sigma N}^2}{G_{K\Lambda N}^2+8G_{K\Sigma N}^2}$
γ_5	γ_5	$-\frac{G_\pi^2}{4\pi\hbar c}\,0.41\,\frac{G_{K\Lambda N}^2+5G_{K\Sigma N}^2}{G_{K\Lambda N}^2+G_{K\Sigma N}^2}$

We note that the ratio is always negative for any parities and values of the coupling constants and that for $G_\pi^2/4\pi\hbar c = 15$ its extreme values are -0.9 (for $G_{K\Sigma N}=0$, $\Gamma_{K\Lambda N}=1$) and -30 (for $G_{K\Lambda N}=0$ $\Gamma_{K\Sigma N}=\gamma_5$).

The matrix element for the graph considered presents thus the desired features, having the convenient sign and

(*) Supported by the National Research Council of Brazil.

(**) On leave of absence from the Centro Brasileiro de Pesquísas Físicas, Rio de Janeiro.

(1) W. Alles, N. N. Biswas, M. Ceccarelli and J. Crussard: *Nuovo Cimento*, **6**, 571 (1957).

(2) R. H. Dalitz: *Proc. of the Geneva Conference* (1958), p. 187.

being large enough to compensate the second order term.

The K^--proton system is a mixture of $T=1$ and $T=0$ isotopic spin states. It is interesting to note that if we assume that only one of these states contribute to the interaction, the potential derived from our graph is still attractive for all possible parities and values of coupling constants. That is, no minus sign arises in the splitting into iso-spin states, For example, in the case of equal parities attributed to the Λ and Σ hyperons, the $T=1$ state will give a matrix element proportional to $G^2_{K\Lambda N}+2G^2_{K\Sigma N}$, and the $T=0$ one will be proportional to $3G^2_{K\Sigma N}$: This equality of signs of the $T=1$ and $T=0$ interactions is in agreement with the result of the phenomenological analysis presented by R. H. Dalitz (see reference (²), p. 189).

* * *

We are greatly indebted to Professor A. Salam and Dr. P. T. Matthews for guidance and encouragement.

Quadratic Lagrangians in Relativistic Hydrodynamics.

F. Halbwachs, P. Hillion and J.-P. Vigier
Institut Henri Poincaré - Paris

(ricevuto il 12 Febbraio 1959)

In a preceding paper [1] we proposed a lagrangian formalism for relativistic fluids made of extended rotating dropplets, defined within time-like tubes along the lines of flow. Because the canonical tensors deduced from our lagrangians and satisfying the well known conservation relations $\partial_\nu t_{\mu\nu}=0$ and $\partial_\lambda f_{[\mu\nu]\lambda}=\frac{1}{2}(t_{\mu\nu}-t_{\nu\mu})$ take the particular forms

$$t_{\mu\nu}=g_\mu u_\nu \qquad \text{and} \qquad f_{[\mu\nu]\lambda}=\tfrac{1}{2}m_{[\mu\nu]}u_\lambda\,, \tag{1}$$

the vector g_μ (linear momentum density) and $m_{\mu\nu}$ (angular momentum density) obey the equations:

$$\dot{g}_\mu=0 \qquad \text{and} \qquad \dot{m}_{\mu\nu}=g_\mu u_\nu-g_\nu u_\mu\,, \tag{2}$$

as a necessary consequence. If we suppose the internal tensions between the individual droplets to be negligible, the latter satisfy consequently Weyssenhoff's equations of motion:

$$\dot{G}_\mu=0\,, \qquad \dot{M}_{\mu\nu}=G_\mu u_\nu-G_\nu u_\mu\,.$$

However the proposed lagrangians with a proper rotation energy term $\frac{1}{2}M_{\mu\nu}\dot{b}_\mu^{(\xi)}b_\nu^{(\xi)}$ rested on the special assumption that $M_{\mu\nu}$ did not depend on the derivation of the EK variables $b_\mu^{(\xi)}$, so that the non relativistic approximation furnished as rotation energy a term depending linearly of the angular velocity $\omega_{ij}=\dot{b}_i^{(\xi)}b_j^{(\xi)}-\dot{b}_j^{(\xi)}b_i^{(\xi)}$), thus different from the usual classical expression

$$T=\tfrac{1}{2}I_{il}\omega_i\omega_l\,, \tag{3}$$

where $\omega_i=\varepsilon_{ijk}\omega_{jk}$ and I_{il} denotes the usual symmetrical tensor of inertia. The quantization of such an expression would naturally raise special difficulties.

---

[1] F. Halbwachs, P. Hillion and J.-P. Vigier: *Nuovo Cimento*, **10**, 817 (1958).

We shall now show that the preceding assumption is not necessary and that more general Lagrangians quadratic with respect to $\omega_{\mu\nu}$ give correctly, not only relations (2), but also the usual non relativistic rotation energy (3). We first define the relativistic generalization of the tensor of inertia through the relation

$$M_{\alpha\beta} = \tfrac{1}{2} I_{\underset{\smile}{\alpha\beta}\,\underset{\smile}{\gamma\delta}} \omega_{\gamma\delta} \quad (^2) ,$$

where $M_{\alpha\beta}$ is the particle angular momentum and the tensor $I_{\underset{\smile}{\alpha\beta}\,\underset{\smile}{\gamma\delta}}$ is antisymmetric with respect to α and β, and to γ and δ, and symmetric with respect to substitution of the pair of indices $(\alpha\beta)$ with $(\gamma\delta)$. We take as rotation energy density

$$T = \tfrac{1}{8} I_{\alpha\beta\gamma\delta} \omega_{\alpha\beta} \omega_{\gamma\delta} = \tfrac{1}{4} M_{\alpha\beta} \omega_{\alpha\beta} , \qquad \omega_{\alpha\beta} = \tfrac{1}{2} (\dot{b}_\alpha^{(\xi)} b_\beta^{(\xi)} - \dot{b}_\beta^{(\xi)} b_\alpha^{(\xi)}) .$$

And then the non relativistic approximation gives evidently the above classical quadratic expression.

On the other hand, we make the supplementary assumption that this tensor $I_{\alpha\beta\gamma\delta}$ does not depend on the derivatives $\partial_\lambda b_\mu^{(\xi)}$ of the EK variables.

Let us start from the lagrangian

$$\mathcal{L} = \varrho m_0 c^2 + ic\varrho b_\mu^{(4)} \partial_\mu S + \tfrac{1}{8} \varrho I_{\alpha\beta\gamma\delta} \omega_{\alpha\beta} \omega_{\gamma\delta} + \lambda_{\mu\nu} (b_\mu^{(\xi)} b_\nu^{(\xi)} - \delta_{\mu\nu}) .$$

Because $\mathcal{L} = 0$ (as a consequence of $\partial\mathcal{L}/\partial\varrho = 0$ and $b_\mu^{(\xi)} b_\nu^{(\xi)} = \delta_{\mu\nu}$) the two canonical tensors $t_{\mu\nu}$ and $f_{\mu\nu\lambda}$ depend only on the derivatives of $\mathcal{L}$ with respect to the derivatives $\dot{b}_\mu^{(\xi)}$ (and also $\partial_\mu S$) namely:

$$f_{\mu\nu\lambda} = \tfrac{1}{2} \varrho i c b_\lambda^{(4)} M_{\alpha\gamma} b_\gamma^{(\xi)} b_\beta^{(\xi)} \cdot \tfrac{1}{2} (\delta_{\alpha\mu} \delta_{\beta\nu} - \delta_{\beta\mu} \delta_{\alpha\nu}) ,$$

that is, because $b_\beta^{(\xi)} b_\gamma^{(\xi)} = \delta_{\gamma\beta}$

$$f_{\mu\nu\lambda} = \tfrac{1}{2} \varrho M_{\mu\nu} u_\lambda ,$$

$$t_{\mu\nu} = ic\varrho b_\nu^{(4)} \partial_\mu S + \tfrac{1}{2} \varrho i c b_\nu^{(4)} b_\gamma^{(\xi)} M_{\alpha\gamma} \partial_\mu b_\alpha^{(\xi)} =$$

$$= \varrho u_\nu (\partial_\mu S + \tfrac{1}{2} M_{\alpha\beta} \partial_\mu b_\alpha^{(\xi)} b_\beta^{(\xi)}) .$$

Thus we obtain the correct form for these two tensors and our formalism satisfies the equation of Weyssenhoff with

$$g_\mu = \varrho (\partial_\mu S + \tfrac{1}{2} M_{\alpha\beta} \partial_\mu b_\alpha^{(\xi)} b_\beta^{(\xi)}) , \qquad m_{\mu\nu} = \varrho M_{\mu\nu} .$$

(²) The symbols $\smile$ and — denote skew symmetric and symmetric tensors.

Note on Possible Parity Non-Conservation in Strong Interactions.

L. M. Brown (*)

Istituto di Scienze Fisiche dell'Università - Milano
Istituto Nazionale di Fisica Nucleare - Milano

(ricevuto il 23 Febbraio 1959)

As experimental tests of the conservation of parity in strong interactions have not been completed, it may be of interest to observe that a principle which has already been successfully applied to the theory of the weak interactions may allow a distinction to be made between the strong interaction terms of the Lagrangian which do, and those which do not conserve parity. We refer to the principle of chirality invariance [1], or its equivalent expression in terms of the two-component fermion theory [2]. Whether the presence of such parity non-conserving terms in the strong interaction Lagrangian would necessarily imply prominent parity non-conserving effects in pion-nucleon or nucleon-nucleon interaction at moderate energies is an open question related to the role which virtual strange particles play, in general, in such processes [3].

In order to apply the chirality invariance principle, we may suppose that the strong interactions, like the weak, can in some sense be represented as direct four-fermion interactions and adopt the model of the pion as a nucleon-antinucleon compound, following Fermi and Yang [4]. Similarly we represent the K-meson as a compound of nucleon and lambda [5].

A consideration of this type on the part of Okun [6], but assuming parity conservation in the strong interactions, led him to propose that not all the known baryon fields are fundamental, but that the Σ and the Ξ are compounds

(*) On leave from Northwestern University, U.S.A., for the academic year 1958-59 as a Fulbright Research Scholar in Italy.

(1) J. Tiomno: *Nuovo Cimento*, **1**, 226 (1955); S. Watanabe: *Progr. Theor. Phys.*, **15**, 81 (1956); E. G. C. Sudarshan and R. E. Marshak: *Phys. Rev.*, **109**, 1860 (1958); J. J. Sakurai: *Nuovo Cimento*, **7**, 649 (1958).

(2) R. P. Feynman and M. Gell-Mann: *Phys. Rev.*, **109**, 193 (1958); L. M. Brown: *Phys. Rev.*, **111**, 957 (1958).

(3) A. Pais: *Phys. Rev. Lett.*, **1**, 418 (1958). Pais has discussed how parity nonconserving effects can be limited by imposing other exact or approximate symmetry principles.

(4) E. Fermi and C. N. Yang: *Phys. Rev.*, **76**, 1739 (1949).

(5) S. Sakata: *Progr. Theor. Phys.*, **16**, 686 (1956).

(6) L. B. Okun': *Proc. Annual International Conference on High Energy Physics at CERN* (1958), p. 223.

of the others. Here, instead, we assume that each baryon field is fundamental and see what the postulate of chirality invariance tells us about parity conservation. The isotopic spin is omitted in the writing as it is irrelevant to this question (7). We treat each isotopic multiplet given by Gell-Mann-Nishijima scheme as a single field.

The chirality transformation $\psi \to \gamma_5\psi$, $\overline{\psi} \to -\overline{\psi}\gamma_5$ (with $\gamma = 1$) is to be applied to each fundamental baryon field *separately*. When the same fermion field occurs twice in a bracket, for example,

$$(1a) \quad (\overline{\psi}^{(1)}O_i\psi^{(1)}) \to (\overline{\psi}^{(1)}O_i\psi^{(1)}), \text{ for } O_i = V, A;$$

$$(1b) \quad \to -(\overline{\psi}^{(1)}O_i\psi^{(1)}), \quad \text{for } O_i = S, T, P,$$

independent of the transformation character of the field $\psi^{(1)}$ under γ_5. But when two different fields occur,

$$(2) \quad (\overline{\psi}^{(2)}O_i\psi^{(1)}) \to (\overline{\psi}^{(2)}O_i\gamma_5\psi^{(1)}) = \\ = \pm(\overline{\psi}^{(2)}O_i\psi^{(1)}),$$

the equality holding only when $\psi^{(1)}$ or $\psi^{(2)}$ are chosen to be eigenfunctions of γ_5. In order to form a chirality invariant four-fermion interaction with other fields from expressions like (2), it is clear that $\psi^{(1)}$ and $\psi^{(2)}$ must belong to the *same* eigenvalue of γ_5. (Note that $\gamma_5\psi = \pm\psi$ implies $-\overline{\psi}\gamma_5 = \pm\overline{\psi}$). For (2) to be non-vanishing it follows then that O_i is either V or A.

Thus while chirality invariance imposes severe restrictions on the interaction form when two different fields are in the same bracket, it gives much weaker results when the fields are the same. We shall minimize the restriction in writing the interactions by putting, whenever possible, the same fields in one bracket.

Adopting the model of Fermi-Yang, we see that the pseudoscalar pion field can be represented by an expression of type (1*b*). The « vertex » interaction

$$(3) \quad (\overline{\mathrm{N}}\gamma_5\mathrm{N})\cdot(\overline{\mathrm{N}}\gamma_5\mathrm{N}),$$

where the second bracket represents the pion, is thus automatically parity and chirality invariant. Pseudoscalar interactions between this pion and the other baryons ($\Sigma\Sigma\pi$), ($\Xi\Xi\pi$) cannot be written in chirality invariant form, but only as V or A direct interactions, according to Eq. (1). With this restriction they can still conserve parity. When three fundamental fields are involved, however, this is not the case.

Consider, for example, $\Sigma + \mathrm{N} \to \Lambda + \mathrm{N}$,

$$(4) \quad (\overline{\Lambda}O_i\Sigma)\cdot(\overline{\mathrm{N}}O_i\mathrm{N}).$$

Here the nucleon bracket is chirality invariant if O_i is V or A, but it is necessary for Σ and Λ to be positive eigenfunctions of the chirality operator. In this case we get maximum parity non-conservation. Similarly, considering the K-meson as a nucleon-Λ compound we conclude that (KNΛ) can be parity conserving, while (KNΣ) is parity violating.

In summary, we can classify the strong interactions as follows, letting a, b, c, d represent the four fundamental baryon fields, and letting a^+, a^- be the positive and negative chirality parts of a, etc.

Class I: requiring V, A interaction *and* parity violation. For (a, b, c, d) we must have a_+, b_+, c_+, d_+; for ($aacd$) we must have c_+, d_+. This class includes the interactions (NN)($\Lambda\Sigma$) or $\pi\Lambda\Sigma$ or KNΣ; (NΞ)($\Lambda\Lambda$) or K$\Xi\Lambda$; (NΞ)($\Lambda\Sigma$) or K$\Xi\Sigma$; (NΞ)($\Sigma\Sigma$).

Class II: requiring V, A interaction but not requiring parity violation, form

(7) Of course, if one requires charge independence, then the isotopic spin is relevant. In fact SOLOVIEV has shown that in renormalizable pseudoscalar meson theory, imposing CP invariance and charge independence requires parity conservation. See V. G. SOLOVIEV: *Nucl. Phys.*, **6**, 618 (1958).

$(a\ a\ b\ b)$. This class includes (NN)($\Lambda\Lambda$) or KΛN; (NN)($\Sigma\Sigma$) or $\pi\Sigma\Sigma$; (NN)($\Xi\Xi$) or $\pi\Xi\Xi$.

Class III: no restriction, form $(a\ a\ a\ a)$. This class includes (NN)(NN) or πNN.

With regard to the question of renormalizability it may be remarked that, in principle, this question has nothing to do with the strength of coupling. The objection on ground of mathematical consistency is the same here as for the usual formulation of the weak interactions. If this is resolved, for example by the attribution of an intrinsic non-locality of some type, the same solution could apply here.

On Ionization Measurements in a Hydrogen Bubble Chamber.

I. Derado and N. Schmitz

Max-Planck-Institut für Physik und Astrophysik - München

(ricevuto il 9 Marzo 1959)

Using bubble chamber photographs from the 10 in. hydrogen chamber of the Alvarez Group (Berkeley) we have examined the inelastic π^--p-scatterings resulting from an exposure of the chamber to a π^--beam of 1.14 GeV/c from the bevatron. Mainly, in addition to multiple production, two reactions occur

$$(a) \qquad \pi^- + p \to \pi^- + p + \pi^0 ,$$

$$(b) \qquad \pi^- + p \to \pi^- + n + \pi^+ .$$

For most of the events we were able by using the conservation laws for energy and momentum to decide whether a reaction of type (*a*) or type (*b*) had occurred. However, in some cases it was impossible by this method to distinguish between the two types of reactions. (The reasons for this will be discussed in a later paper.)

In order to decide also in these cases whether the positive particle was a proton or a π^+ we have examined the momentum dependence of the bubble density σ both for proton and pion tracks, using elastic events

$$\pi^- + p \to \pi^- + p ,$$

where the particles can be identified and where the momenta follow exactly from the scattering angles. In all cases the measured values for σ lay between 20 and 25 cm^{-1} ($\sigma_{average} = (22.5 \pm 2.5)$ cm^{-1}) regardless of the momentum and of whether the track was that of a proton or of a pion. This means that no momentum dependence for σ could be established. The reason for this apparent independence lies probably in the fact that the bubbles had rather large radii in our films and that even at momenta for which theoretically minimum ionization was to be expected the bubble density was so high that the bubbles almost bordered on one another thus preventing a resolution of higher density. Besides, in the case of small momenta several bubbles had often grown together to form one lengthy blob or a larger bubble thus making the measurement of the bubble density unsuitable.

In the course of these examinations we noticed, however, that at momenta lower than 650 MeV/c a proton track presents a visual form quite different from that of a pion track of the same momentum. In the case of the pion

track the bubbles are comparatively small and seem to be arranged exactly

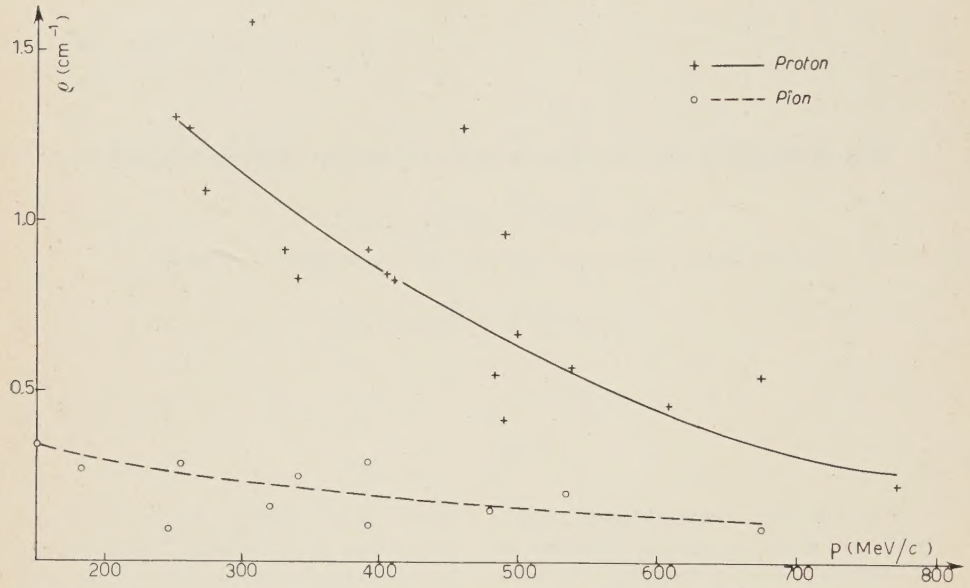

Fig. 1.

on a line whereas in the case of the proton track the bubbles are larger as a result of several bubbles growing together and are not all lying on a line; instead, many bubbles lie outside the proper track (δ-rays) thus causing a quite different visual impression of the track. This difference ceases to exist at

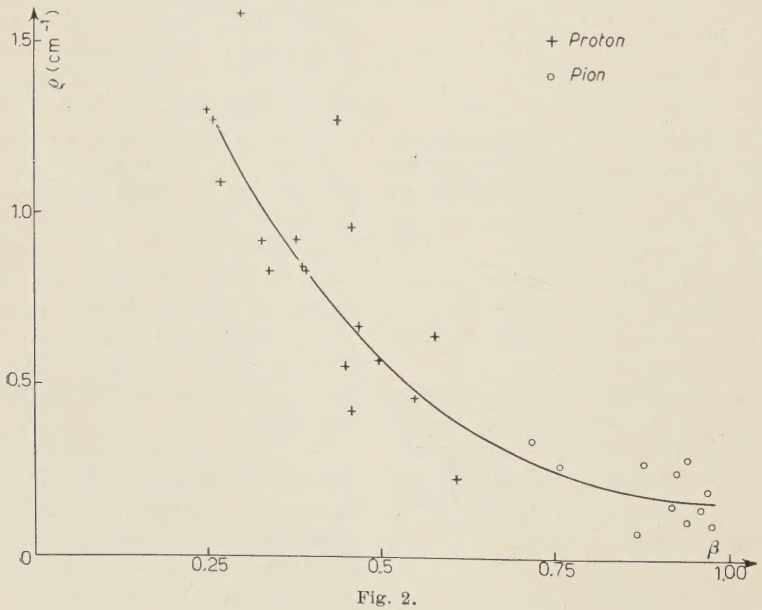

Fig. 2.

higher momenta where approximately minimum ionization for both particles is to be expected. In a quantitative examination we have measured the δ-ray density ϱ for many tracks of elastic events having a dip angle $<50°$. A « δ-ray » was counted if one or more bubbles lay clearly outside the track. The results of these measurements for 29 tracks are shown in the two figures. Fig. 1 gives the « δ-ray » density ϱ as a function of the momentum p, Fig. 2 as a function of the velocity β. (Crosses correspond to identified protons, circles to pions. The curves are drawn as a best fit through the experimental points.) From Fig. 1 it can be seen clearly that for momenta smaller than 650 MeV/c the « δ-ray » density of a proton track is considerably larger than for a pion track so that at these momenta a distinction between a proton and a pion is possible by the measurement of the « δ-ray » density.

* * *

We are grateful to Dr. K. GOTTSTEIN for a valuable discussion and to Dr. L. W. ALVAREZ for the loan of the bubble chamber films.

LIBRI RICEVUTI E RECENSIONI

G. Toraldo di Francia – *La diffrazione della luce*; pagg. XI+530; figg. 159. Edizioni Scientifiche Einaudi, L. 8 000.

Il presente testo costituisce quanto di più moderno sia disponibile nella bibliografia internazionale in merito ai fenomeni di diffrazione della luce.

Lo studio teorico di questi fenomeni è ricondotto alla ricerca di autofunzioni e di autovalori utilizzando un metodo già usato in vari articoli originali ma mai fino ad ora nei libri di ottica, dove si era preferita la più intuitiva via tradizionale.

Questa nuova trattazione è il pregio fondamentale del libro sia perchè rende possibile una notevole semplificazione della trattazione matematica che risulta così più coerente e compatta, sia perchè rende più accessibile al fisico moderno, abituato dalla meccanica quantistica a ragionare in termini di autovalori e autofunzioni, una materia molto specializzata.

Il libro è diviso in cinque parti delle quali la prima è solo una premessa matematica per rendere intellegibile il seguito anche ad uno studente con la preparazione del biennio di ingegneria.

La seconda, che è forse la parte più bella, è dedicata ad un vasto ed accurato studio dei fenomeni di Fraunhofer. Vi si trova una precisa trattazione di tutti i vari tipi di reticoli, dal primo reticolo a fili dello stesso Fraunhofer ai reticoli di fase; dai reticoli finiti a quelli infinitamente estesi, dai reticoli a trasparenza a quelli a riflessione, con la giusta precisazione che i reticoli incisi sono reticoli a trasparenza e di fase. Non manca un paragrafo sulla verifica sperimentale dell'esistenza delle onde evanescenti, verifica eseguita dall'autore sia con la luce sia con le microonde. Completa queste parti la teoria dei diaframmi non periodici e del potere risolutivo di molti strumenti ottici.

La teoria diffrazionale delle immagini sia in luce coerente sia in luce incoerente è trattata nella III parte. Si trova qui una interessante e approfondita discussione sul potere risolutivo del microscopio e sulle informazioni contenute in una immagine in luce coerente. Non ci sembra invece sufficiente il rilievo dato alla microscopia in contrasto di fase.

Un brillante capitolo sui paradossi ottici ai quali può dar luogo la teoria della diffrazione è inserito nella quarta parte dedicata ai fenomeni di Fresnel. Son qui descritti tra l'altro i paradossi ottici di Poisson, di Lord Rayleigh, di Gouy e la propagazione anomala delle onde sferiche con una ingegnosa verifica sperimentale.

Lo studio diffrazionale delle aberrazioni si trova infine nell'ultima parte che è molto utile per le applicazioni pratiche.

Notiamo uno strano errore tipografico, più volte ripetuto che fa diventare infinitesimali i reticoli infinitamente estesi.

E. Polacco